

DTIC FILE COPY

4

AD-A202 113

AFGL-TR-88-0228

CALCULATION OF MOLECULAR ABSORPTION PARAMETERS  
AND UPDATING THE AFGL ATMOSPHERIC LINE PARAMETER  
COMPILATION

Robert R. Gamache

University of Lowell  
Center for Atmospheric Research  
450 Aiken Street  
Lowell, Massachusetts 01824

15 September 1988

Final Report

May 31, 1985 to May 30, 1988

Approved for public release; distribution unlimited.

DTIC  
ELECTE  
DEC 16 1988  
S D  
E

AIR FORCE GEOPHYSICS LABORATORY  
AIR FORCE SYSTEMS COMMAND  
UNITED STATES AIR FORCE  
HANSCOM AFB, MASSACHUSETTS 01731

88 12 14 060

"This technical report has been reviewed and is approved for publication"



(Signature)

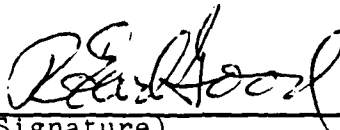
LAURENCE ROTHMAN  
Contract Manager



(Signature)

GEORGE A. VANASSE  
Branch Chief

FOR THE COMMANDER



(Signature)

R. EARL GOOD  
Director

This report has been reviewed by the ESD Public Affairs Office (PA) and is releasable to the National Technical Information Service (NTIS).

Qualified requestors may obtain additional copies from the Defense Technical Information Center. All others should apply to the National Technical Information Service.

If your address has changed, or if you wish to be removed from the mailing list, or if the addressee is no longer employed by your organization, please notify AFGL/DAA, Hanscom AFB, MA 01731. This will assist us in maintaining a current mailing list.

Do not return copies of this report unless contractual obligations or notices on a specific document requires that it be returned.

UNCLASSIFIED

SECURITY CLASSIFICATION OF THIS PAGE

REPORT DOCUMENTATION PAGE				Form Approved OMB No 0704-0188	
1a REPORT SECURITY CLASSIFICATION Unclassified			1b RESTRICTIVE MARKINGS		
2a SECURITY CLASSIFICATION AUTHORITY			3 DISTRIBUTION/AVAILABILITY OF REPORT Approved for public release; distribution unlimited.		
2b DECLASSIFICATION/DOWNGRADING SCHEDULE					
4 PERFORMING ORGANIZATION REPORT NUMBER(S) ULRF-446/CAR			5 MONITORING ORGANIZATION REPORT NUMBER(S) AFGL-TR-88-0228		
6a NAME OF PERFORMING ORGANIZATION University of Lowell		6b OFFICE SYMBOL (If applicable)	7a NAME OF MONITORING ORGANIZATION Air Force Geophysics Laboratory		
6c ADDRESS (City, State, and ZIP Code) Center for Atmospheric Research 450 Aiken Street Lowell, MA 01854			7b ADDRESS (City, State, and ZIP Code) Hanscom AFB Massachusetts 01731-5000		
8a NAME OF FUNDING SPONSORING ORGANIZATION Air Force Geophysics Laboratory		8b OFFICE SYMBOL (If applicable) OPI	9 PROCUREMENT INSTRUMENT IDENTIFICATION NUMBER F19628-85-K-0044		
8c ADDRESS (City, State, and ZIP Code) Hanscom AFB, MA 01731			10 SOURCE OF FUNDING NUMBERS		
			PROGRAM ELEMENT NO 61102F	PROJECT NO 2310	TASK NO G1
					WORK UNIT ACCESSION NO BJ
11 TITLE (Include Security Classification) CALCULATION OF MOLECULAR ABSORPTION PARAMETERS AND UPDATING THE AFGL ATMOSPHERIC LINE PARAMETER COMPILATION					
12 PERSONAL AUTHOR(S) Robert R. Gamache					
13a TYPE OF REPORT Final		13b TIME COVERED FROM 5/31/85 TO 5/30/88		14 DATE OF REPORT (Year, Month, Day) 1988 September 15	
15 PAGE COUNT 184					
16 SUPPLEMENTARY NOTATION					
17 COSATI CODES			18 SUBJECT TERMS (Continue on reverse if necessary and identify by block number)		
FIELD	GROUP	SUB-GROUP	Molecular Spectroscopy, Total Internal Partition Sums, Collision Broadened Halfwidths and Line Shifts, Temperature Dependence of Halfwidths, and Line Shifts.		
19 ABSTRACT (Continue on reverse if necessary and identify by block number) The changes and updates made that produced the 1986 version of the HITRAN database are discussed. The new format adopted and the programs and files that are distributed with the database are reviewed. We present the new parameters added to the database and the sources of the data. We briefly discuss our work on the temperature dependence of the $N_2$ -broadened halfwidths and line shifts for ozone and water vapor. The work done on the calculation of line intensities for transitions in the visible region of the spectrum for water vapor is given. We discuss many of the miscellaneous tasks relating to the database that were done under this contract. Finally the work done on calculating the total internal partition sums and their temperature dependence for the species on the database is presented.					
20 DISTRIBUTION/AVAILABILITY OF ABSTRACT <input checked="" type="checkbox"/> UNCLASSIFIED UNLIMITED <input type="checkbox"/> SAME AS RPT <input type="checkbox"/> DTIC USERS			21 ABSTRACT SECURITY CLASSIFICATION Unclassified		
22a NAME OF RESPONSIBLE INDIVIDUAL Laurence S. Rothman			22b TELEPHONE (Include Area Code)		22c OFFICE SYMBOL AFGL/OPI

## TABLE OF CONTENTS

	Page
1.0 HITRAN DATABASE	1
2.0 TEMPERATURE DEPENDENCE OF THE HALFWIDTH	26
2.1 Temperature Dependence of Ozone Halfwidths	26
2.2 Temperature Dependence of Halfwidths of Water Vapor	27
3.0 WATER VAPOR DATA IN THE VISIBLE SPECTRAL REGION	32
4.0 MISCELLANEOUS TASKS	44
4.1 Ozone Data for Minor Isotopic Species	44
4.2 Ozone Halfwidths for the GEISA Atlas	44
4.3 Halfwidth and Temperature Dependence of Halfwidths for Database	45
4.4 Ozone Halfwidth and Shift Data Requested by Outside Groups	46
4.5 Halfwidths for Water Vapor for HOT Gas Atlas	48
4.6 CO <sub>2</sub> Data from L. Rosenmann	50
4.7 Updates to the Program SELECT	51
5.0 PARTITION SUMS FOR THE DATABASE SPECIES	52
5.1 Water Vapor	72

## TABLE OF CONTENTS (Continued)

	Page
5.2 Carbon Dioxide	78
5.3 Ozone	78
5.4 N <sub>2</sub> O	82
5.4.1 CO	117
5.5 Methane	119
5.6 Nitrogen Dioxide	119
5.7 Approximate Partition Sums	137
5.8 Nuclear Statistical Factors for Non-Symmetric Nuclei	141
6.0 REFERENCES	146
7.0 ACKNOWLEDGEMENT	150

APPENDIX A     Presentations Made Under Contract

APPENDIX B     Publications Made Under Contract



Accession For	
NTIS GRA&I	<input checked="" type="checkbox"/>
DTIC TAB	<input type="checkbox"/>
Unannounced	<input type="checkbox"/>
Justification	
By	
Distribution/	
Availability Codes	
Avail and/or	
Dist	Special
<div style="font-size: 2em; font-weight: bold; margin-left: 10px;">A-1</div>	

## LIST OF FIGURES

Figure No.		Page
1	File Structure of HITRAN	17
2	Custom Editor Menu	23
3	Screen for Editing Records	24
4	$\ln(\gamma(T)/\gamma(T_0))$ vs. $\ln(T_0)/(T)$ for the $^{27}_{15}\text{O} \leftarrow ^{27}_{13}\text{O}$ Transition of Ozone, $n = 0.76$	28
5	Total Partition Function vs. Energy for $\text{H}_2\text{O}$ and $\text{CO}_2$ at Various Temperatures $\text{H}_2\text{O}$ at 9.375 K (Principle Isotope)	56
6	Total Partition Function vs. Energy for $\text{H}_2\text{O}$ and $\text{CO}_2$ at Various Temperatures $\text{H}_2\text{O}$ at 100 K (Principle Isotope)	57
7	Total Partition Function vs. Energy for $\text{H}_2\text{O}$ and $\text{CO}_2$ at Various Temperatures $\text{H}_2\text{O}$ at 200 K (Principle Isotope)	58
8	Total Partition Function vs. Energy for $\text{H}_2\text{O}$ and $\text{CO}_2$ at Various Temperatures $\text{H}_2\text{O}$ at 296 K (Principle Isotope)	59
9	Total Partition Function vs. Energy for $\text{H}_2\text{O}$ and $\text{CO}_2$ at Various Temperatures $\text{H}_2\text{O}$ at 500 K (Principle Isotope)	60
10	Total Partition Function vs. Energy for $\text{H}_2\text{O}$ and $\text{CO}_2$ at Various Temperatures $\text{H}_2\text{O}$ at 1000 K (Principle Isotope)	61
11	Total Partition Function vs. Energy for $\text{H}_2\text{O}$ and $\text{CO}_2$ at Various Temperatures $\text{CO}_2$ at 296 K (Principle Isotope)	62
12	Total Partition Function vs. Energy for $\text{H}_2\text{O}$ and $\text{CO}_2$ at Various Temperatures $\text{CO}_2$ at 500 K (Principle Isotope)	63

# LIST OF FIGURES (Continued)

Figure No.		Page
13	Total Partition Function vs. Energy for H <sub>2</sub> O and CO <sub>2</sub> at Various Temperatures CO <sub>2</sub> at 1000 K (Principle Isotope)	64
14	Total Partition Function vs. Energy for H <sub>2</sub> O and CO <sub>2</sub> at Various Temperatures CO <sub>2</sub> at 1000 K (636 Isotope)	65
15	Total Partition Function vs. Energy for H <sub>2</sub> O and CO <sub>2</sub> at Various Temperatures CO <sub>2</sub> at 1000 K (637 Isotope)	66
16	Total Partition Function vs. Energy for H <sub>2</sub> O and CO <sub>2</sub> at Various Temperatures CO <sub>2</sub> at 1000 K (828 Isotope)	67
17	Convergence of Partition Sums vs. Energy (161) Water Vapor at T = 100, 200, 300, and 400 K	77
18	% Error [Q(T)-Polynomial/QT] vs. T for H <sub>2</sub> <sup>16</sup> O	79
19	% Error [Q(T)-Polynomial/QT] vs. T for HDO	80
20	% Error [Q(T)-Polynomial/QT] vs. T for CO <sub>2</sub>	81
21	Partition Sum vs. Energy for <sup>12</sup> CH <sub>4</sub> and <sup>13</sup> CH <sub>4</sub> at 400 K	121
22	Q(T) Calc, Q <sub>v</sub> (T)*Q <sub>r</sub> (T), Q <sub>v</sub> (T)*Q <sub>r</sub> (T) Classical, vs. Temperature and % Error vs. Temperature	139
23	Q(T) Calc, Q <sub>v</sub> (T)*Q <sub>r</sub> (296K)*(T/T <sub>0</sub> ) <sup>1.5</sup> vs. Temperature and % Error vs. Temperature, i.e. the FASCODE Approx.	140

## LIST OF TABLES

Table No.		Page
1	Format of Rotational Quantum Numbers	3
2	Relative Natural Abundances of the Species on the HITRAN Database	5
3	Statistical Weights for Symmetric Tops with Three Identical Nuclei	8
4	Statistical Weights for Symmetric Tops with Four Identical Nuclei	9
5	Range of Air-Broadened Halfwidths and Temperature Dependences	15
6	Example of Direct Image of Lines on the 1986 HITRAN Database	18
7	Approximate Absorption Cross-Sections on File 4 of HITRAN Tape	20
8	Structure for Database: AGENDA.dbf	22
9	Temperature Exponents for the H <sub>2</sub> O-N <sub>2</sub> System	30
10	Vibrational Bands Present in the Water Vapor Data from Camy-Peyret et al.	33
11	IER Values for Wavenumber and Intensity	35
12	Average Value of the Effective Constant $\beta$	39
13	Flaud's Notes for Lines with P > 500	41



# LIST OF TABLES (Continued)

Table No.		Page
14	Corrected H <sub>2</sub> O Lines for which $P > 500$	42
15	Ozone Halfwidths Sent to Dr. M. Abbas	49
16	Nuclear Spin Degeneracy Factors for Non-Symmetrical Nuclei	54
17	Selected Energy Levels for Water Vapor in cm <sup>-1</sup>	69
18	Selected Energy Levels for O <sub>3</sub> in cm <sup>-1</sup>	70
19	Ground State Watson Hamiltonian Constants for the Four Isotopic Species of H <sub>2</sub> O	73
20	Watson Hamiltonian Constants for O <sub>3</sub> from Flaud et al.	83
21	Partition Sums from a "Complete" Set of O <sub>3</sub> Energy Levels	101
22	Error Analysis for the Isotopic Species of O <sub>3</sub>	102
23	Test of Approximation $Q_{\text{actual}} = Q_{\text{vib}} \cdot Q_{\text{rot}}$ for the Principle Species of O <sub>3</sub>	103
24	Vibrational-Rotational Hamiltonian Constants for N <sub>2</sub> O from Toth	104
25	Last J-Level for N <sub>2</sub> O Data from the AFGL Database	116
26	Band Origins for the Various Vibrational Levels of N <sub>2</sub> O	117
27	Partition Sums for N <sub>2</sub> O from a "Complete" Set of Energy Levels	118

# LIST OF TABLES (Continued)

Table No.		Page
28	Partition Functions for CH <sub>4</sub> vs. T	120
29	Comparison of Calculated Energies in cm <sup>-1</sup> with Published Values	124
30	Watson Hamiltonian Constants for Eleven Vibrational Bands of NO <sub>2</sub>	125
31	Spin Rotation Interaction Constants for NO <sub>2</sub>	136
32	Vibrational Energies in cm <sup>-1</sup> for H <sub>2</sub> O, HDO and O <sub>3</sub>	141

## 1.0 HITRAN DATABASE

Work done under this contract produced several major changes to the AFGL line parameter compilations. First, the two line parameter compilations (the main and trace gas atlases) were merged into a single entity and called **high-resolution transmission molecular absorption database (HITRAN)**. Next, the format of the database was changed and other parameters corresponding to each quantum transition were added. Each record of a transition now consist of 100 characters of information rather than the previous 80 characters. Finally, the database is now distributed with several other files that assist in reading and using the database and which give useful information relating to the database.

The first version of the combined databases was issued in late 1986 and was called the HITRAN database: 1986 edition. It was formed from merging the 1982 editions of the AFGL main gas compilation<sup>1</sup> and the trace gas compilations.<sup>2</sup> In merging these two compilations, much new data was added with the corresponding previous data being removed. All of these changes were described in an accompanying publication.<sup>3</sup> Originally the database contained the following molecular parameters for each quantum transition: (1) resonant wavenumber; (2) line intensity; (3) air-broadened halfwidth; and (4) lower state energy (as well as the unique quantum state identifications). New parameters have been added to this list to allow the database to be applicable to remote sensing in the atmosphere and capabilities to deal with non-local thermodynamic equilibrium effects in the upper atmosphere. The new parameters are: the transition probability, the self-broadened halfwidth, and the exponent of temperature dependence of the air-broadened halfwidth. Data fields have also been reserved for the pressure shift of the transition, accuracy criteria for the three principal parameters, and references to the sources of the latter parameters. The card

image concept (80 characters/transition) was abandoned and 100 characters/transition was adopted. In order not to exceed 100 characters, the isotope labels and vibrational state labels were indexed. Recalling of the information is accomplished via the program SELECT which is distributed with the database. This program is discussed later.

The creation of a new database gave us an opportunity to clean up many of the minor errors that were present on the 1982 versions. Many of these errors were not serious, e.g. many species had the quantum designations present in several formats, different symmetry labels were used for the same designations, etc. Some errors were more serious, parts of or the entire quantum field was missing, thus the data can not be associated with a specific transition. The reformatting allowed us to define six groups of rotational quantum number formats for the molecules and ensures that the 1986 version will have a single format for each species. The rotational formats are given in Table 1.

One of the new parameters being added is the transition probability,  $R_{if}$ , in Debyes squared. This parameter is independent of both temperature and isotopic abundance. The transition probability is related to the intensity of a transition,  $S_{if}$ , from state  $i$  to state  $f$  by

$$S_{if}(T) = \frac{8\pi^3}{3hc} \nu_{if}^3 \left[ 1 - \exp(-c_2 \nu_{if}/T) \right] \frac{g_i I_a}{Q(T)} \cdot \exp(-c_2 E_i/T) R_{if} \cdot 10^{-36} \quad (1)$$

Here  $\nu_{if}$  is the resonant frequency of the line in wavenumbers,  $E_i$  is the lower state energy of the transition,  $g_i$  is the nuclear spin degeneracy of the lower level,  $Q(T)$  is the total internal partition sum,  $I_a$  is the natural isotopic abundance, and  $c_2$  is the second radiation constant ( $hc/k$ ). The transition probability on the database was obtained by removing all terms on the right hand side of eq. (1)

Group 1: Asymmetric Rotors,

H<sub>2</sub>O, O<sub>3</sub>, SO<sub>2</sub>, NO<sub>2</sub>, HNO<sub>3</sub>, H<sub>2</sub>CO, HOCl, H<sub>2</sub>O<sub>2</sub>, H<sub>2</sub>S

J', K<sub>a</sub>', K<sub>c</sub>', F', Sym'; J'', K<sub>a</sub>'', K<sub>c</sub>'', F'', Sym"  
 I2, I2, I2, I2, A1; I2, I2, I2, I2, A1

Group 2: Diatomic and Linear Molecules with Integer J

CO<sub>2</sub>, N<sub>2</sub>O, CO, HF, HCl, HBr, HI, OCS, N<sub>2</sub>, HCN, C<sub>2</sub>H<sub>2</sub>

\_\_\_\_ Br, F', \_\_\_\_; \_\_\_\_ Br, J'', Sym"  
 5X, A1, I2, 1X; 4X, A1, I3, A1

Group 3: Spherical Rotors

Methane (CH<sub>4</sub> only, not CH<sub>3</sub>D)

J', R', C', N', Sym'; J'', R'', C'', N'', Sym"  
 I2, I2, A2, I2, A1; I2, I2, A2, I2, A1

Group 4: Symmetric Rotors

CH<sub>3</sub>D, NH<sub>3</sub>, CH<sub>3</sub>Cl, C<sub>2</sub>H<sub>6</sub><sup>\*</sup>, PH<sub>3</sub>

J', K', C', \_\_\_\_, Sym'; J'', K'', C'', \_\_\_\_, Sym"  
 I2, I2, A2, 2X, A1; I2, I2, A2, 2X, A1

Group 5: Triplet Ground Electronic States

O<sub>2</sub>

\_\_\_\_ Br, F'', \_\_\_\_; Br, N'', Br, J'', \_\_\_\_, Sym"  
 3X, A1, F4.1, 1X; A1, I2, A1, I2, 2X, A1

Group 6: Doublet Ground Electronic States (Half Integer J)

NO, OH, ClO

\_\_\_\_ Br, F'', \_\_\_\_; \_\_\_\_ Br, J'', Sym"  
 5X, A1, I2, 1X; 3X, A1, F4.1, A1

Notes: Prime and double primes refer to upper and lower states respectively; Br is the P-, Q-, or R- branch symbol; J is the rotational quantum number; Sym is e or f for l-type doubling, + or - for symmetry, etc. (for further explanation see references).

\* presently using group 2 quantum notation on the tape.

Table 1. Format of Rotational Quantum Numbers

(except  $Q(T)$ ) out of  $S_{if}$ . (The partition sums were not all known at the time of producing this version.) The data for the line strength, resonant frequency, and lower state energy come off the database. The reference temperature of the database is 296 K. The isotopic abundances used, now supplied as part of the third file distributed with the database, are given in Table 2. The nuclear spin degeneracy factor,  $g_i$ , depends on the particular isotope symmetry. These were calculated for each isotopic variant on the database.

When there are equivalent nuclei in a molecule, i.e. identical isotopes of the same element which have exactly the same molecular environment, the nuclear spin statistics will affect the populations of the molecular states and hence the transition intensities.

Consider first two equivalent nuclei. The molecule has a two-fold axis of symmetry, and coordinates of the two equivalent nuclei may be interchanged by a  $180^\circ$  rotation about this symmetry axis, or by combinations of inversion and  $180^\circ$  rotations about various axes. If the nuclei obey Bose-Einstein (integer spin) statistics, an interchange of both the position and spin coordinates must leave the wave function unchanged; if they obey Fermi-Dirac (half-integer spin) statistics, the wave function must change sign. It can be shown<sup>4</sup> that the total number of symmetric spin functions possible (hence the weight) is

$$n_{\text{sym}} = g_s = (2I + 1) (I + 1) \quad (2a)$$

and of antisymmetric spin functions possible is

$$n_{\text{antisym}} = g_a = (2I + 1) (I). \quad (2b)$$

A molecular rotation of  $180^\circ$  about the symmetry axis and an exchange of spin coordinates of the two equivalent nuclei amounts to an exchange of all coordinates of these two nuclei. Hence if Bose-Einstein statistics apply to the two nuclei, the symmetric spin

Relative Natural Abundance of Molecular Species on Database

Molecule	AFGL isotope code	relative natural abundance	Molecule	AFGL isotope code	relative natural abundance
H2O	161	0.9973	HNO3	146	0.9891
	181	0.0020			
	171	0.0004	OH	61	0.9975
	162	0.0003		81	0.0020
				62	0.00015
CO2	626	0.9842	HF	19	0.99985
	636	0.0110			
	628	0.0039	HCl	15	0.7576
	627	0.0008		17	0.2423
	638	0.000044			
	637	0.000009	HBr	19	0.5068
	828	0.0000040		11	0.4930
	728	0.000002			
O3	666	0.9928	HI	17	0.99985
	668	0.0040			
	686	0.0020	ClO	56	0.7559
				76	0.2417
N2O	446	0.9904	OCS	622	0.937
	436	0.0036		624	0.0416
	546	0.0036		632	0.0105
	448	0.0020		822	0.0019
	447	0.0004			
CO	26	0.9865	H2CO	126	0.9862
	36	0.011		136	0.0111
	28	0.0020		128	0.0020
	27	0.0004			
CH4	211	0.9883	HOCl	165	0.7558
	311	0.0111		167	0.2417
	212	0.00059	N2	44	0.9928
O2	66	0.9952	HCN	124	0.9852
	68	0.0040		134	0.0111
	67	0.0008		125	0.0036
NO	46	0.9940	CH3Cl	215	0.7490
	56	0.0036		217	0.2395
	48	0.0020			
SO2	626	0.9454	H2O2	1661	0.9949
	646	0.0420	C2H2	1221	0.9776
NO2	646	0.9916		1231	0.0219
NH3	4111	0.9960	C2H6	1221	0.9776
	5111	0.0036	PH3	1111	0.99955

Table 2

functions must be used with rotational functions which are symmetric with respect to a rotation around the symmetry axis, the antisymmetric spin functions with antisymmetric rotational functions. The opposite is the case for Fermi-Dirac statistics. The ratio of the number of spin states or the statistical weights of the levels which are symmetric to those which are antisymmetric with respect to a  $180^\circ$  rotation about the symmetry axis is,

$$\begin{aligned} \text{For Bose-Einstein statistics: } & \frac{I+1}{I} \\ \text{For Fermi-Dirac statistics: } & \frac{I}{I+1}. \end{aligned} \quad (3)$$

The line strength for molecules with two equivalent atoms contains the nuclear spin statistical weight factor from eq. (2).

If there are more than one pair of equivalent nuclei in a molecule the symmetry properties of each pair may be taken into account. An example is  $\text{CH}_2\text{Cl}_2$ . If we let the spins of the two different types of nuclei be  $I_1$ , and  $I_2$  we have

$$n_{\text{sym}} = (2I_1 + 1)(2I_2 + 1)(2I_1I_2 + I_1 + I_2 + 1) \quad (4a)$$

and

$$n_{\text{anti}} = (2I_1 + 1)(2I_2 + 1)(2I_1I_2 + I_1 + I_2). \quad (4b)$$

In general, for a molecule with  $n$  pairs of identical nuclei, the number of symmetric spin functions which can be formed is

$$n_{\text{sym}} = \left[ \prod_{i=1}^n (2I_i + 1) \right] \left[ \prod_{i=1}^n (2I_i + 1) + 1 \right] \quad (5a)$$

and the number of antisymmetric functions is



$$n_{\text{anti}} = \frac{1}{2} \left[ \prod_{i=1}^n (2I_i + 1) \right] \left[ \prod_{i=1}^n (2I_i + 1) - 1 \right] \quad (5b)$$

If the molecule has a two-fold axis of symmetry and the  $n$  pairs of nuclei are interchanged by a  $180^\circ$  rotation around this axis, the ratio of intensities of rotational levels of odd and even  $K$  is given by eq. (5).

The cases described above, i.e.  $180^\circ$  rotations, apply to linear and asymmetric-top molecules. Next we consider symmetric top molecules which may have three or four equivalent nuclei in a molecule. For molecules with three equivalent nuclei, the levels with  $K$  a multiple of three always have greater weight. The statistical weights for these levels are given in Table 3. Similarly for symmetric top molecules with four identical nuclei equidistant around the axis, the statistical weights are in Table 4.

The nuclear statistical weights for species present on the atlas can now be given.

**H<sub>2</sub>O** This is an asymmetric rotor with two identical nuclei for the species 161, 171, and 181. From eq. (2) we have

$$n_{\text{sym}} = g_s = (2I+1)(I+1); \quad n_{\text{anti}} = g_a = (2I+1)(I).$$

For hydrogen  $I = 1/2$ , which gives  $g_s = 1$  and  $g_a = 3$  where the even-(odd)ness is determined by the even or odd-ness of  $K_a + K_c + v_3$ . For HDO there are no equivalent nuclei, thus  $g_s = g_a = 1$ .

**CO<sub>2</sub>** There are eight isotopic species in the atlas for CO<sub>2</sub>. Of these, only three have a pair of identical nuclei, 626, 636, and 828. All other species do not have interchangeable nuclei and  $g_a = g_s = 1$ . For the species which have nuclear

Table 3. Statistical Weights for Symmetric Tops with Three  
Identical Nuclei

State	Statistical Weight
K a multiple of 3, but not 0	$\frac{1}{3} (2I + 1)(4I^2 + 4I + 3)$
K not a multiple of 3	$\frac{1}{3} (2I + 1)(4I^2 + 4I)$

Table 4. Statistical Weights for Symmetric Tops with Four Identical Nuclei

$K = 0$

$(I+1)(2I+1)(2I^2+I+1)$	for $K$ a multiple of four	Bose-Einstein statistics <u>or</u>
	$K$ even, for $K$ <u>not</u> a multiple of four	Fermi-Dirac statistics
$I(2I+1)(2I^2+3I+2)$	for $K$ a multiple of four	Fermi-Dirac statistics
	$K$ even, $K$ <u>not</u> a multiple of four	Bose-Einstein statistics
$I(I+1)(2I+1)^2$	$K$ odd	

$K = 0$

Bose-Einstein Statistics		Fermi-Dirac	
$1/2 (I+1)(2I+1)(2I^2+3I+2)$	$J$ even	$1/2 I (2I+1)(2I^2+I+1)$	$J$ even
$1/2 I (I+1)(2I-1)2I+1)$	$J$ odd	$1/2 I (I+1)(2I+1)(2I+3)$	$J$ odd

weights, we note both  $^{16}\text{O}$  and  $^{18}\text{O}$  have  $I = 0$  so all three species have the same nuclear statistical weights, namely

$$g_s = (2(0)+1)(0+1) = 1 \text{ and } g_a = (2(0)+1)(0) = 0.$$

All  $\text{CO}_2$  lines on the database have  $g_i = 1$ .

$\text{O}_3$  The 668 species has no interchangeable nuclei thus  $g = 1$ , the other two species have  $^{16}\text{O}$  as the equivalent nuclei related by a  $180^\circ$  rotation hence from eq. (2)  $g_s = 1$  and  $g_a = 0$ . For ozone all lines present on the atlas have  $g_i = 1$ .

$\text{N}_2\text{O}$  This molecule has the structure,  $\text{NNO}$ , and there are no nuclei that are equivalent. There are many molecules on the atlas that are similar to this and are listed below. Note for all isotopes of these species there are no nuclear statistical weight factors to consider for coupling with rotational wave functions:  $g_i = 1$  for

$\text{N}_2\text{O}$ ,  $\text{CO}$ ,  $\text{NO}$ ,  $\text{OH}$ ,  $\text{HF}$ ,  $\text{HCl}$ ,  $\text{HI}$ ,  $\text{HBr}$ ,  $\text{OCS}$ ,  $\text{HOCl}$ , and  $\text{HCN}$ .

$\text{CH}_4$  Methane is a symmetric top molecule with four equivalent nuclei for the atlas species 211 and 311. The nuclear statistical weights can be obtained from Table 4 or can be related to the labels used to describe the state, A, E or F. This gives the following association for  $g_i$ : for A species  $g_i = 5$ , for E species  $g_i = 2$  and for F species  $g_i = 3$ .

The deuterated species,  $\text{CH}_3\text{D}$ , has three equivalent nuclei which gives from Table 3 with  $I = 1/2$

$$g_i = 4 \text{ for } K \text{ a multiple of } 3$$

$$g_i = 2 \text{ K } \underline{\text{not}} \text{ a multiple of three (includes 0)}$$

- O<sub>2</sub> Here the two oxygen atoms are equivalent for the 66 species which gives  $g_s = 1$  and  $g_a = 0$ , and not equivalent for the 67 and 68 species so  $g_i = 1$ .
- SO<sub>2</sub> The two species present on the atlas 626 and 646 have equivalent <sup>16</sup>O nuclei hence  $g_s = 1$  and  $g_a = 0$ .
- NO<sub>2</sub> The 646 species is the only one present on the atlas and has  $g_s = 1$  and  $g_a = 0$ .
- NH<sub>3</sub> Ammonia is a symmetric top with three equivalent H atoms for both species on the atlas. From Table 3 we find
- K a multiple of three but not 0  $g = 4$
- K not a multiple of three (including 0)  $g = 2$
- HNO<sub>3</sub> The structure of nitric acid is such that there are no equivalent <sup>16</sup>O nuclei. This implies that  $g_i = 1$ .
- H<sub>2</sub>CO All three species on the atlas contain a pair of equivalent hydrogen nuclei. We have for levels with  $K_a + K_c + v_3$  even  $g_s = 1$  and with  $K_a + K_c + v_3$  odd  $g_a = 3$ .
- N<sub>2</sub> The nitrogen atoms are symmetric by 180° rotation,  $I(^{14}\text{N}) = 1$  so
- $g_s = (2(1) + 1)(1 + 1) = 6$
- and
- $g_a = (2(1) + 1)(1) = 3$ .
- CH<sub>3</sub>Cl Both species on the atlas have three identical hydrogen nuclei, thus we have

$g = 4$  when  $K$  is a multiple of three but not 0 and

$g = 2$  when  $K$  is not a multiple of three, including 0.

$H_2O_2$  In this cis-conformation a rotation through  $180^\circ$  exchanges both the oxygens and hydrogens. In the trans-conformation inversion through the center of gravity of the molecule does the same. The nuclear statistics are given by eq. (4) where  $I_1 = 1/2$  and  $I_2 = 0$ . The even-oddness is determined by  $K_a + K_c + v_3$  for the state

$g_s$  or even  $= 3$  and  $g_a$  or odd  $= 1$ .

$C_2H_2$  Acetylene when rotated  $180^\circ$ , exchanges the carbon and hydrogen atoms so again we use equation (4) where  $I_1 = 1/2$  and  $I_2 = 0$  to give  $g_s = 3$  and  $g_a = 1$ .

$C_2H_6$  The structure of the molecule,  $H_3C - CH_3$ , is such that a rotation along the internuclear axis by  $120^\circ$  or  $240^\circ$  leaves the molecule unchanged. Thus the hydrogen atoms at either end are equivalent. This gives  $g = 4$  when  $K$  is a multiple of 3 and  $g = 2$  when  $K$  is zero or not a multiple of three.

$PH_3$  This has three identical nuclei with spin  $1/2$  thus  $g = 4$  when  $K$  is a multiple of three and  $g = 2$  when  $K$  is zero or not a multiple of three.

The other new parameter added to the database is the temperature dependence of the air-broadened halfwidth. This is called the temperature exponent because it appears as an exponent of the temperature ratio. This becomes clear once the formulation is considered. The halfwidth can be considered as a function of density or pressure, i.e.

$$\gamma \text{ proportional to } \rho \text{ v } \sigma \text{ (density)} \quad (6a)$$

or

$\gamma$  proportional to  $p \propto \sigma$  (pressure). (6b)

In the first case the halfwidth has the units  $\text{cm}^{-1}/\text{atm}$  or  $\text{MHz}/\text{torr}$ , the second being  $\text{cm}^{-1}$  or  $\text{MHz}$ . Formula (6a) leads to the following temperature dependence (assuming the optical cross-section,  $\sigma$ , is temperature independent)

$$\frac{\gamma(T_1)}{\gamma(T_2)} = \left( \frac{T_1}{T_2} \right)^{-1/2} \quad (7)$$

To remove the negative sign of the exponent this is often rewritten as

$$\frac{\gamma(T_1)}{\gamma(T_2)} = \left( \frac{T_2}{T_1} \right)^{1/2} \quad (7a)$$

When the temperature dependence of the optical cross-section is added (assuming the form  $\sigma(T) = \sigma_0 T^m$ ) the resulting formula is

$$\frac{\gamma(T_1)}{\gamma(T_2)} = \left( \frac{T_2}{T_1} \right)^n \quad (8)$$

Working in the other formulation (eq. 6b) gives ( $\sigma$  temperature independent)

$$\frac{\tilde{\gamma}(T_1)}{\tilde{\gamma}(T_2)} = \left( \frac{T_1}{T_2} \right)^{1/2} \quad (9)$$

The tilde above  $\gamma$  is to indicate the pressure dependent halfwidth in  $\text{cm}^{-1}$  or  $\text{MHz}$  units. The confusion arises in the similarity between eqs. (9) and (7a) in the exponents. Only on closer inspection does one find the temperatures are inverted. When the temperature dependence of  $\sigma$  is added to eq. (9) we write the exponent as  $m$  and note that  $m = n + 1$ . The formulation most often used is eq. (7a) with

the halfwidths given in (frequency per unit pressure) units. Here we use equation (8) to describe the temperature dependence so we need not worry about the negative sign. With this in mind we now review the temperature exponents to be used on the atlas.

Table 5 lists the temperature exponents used on the database. We compare our values with those found on the GEISA atlas.<sup>5</sup> The values used on the database are from references 6-20. For water, GEISA states a value of  $n = 0.65$  for pure rotation from the work of Bauer et al<sup>6</sup> and  $n = 0.5$  for all other bands from the work of Davies and Oli.<sup>7</sup> In reference 6 we found that the average value of  $n = 0.65$  was for self-broadening of H<sub>2</sub>O from ATC and QFT calculations cited in the references. Bauer's experimental measurements for self-broadening given  $n = 1.17 \pm 0.06$ . For air-broadening Bauer reports "the size of the errors is such that the temperature dependence cannot be determined" and no value is given. The reference of  $n = 0.5$  from Davies and Oli is merely a statement of the classical value of  $n$  (i.e. the assumption of a temperature independent optical cross-section). Thus both reported values are not correct.

In the Davies and Oli paper, four transitions were studied for temperature dependence, three pure rotation and one  $\nu_2$  line. The average exponent for N<sub>2</sub>-broadening of the pure rotation lines was  $n = 0.64$ , and the value for the  $\nu_2$  line was  $n = 0.45$ . We have discussed the results with Dr. Richard W. Davies and feel that the value for the  $6\ 4\ 2 \rightarrow 7\ 5\ 3\ \nu_2$  transition ( $n = 0.45$ ) represents more how the temperature exponent can vary from line to line rather than being indicative of the average value. Until further calculations are made it is suggested the value  $n = 0.64$  be used for all water lines.

The compilation will have several other temperature exponents that do not agree with the GEISA values. This arises from recent measurements not yet added to the GEISA database.



Molecule	HWHM		n	
	min.	max.	min.	max.
H <sub>2</sub> O	0.0061	0.1046	--	0.64 --
CO <sub>2</sub>	0.0559	0.0899	0.75	0.79
O <sub>3</sub>	0.045	0.077	--	0.76 --
N <sub>2</sub> O	0.0686	0.0974	0.64	0.82
CO	0.047	0.088	--	0.69 --
CH <sub>4</sub>	0.0445	0.0920	0.63	1.00
O <sub>2</sub>	0.032	0.062	--	0.5 ---
NO	0.043	0.063	--	0.5 ---
SO <sub>2</sub>	0.110	0.152	--	0.5 ---
NO <sub>2</sub>	0.062	0.073	--	0.5 ---
NH <sub>3</sub>	0.043	0.090	--	0.5 ---
HNO <sub>3</sub>	-- 0.13	--	--	0.5 ---
OH	-- 0.083	--	--	0.5 ---
HF	0.020	0.126	--	0.5 ---
HCl	0.0135	0.0953	0.20	0.88
HBr	0.015	0.123	--	0.5 ---
HI	0.008	0.100	--	0.5 ---
ClO	-- 0.085	--	--	0.5 ---
OCS	-- 0.07	--	--	0.5 ---
H <sub>2</sub> CO	0.107	0.108	--	0.5 ---
HOCl	-- 0.06	--	--	0.5 ---
N <sub>2</sub>	-- 0.06	--	--	0.5 ---
HCN	0.0819	0.1566	--	0.5 ---
CH <sub>3</sub> Cl	-- 0.08	--	--	0.5 ---
H <sub>2</sub> O <sub>2</sub>	-- 0.10	--	--	0.5 ---
C <sub>2</sub> H <sub>2</sub>	0.0400	0.1158	--	0.75 --
C <sub>2</sub> H <sub>6</sub>	-- 0.10	--	--	0.5 ---
PH <sub>3</sub>	-- 0.075	--	--	0.5 ---

Table 6. Range of Air-Broadened Halfwidths and Temperature Dependences

For ozone the recent work of Gamache<sup>15</sup> gives a value of  $n = 0.76$  for air-broadening temperature dependence. For CO, there are several references; the work of Bouanich et al.<sup>16</sup> giving  $N = 0.75$  and  $n = 0.77$  for the temperature ranges 200 - 300 K and 93 - 300 K. The work of Hartmann et al.<sup>17</sup> giving  $n_{N_2} = 0.69 \pm 0.02$  and that of Connor and Radford<sup>18</sup> giving  $n_{air} = 0.74 \pm 0.10$ . We have decided to use the value reported by Hartmann et al. for the temperature exponent,  $n = 0.69$ .

For NO<sub>2</sub>, measurements by Devi et al.<sup>19-20</sup> for ten transitions give an average value of  $n = 0.97$ . This will be used for all NO<sub>2</sub> lines.

With the new parameters defined, we reformatted the two atlases and merged them into one database. This procedure employed the use of many programs to check for the consistency of the data, proper formats, etc. From the many checks, we are reasonably confident the database is free from format errors. Because of the new structure of the database and the additional parameters, the 1986 version is distributed with a user friendly program that will extract information from the database and generate files of several specific forms. The intent was to ease the change to the new form for users conditioned to the old format. The program, called SELECT, uses help screens in the interactive mode to prompt the user for specifics. Any incorrect or inconsistent data entries are sensed and the question reissued to the user. The program considers up to ten choices of molecule, isotope, vibrational band, and intensity level in a specified frequency range. From the selection, output can be generated in several specific forms.

The new file structure of HITRAN is shown in Figure 1. A complete description of the changes and improvements to HITRAN as well as sources of the data, band sums, etc. can be found in Table 3. Table 6 illustrates the actual image of the new database for individual quantum transitions for a small frequency range. The

# HITRAN

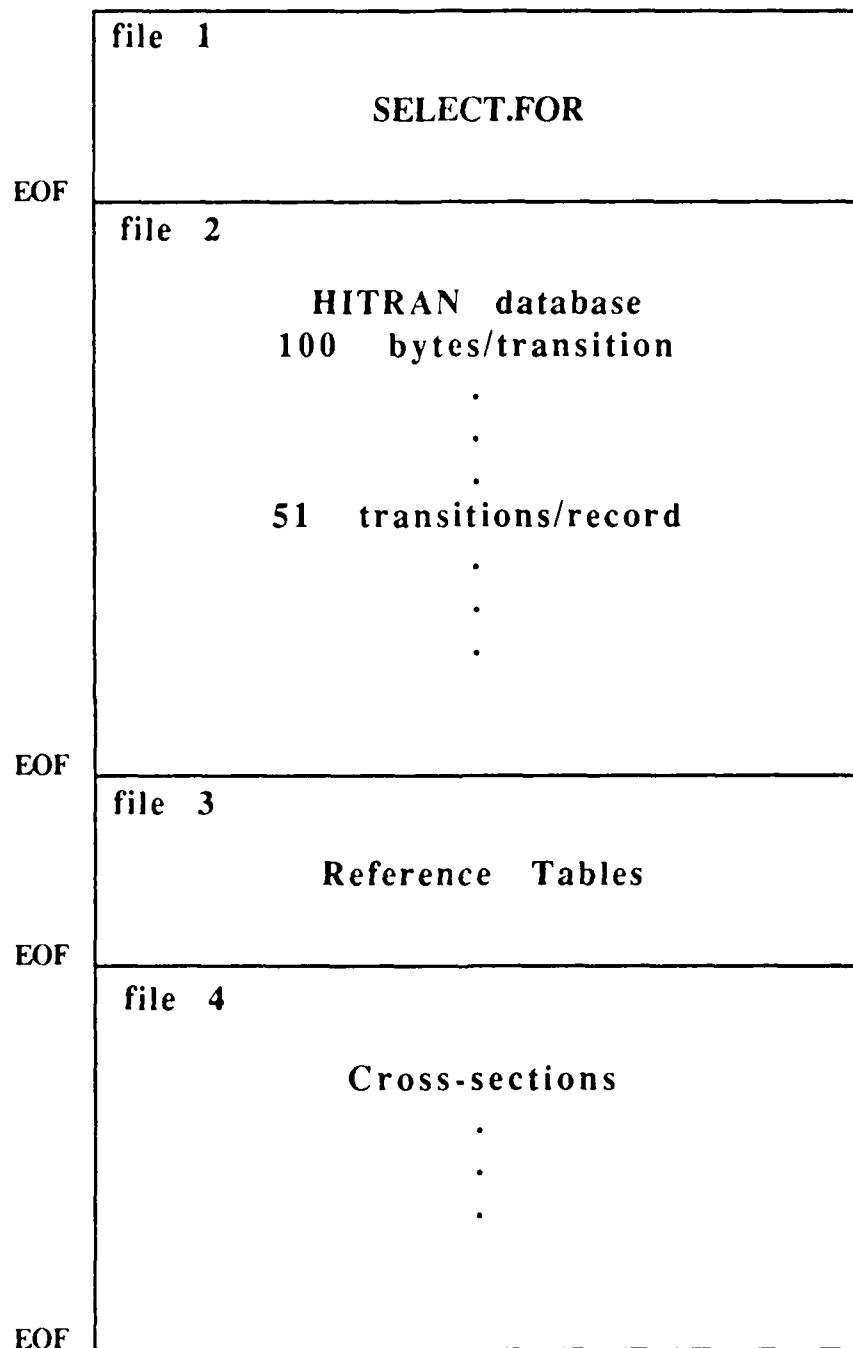


Figure 1. File Structure of HITRAN

iso	Frequency	Intensity													
Mo	$\nu$	S	R	$\gamma$	$\gamma_s$	E"	$\tau$	$\delta$ or $y$	$v'$	$v''$	Q'	Q"	IER	IRef	
31	800.276500	4.316E-25	3.777E-07	0599	0000	1162.00600	.76	0.00000	2	12418	6	2517	9	382	
281	800.287000	2.270E-23	4.717E-05	0750	0000	1483.94700	.50	0.00000	2	1177		18		381	
101	800.301900	4.680E-23	2.421E-07	0630	0000	105.93600	.50	0.00000	2	1844		9		381	
31	800.304700	1.286E-24	1.131E-05	0618	0000	1636.93510	.76	0.00000	2	1599		15		381	
31	800.322500	1.243E-23	1.274E-06	0610	0000	720.65800	.76	0.00000	2	11615	1	1714		381	
101	800.322700	1.840E-22	2.195E-06	0630	0000	277.86000	.50	0.00000	2	126224		25		381	
23	800.326900	5.380E-26	2.668E-05	0793	.1103	1326.41920	.75	0.00000	8	3				381	
271	800.332030	1.100E-22	3.212E-02	1000	0000	2354.24000	.50	0.00000	19	14				381	
101	800.361600	1.910E-22	2.278E-06	0630	0000	277.80700	.50	0.00000	2	126224		25		381	
31	800.379600	6.830E-24	6.554E-0	0602	0000	707.21200	.76	0.00000	2	11615	1	1714		381	
101	800.416400	5.300E-23	1.025E-01	0630	0000	851.01800	.50	0.00000	2	14				381	
101	800.416750	1.330E-22	2.035E-02	1000	0000	2321.36110	.50	0.00000	19	14				381	
31	800.434100	4.723E-25	2.225E-05	0618	0100	1982.04700	.76	0.00000	3	2517		45		381	
22	800.444000	6.390E-26	1.396E-04	0623	.0746	1844.81850	.75	0.00000	8	3				381	
101	800.447000	5.180E-23	1.002E-05	0630	0000	851.04100	.50	0.00000	2	141244		24		381	
21	800.451200	3.210E-26	1.731E-05	0661	.0872	2481.56150	.75	0.00000	14	6				381	

FORMAT (I2,I1,F12.6,1P2E10.3,OP2F5.4,F10.4,F4.2,F8.5,I13,2A9,3I1,3I2)  
 - 100 characters per transition

This format corresponds as follows:

Mo - I2 - Molecule number  
 iso- I1 - Isotope number (1- most abundant, 2- second, etc.)  
 $\nu$  - F12.6 - Frequency in  $\text{cm}^{-1}$   
 S - E10.3 - Intensity in  $\text{cm}^{-1}/(\text{molec} \cdot \text{cm}^{-2})$  @ 296K  
 R - E10.3 - Transition probability in Debyes<sup>2</sup> (presently lacking internal partition sum)  
 $\gamma$  - F5.4 - Air-broadened halfwidth (HWHM) in  $\text{cm}^{-1}/\text{atm}$  @ 296K  
 $\gamma_s$  - F5.4 - Self-broadened halfwidth (HWHM) in  $\text{cm}^{-1}/\text{atm}$  @ 296K  
 E" - F10.4 - Lower state energy in  $\text{cm}^{-1}$   
 n - F4.2 - Coefficient of temperature dependence of air-broadened halfwidth  
 y - F8.5 - Shift of transition due to pressure (presently empty; some coupling coefficients inserted)  
 $v'$  - I3 - Upper state global quanta index  
 $v''$  - I3 - Lower state global quanta index  
 Q' - A9 - Upper state local quanta  
 Q" - A9 - Lower state local quanta  
 IER- 3I1 - Accuracy indices for frequency\*, intensity, and halfwidth  
 IRef-3I2 - Indices for lookup of references for frequency, intensity, and halfwidth (not presently used)

\*IER code for frequency when used:

IER	estimated error in wavenumber
0	$\geq 1$
1	$\geq 0.1$ and $< 1.0$
2	$\geq 0.01$ and $< 0.1$
3	$\geq 0.001$ and $< 0.01$
4	$\geq 0.0001$ and $< 0.001$
5	$\geq 0.00001$ and $< 0.0001$
6	$< 0.00001$

Table 6. Example of Direct Image of Lines on the 1986 HITRAN Database

first file on the distribution magnetic tape is the program SELECT discussed above. The file is in a "card" image form, i.e. 80 characters per record and is followed by an end-of-file marker. The program is written in FORTRAN 77, follows all ANSI standards and should run on all systems that have FORTRAN compilers.

The second file on the distribution tape is the database. There are 5100 characters per record for this file followed by an end-of-file marker.

The third file on the tape is presently a table of the isotopic abundances of the species on the database, a copy of this table is given in Table 2. In the future, this file will also contain reference tables, partition sums and information of this nature. This file contains 80 characters per record and ends with an end-of-file marker.

The fourth and last file on the tape is for heavy trace constituents of the atmosphere that have dense spectra comprised of many thousands of lines. In the last file are absorption cross-sections for these species to be used in simulation codes such as FASCODE.<sup>21</sup> The data is from the experimental work of Massie et al.<sup>22</sup> The structure of the file is as follows, a 100 character header card containing the species name, the number of cross-sections, the start and end frequency, and the experimental conditions used to record the data comes first. Next the absorption cross-sections are given in 10E10.3 format per line and the first entry corresponds to the start frequency and for each following entry one must add the frequency interval defined by

$$\Delta f = \frac{(\text{end frequency} - \text{start frequency})}{\text{number of points for the species}}$$

This is repeated for each species given in Table 7. The file is blocked 5100 characters per physical tape record (same as the database) with the end-of-file marker at the end.

Table 7. Approximate Absorption Cross-Sections on File 4 of HITRAN Tape

Species	# Cross-Sections	Frequency $\text{cm}^{-1}$	
		Minimum	Maximum
ClONO <sub>2</sub>	5020	765.0020	819.9980
HNO <sub>4</sub>	5476	770.0070	829.9990
F <sub>2</sub> I	5020	785.0000	839.9950
CCl <sub>4</sub>	1826	786.0010	805.9980
F <sub>1</sub> I	2738	830.0090	859.9990
F <sub>1</sub> I <sub>2</sub>	7301	860.0080	939.9960
F <sub>1</sub> I <sub>4</sub>	12320	1025.0090	1159.9920
F <sub>2</sub> I	4563	1050.0040	1099.9920
F <sub>1</sub> I	3651	1060.0040	1099.9980
F <sub>1</sub> I <sub>2</sub>	10039	1070.0050	1179.9940
F <sub>1</sub> I <sub>3</sub>	12777	1090.0080	1229.9980
F <sub>1</sub> I <sub>4</sub>	11771	1160.0250	1288.9920
N <sub>2</sub> O <sub>5</sub>	4647	1225.0010	1265.0000
HNO <sub>3</sub>	7301	1270.0040	1349.9930
ClONO <sub>2</sub>	3650	1270.007	1309.9910
CF <sub>4</sub>	1095	1275.0030	1286.9900
N <sub>2</sub> O <sub>5</sub>	11616	1680.0030	1780.0000

To aid us in keeping track of all the updates, additions and changes that were to be done, an agenda system was created. The system was based on the dBASE III database language and set up for an IBM-PC environment. The agenda system allowed us to list, track, modify and add update information. Each record pertains to a proposed update from a single source. The structure of the records is given in Table 8.

Several dBASEIII programs have been written to make the database Agenda easier to use. The first is a custom menu editing program. When the command "DO CUMENU" is entered in dBASEIII the screen shown in Figure 2 appears. To modify existing records a 2 is entered and the screen shown in Figure 3 is displayed. The fields of the Agenda are shown in reverse video. Changes are made by typing in the corrections, moving through the various fields is accomplished by the numeric keypad arrows. Addition of a new record (enter 1) gives a screen similar to Figure 3 with no information in the reverse video area. The information is entered, followed by a carriage return or when the field is full the cursor automatically moves to the next field to be entered. The use of a custom screen greatly simplifies the maintenance of the agenda.

The other feature we have added for the agenda is a print program. By entering the command "DO LISTMOL" the following prompt is seen:

ENTER WHICH MOLECULE TO LIST

TYPE 'ALL' TO GET ENTIRE LIST

MOLECULE =

by typing ALL the entire data base is listed three records per page. To get all records pertaining to a particular molecule enter the chemical symbol, e.g. for water enter H<sub>2</sub>O, peroxide H<sub>2</sub>O<sub>2</sub>, etc. A second program, LISTMOL2, creates a file called AGENDA.LST which

Table 8. Structure for Database: AGENDA.dbf

Number of data records: 80

Date of last update: 12/02/85

<u>Field</u>	<u>Field Name</u>	<u>Type</u>	<u>Width</u>	<u>Description of Field</u>
1	MOLECULE	Character	6	Molecule chemical symbol
2	ISOTOPE	Character	8	Isotope, AFGL code
3	FREQUENCY	Character	1	is Frequency to be used, Y or N
4	STRENGTH	Character	1	is Strength to be used, Y or N
5	HW_AIR	Character	1	is air-broadened halfwidth to be used, Y or N
6	HW_SELF	Character	1	is self-broadened halfwidth to be used, Y or N
7	ENERGY	Character	1	is lower state energy to be used, Y or N
8	TDEP_HW	Character	1	is temperature exponent of halfwidth to be used, Y or N
9	SHIFT	Character	1	is shift to be used, Y or N
10	SOURCE	Character	240	Source of data
11	VIBRATION	Character	30	Particular vibrational band
12	VLOWER	Numeric	5	Lowest frequency in range
13	VUPPER	Numeric	5	Highest frequency in range
14	USE	Character	1	Will it be used, Y or N
15	LOCATION	Character	80	Location of data file
16	FILENAME	Character	40	Name of permanent file
17	STATUS	Character	240	Description of the state the data is in
18	COMPLETION	Date	8	Date data is added to atlas
Total			671	



EXIT AGENDA

DO YOU WISH TO

1. ADD A RECORD
2. MODIFY EXISTING RECORD
3. QUIT

ENTER YOUR CHOICE AND PRESS ENTER

Press any key to continue . . .

Figure 2. Custom Editor Menu

ENTER MOLECULE CO2  
ENTER ISOTOPE 11111111

COMPLETION 11/30/85

FREQUENCY	y	STRENGTH	y
HW-AIR	y	HW-SELF	n
ENERGY	y	TDEP-HW	n
SHIFT	n	USE	y
VLOWER	400	VUPPER	9500
VIBRATION	All bands		
LOCATION	File on VAX		
FILE NAME	CO2:CO2LINES.DAT		
SOURCE	Rothman, Global analysis		

STATUS           Needs to have 03301-00001 data from Rinsland added;  
                  needs to have perturbed bands added. Needs to have  
                  self-broadened halfwidth and temp-dependence added.

TO EXIT PRESS PgDn KEY

Figure 3. Screen for Editing Records

can be transferred to the Cyber or Vax systems to be printed by the laser printers. The form is three records followed by a page eject.

We now have an automated means of keeping track of changes (past, present, and future) made to the database.

## 2.0 TEMPERATURE DEPENDENCE OF THE HALFWIDTH

It became apparent during the literature search that the temperature exponents for the halfwidths are not well understood. The values used on the GEISA atlas and many of the HITRAN values come from studies of only a few transitions. We undertook the task of evaluating the temperature dependence of the halfwidths for two asymmetric rotors, H<sub>2</sub>O and O<sub>3</sub>. In our studies we looked at both the vibrational and rotational structure of this parameter.

### 2.1 Temperature Dependence of Ozone Halfwidths

The temperature dependence of N<sub>2</sub>-broadened halfwidths of ozone was studied over a temperature range of 200-500K. We assumed the optical cross-section to vary as a temperature independent part times temperature to a power  $m$  ( $\sigma(T) = \sigma_0 \cdot T^m$ ). This relates the halfwidth at temperature  $T$  to the value at a reference temperature  $T_0$  as

$$\gamma(T) = \gamma(T_0) \left\{ \frac{T_0}{T} \right\}^n \quad (10)$$

The exponent  $n$  was determined by calculating the halfwidth for 126 ro-vibrational transitions of ozone at seven temperatures. The halfwidths were calculated using quantum-Fourier-transform theory with improved dynamics (QFT-ID).<sup>23</sup> The transitions chosen considered a wide range of rotational quantum number,  $J''$  (1 to 35), the full manifold of  $Ka''$  for a particular  $J''$ , and transitions important to stratospheric studies. The vibrational states considered both A- and B-type transitions using constants for the ground state and  $v_3$

bands. All molecular constants were considered the best available at the time of the calculations.

For each transition studied linear regression was applied to the coordinates;  $\ln(T_2/T_1)$  and  $\ln(\gamma(T_1)/\gamma(T_2))$ , where  $T_2$ , the reference temperature was taken at 296K. From linear regression we obtain the slope  $n$ , i.e. the temperature exponent and the correlation coefficient of the fit. Figure 4 shows such a plot for the  $27\ 15\ 12 \leftarrow 27\ 13\ 15$  transition of ozone. For all the transitions studied, the correlation coefficients were equal to one to four significant figures confirming the assumed temperature of the optical cross-section, i.e.  $\sigma_0 \cdot T^m$ .

The results of the calculations give an average temperature exponent of  $n = 0.77$  for nitrogen-broadening. The temperature exponents are transition dependent but the fluctuation about the average value is small ( $\pm 6\%$ ). The value of  $n$  as a function of  $J''$ , and  $K_a''$  was investigated and the work was related to other work in the literature. A complete description can be found in reference 15 or Appendix B. This work lead to an average temperature exponent  $n = 0.76$  for air-broadening of ozone.

## 2.2 Temperature Dependence of Halfwidths of Water Vapor

We have performed calculations to study the temperature dependence of  $N_2$ -broadened halfwidths of  $H_2O$ . In the calculations we employed cutoff-free theory with improved dynamics and ATC interruption functions. Some 50 water vapor transitions were considered for the pure rotation and  $v_2$  bands. The transitions were supplied to us by Dr. Wesley Traub of the Harvard-Smithsonian Center for Astrophysics and represent some stratospherically important lines of water vapor. Nine temperatures were considered from 200 to 1000 K to allow the results to be

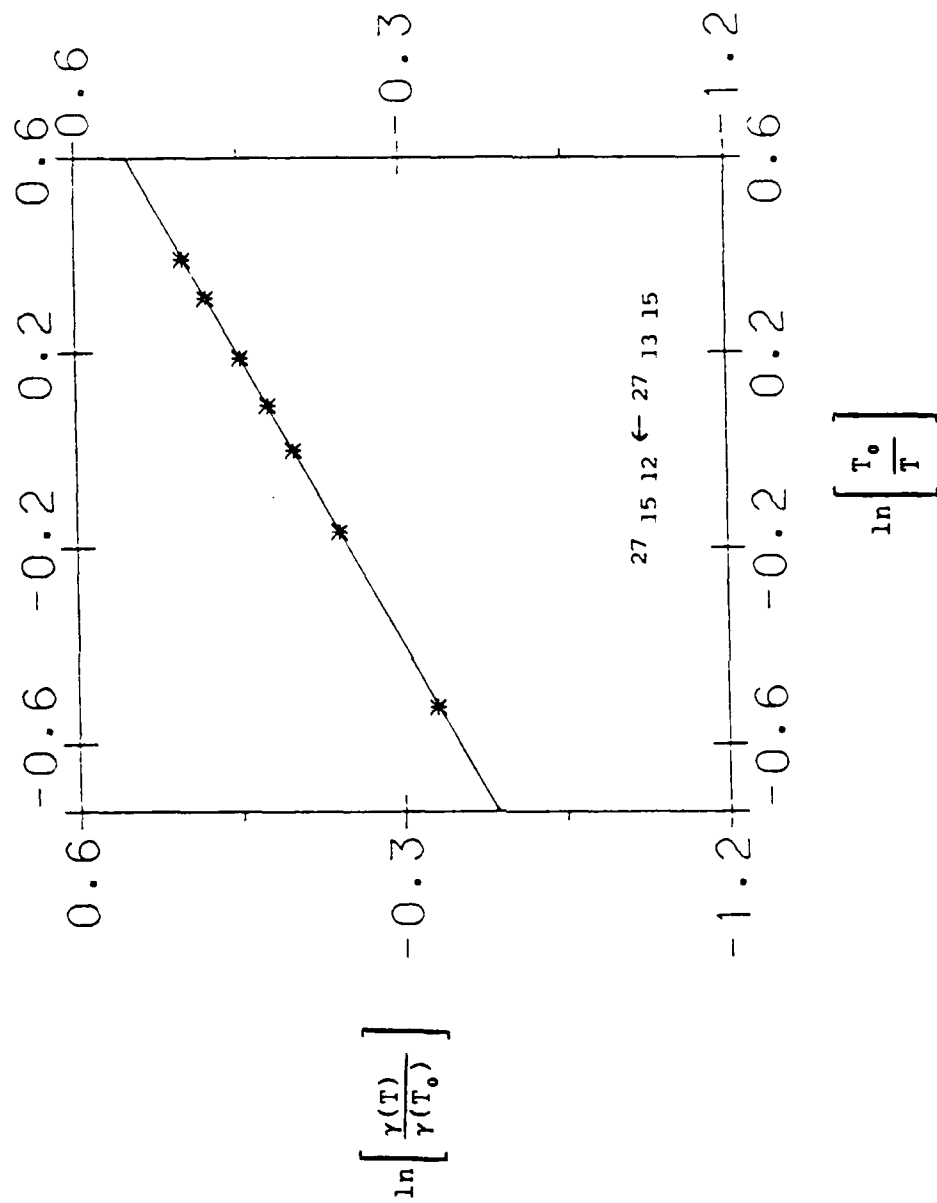


Figure 4.  $\ln(\gamma(T)/\gamma(T_0))$  vs.  $\ln(T_0)/T$  for the 27 15 12 ← 27 13 15 Transition of ozone,  $n = 0.76$

applicable to the stratosphere as well as hot sources. The calculations were done and the results are given in Table 9. One surprising fact was the similar results for the pure rotation and  $v_2$  bands. We had expected more of a dependence on the vibrational band. In general, the  $v_2$  results for  $n$  were lower than the pure rotation  $n$  values. However, there were some exceptions to this. The large variation in  $n$  with the rotational quantum numbers was also surprising. Average values were calculated for each band giving  $n$  (pure rotation) = 0.684 with a +15 to -28% variation about the average and  $n$  ( $v_2$ ) = 0.676 with a +24 to -10% fluctuation about the average. This can be compared with the value we calculated for the ozone-nitrogen system of  $n = 0.77$  with a  $\pm 6\%$  fluctuation. It is suggested that a value of  $n = 0.68$  be used for water vapor and, whenever possible, use a calculated value from Table 9. A complete description of the work is given in reference 24 or Appendix B.

Table 9. Temperature Exponents for H<sub>2</sub>O-N<sub>2</sub> System

Assuming the form,

$$\gamma(T) = \gamma(T_0) \left( \frac{T_0}{T} \right)^n.$$

J''	K <sub>a</sub> ''	Transition				Pure Rotation n	v <sub>2</sub> n
		K <sub>c</sub> ''	J'	K <sub>a</sub> '	K <sub>c</sub> '		
1	1	1	2	0	2	.7182	.7110
1	1	0	2	2	1	.7259	.7067
2	1	1	3	2	2	.7086	.7032
2	2	1	3	3	0	.6786	.6708
2	2	0	3	3	1	.6713	.6737
3	0	3	3	3	0	.7108	.7130
3	1	3	4	2	2	.7394	.7441
3	1	2	4	2	3	.7067	.7074
3	2	1	4	3	2	.6964	.6988
3	3	1	4	4	0	.6507	.6577
3	3	0	4	4	1	.6585	.6641
4	0	4	4	3	1	.7133	.7084
4	0	4	5	1	5	.6859	.6841
4	1	4	5	0	5	.6729	.6664
4	1	4	5	2	3	.7406	.7435
4	1	3	4	4	0	.7045	.7134
4	2	3	5	1	4	.7064	.6997
4	2	3	5	3	2	.7169	.7003
4	2	2	5	3	3	.7171	.7212
4	3	2	4	4	1	.6696	.6643
4	3	1	4	4	0	.6937	.6969
5	0	5	6	1	6	.6106	.6076
5	0	5	5	3	2	.7085	.6954
5	1	5	4	0	4	.6859	.6840
5	1	5	6	0	6	.5939	.5871
5	1	4	5	4	1	.7037	.7052
5	1	4	5	2	5	.7036	.7060
5	2	4	6	1	5	.6682	.6590
5	2	3	6	3	4	.7274	.7301
5	3	3	5	4	2	.6765	.6581



5	3	3	6	2	4	.7277	.7284
5	3	2	5	4	1	.7258	.7169
6	0	6	6	1	5	.6407	.6389
6	1	6	5	4	1	.6262	.6124
6	1	6	6	2	5	.5833	.5689
6	2	5	5	5	0	.6472	.6370
6	2	5	6	3	4	.6378	.6120
6	3	4	6	4	3	.6619	.6430
6	3	3	6	4	2	.7498	.7344
6	5	2	6	6	1	.7192	.7348
6	5	1	6	0	6	.6209	.6211
8	5	3	8	5	4	.6477	.6580
9	3	6	9	5	4	.7087	.6979
9	4	5	8	5	4	.7228	.7058
10	5	5	10	4	6	.7113	.6858
11	4	8	11	5	7	.5868	.5860
12	6	6	12	4	8	.6441	----
14	9	5	14	8	6	----	.5170

### 3.0 WATER VAPOR DATA IN THE VISIBLE SPECTRAL REGION

We have taken the data for water vapor in the visible region of the spectrum from Camy-Peyret et al.<sup>25-26</sup> The data consist of 4612 lines in the region  $13,435\text{ cm}^{-1}$  to  $22,597\text{ cm}^{-1}$ . This compares with 2932 water vapor lines presently on the database in this range. The data contains the bands listed in Table 10 and includes eleven bands that were not present on the 1982 atlas.

The intensities are reported in units of  $\text{cm}^{-2}\text{ atm}^{-1}$  at 300 K and were converted to the units used on the database,  $\text{cm}^{-1}/\text{molec}$   $\text{cm}^{-2}$  and to 296 K, the reference temperature of the database. This first is accomplished by dividing by Loschmidt's constant,  $N_L = (N_a/V_m) = 2.68675 \times 10^{19}\text{ cm}^{-3}\cdot\text{molec}$ , corrected to 300 K by the Ideal Gas Law, i.e.

$$N_L(300\text{K}) = N_L(273.15\text{K}) \cdot (273.15/300).$$

After which the temperature correction must be done.

The data file contains the wavenumber of the transition and the corresponding error, the measured intensity and estimated uncertainty, the vibrational and rotational quantum numbers, and the absorption at the line center in tenths of a percent. Many of the lines in the data do not contain the intensity and some are unassigned lines. The data file was split into lines with the measured intensity, 1319 lines, and the lines without a measured intensity, 3293 lines. The lines that have intensities can be put into the new format without difficulty. Those without intensities cannot be used without some estimation of the intensities for the lines. Fortunately the absorption at the line center is given and can be related to the intensity of the line.

Table 10. Vibrational Bands Present in the Water Vapor Data from  
Camy-Peyret et al.

Vibrational Bands

Bands present in 1982 Atlas	221, 301, 202, 042, 320, 141, 023
Bands New to the Database	331, 213, 312, 411, 501, 313, 303, 403, 402, 421, 412

For the lines with intensities, the intensity was converted to the AFGL units by division by Loschmidt's number at 300 K. The temperature correction of the intensity to 296 K was then done. The file was reformatted into the 1986 format and the halfwidths of Gamache and Davies<sup>27</sup> added to the lines. The error estimates for the data were added to the new format in the IER field. The values used for IER are listed in Table 11.

For lines that only have peak absorption values the intensities must be estimated by a model. A simple Lorentz model of the line shape was used to relate the peak absorption values to the line intensity.

Of the lines of data that have no measured intensities, 1842 of these have quantum assignments (this leaves 1451 unassigned lines). For all the lines the peak absorption at the center of the line is given. The intensities for these lines can be estimated from the peak absorption values for the lines that have measured intensities and a model that relates peak absorption to the measured intensity. The model of line absorption chosen for this was the Lorentz line shape. The absorption coefficient for the Lorentz line shape is given by

$$k_v = \frac{S}{\pi} \frac{\gamma}{(\nu - \nu_0)^2 + \gamma^2} \quad (11)$$

Where S is the integrated line intensity and

$\gamma$  is the Lorentz halfwidth and

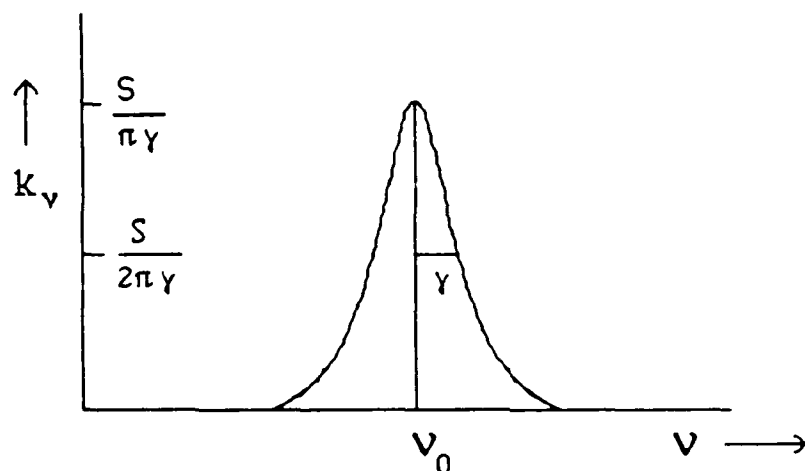
$\nu_0$  is the frequency at line center.

The Lorentz shape has the following form.

Table 11. IER Values for Wavenumber and Intensity

IER Value	Estimated Error in Wavenumber
0	$> .99999$
1	$\geq .1$ and $< .9$
2	$\geq .01$ and $< .1$
3	$\geq .001$ and $< .01$
4	$\geq .0001$ and $< .001$
5	$\geq .00001$ and $< .0001$
6	$< .00001$

IER Value	Estimated Error in Intensity
0	$< 1\%$
1	$1\% \text{ and } \leq 2.5\%$
2	$> 2.5\% \text{ and } \leq 5.0\%$
3	$> 5.0\% \text{ and } \leq 10.0\%$
4	$> 10.0\% \text{ and } \leq 15.0\%$
5	$> 15.0\% \text{ and } \leq 20.0\%$
6	$> 20.0\%$
7	Estimated Intensities



Peak absorption at the center of the line can be associated with  $S/\pi\gamma$ . From the 1319 lines of data that contain both  $S$  and peak absorption,  $P$ , at the line center, we can equate the two via a scale factor, i.e.

$$\frac{S}{\pi\gamma} = fP \quad (12)$$

In the calculations, the factors of  $\pi$  and  $\gamma$  have been absorbed into the scale factor so for each of the 1319 lines  $f = S/P$  is calculated for each line. Before the scaling was done the intensities were converted from  $\text{cm}^{-2} \text{ atm}^{-1}$  units to the units used by AFGL,  $\text{cm}^{-1}/\text{molec cm}^{-2}$ . The average value of the scale factor was calculated from the data giving  $f = 0.583 \times 10^{-25}$ . Multiplying the peak absorption of a line by  $f$  will give the estimated strength at 300 K in AFGL units. This was tested by recalculating the intensity for the 1319 lines using  $f$  and comparing these values with the measured strengths.

This approach did not work; the average error from the method was approximately 2000. The reason for this was that three lines had a scale factor of order  $10^{-22}$  to  $10^{-23}$ , whereas all the other lines were of order  $10^{-26}$ . Hence the average factor essentially came

from the three large factors. To correct for this the three troublesome lines were removed. Then the standard deviation of the scale factor was calculated and then a scale factor was calculated using only factors within  $\pm 1 \sigma$  of the first average. This gave (note three troublesome factors were removed)

# Lines	ave f	$\sigma$	# Lines within $1 \sigma$	ave f within $1 \sigma$
1316	$0.408 \times 10^{-26}$	$0.315 \times 10^{-26}$	1259	$0.356 \times 10^{-26}$

The new value,  $f = 0.356 \times 10^{-26}$  was then used to recalculate the strengths and compared with the experimental values for the 1319 measured lines (note three "troublesome" lines included here) the results were

$$\text{Average \% Dif} = -1.353$$

$$\text{Average Absolute \% Dif} = 16.912$$

These results suggest the model can supply the line intensities for the lines where only a peak value is given. The lines of data without a line intensity were taken and the intensity estimated via the model, i.e.  $S = fP$  with  $f = 0.356 \times 10^{-26}$ . This produced a line file (at 300 K) that can be incorporated into the AFGL database after rescaling to 296 K.

The simple Lorentz line shape model was discussed with Jean-Marie Flaud, University of Paris. He has suggested that a different model, based on the curve-of-growth (COG) method, be tried. In the COG model, the peak absorption is given by

$$P = A(\sigma_0) = 1 - e^{\left( -k_0^N \int_0^{\sigma_0} \sigma_0 \right)}, \quad (13)$$

which assumes a Voigt profile,

$$\phi_v(\sigma_0) = \frac{1}{\gamma_D} \left[ \frac{\log 2}{\pi} \right]^{1/2} k(0, \log 2)^{1/2} \frac{\gamma_L}{\gamma_D} \quad (14)$$

If one assumes that the variation of  $\phi_v(\sigma_0)$  is mainly due to the variation of  $\gamma_D$  which is proportional to  $\sigma_0$  one has

$$\phi_v(\sigma_0) = \frac{\alpha}{\sigma_0}, \quad \alpha \equiv \text{effective constant} \quad (15)$$

Thus equation 13 can be written as

$$P = 1 - e^{(-k_\sigma^N N / \alpha / \sigma_0)} \quad (16)$$

and with the definition  $\beta = N\alpha$  the following can be obtained

$$k_\sigma^N = - \frac{\sigma_0}{\beta} \ln(1-P). \quad (17)$$

From the values of line intensity and peak absorption, the constant  $\beta$  is evaluated after which the intensities can be estimated for lines that have only peak absorption values using the average  $\beta$  value. In the data set there are 1311 lines that have intensities and peak absorption values reported. The effective constant  $\beta$  has been evaluated for these lines. At the suggestion of Flaud, we have averaged  $\beta$  for the two regions 13500-16500  $\text{cm}^{-1}$  and 16500-23000  $\text{cm}^{-1}$  (see Table 12). An average over all lines was done and an average as a function of  $P$  for the ranges shown in Table 12. For peak absorption values greater than 150 the average  $\beta$  values are similar for both regions. For the values less than 150 there is considerable change for the lines greater than and less than 16500  $\text{cm}^{-1}$ , especially for the peak absorption lines between 75 and 150 in the upper wavenumber region.



Table 12. Average Values of the Effective Constant b

P	All Lines		Lines < 16500 cm-1		Lines > 16500 cm-1	
	# Lines	$\beta \times 10^9$	# Lines	$\beta \times 10^9$	# Lines	$\beta \times 10^9$
P<25	258	0.21	1	0.0014	257	0.21
25 $\geq$ P<75	337	0.21	115	0.18	222	0.22
75 $\geq$ P<150	242	0.20	162	0.19	80	0.26
150 $\geq$ P<400	249	0.21	198	0.22	51	0.22
400 $\geq$ P	225	0.22	211	0.23	14	0.21
All Lines	1311	0.2112	687	0.2072	624	0.2215

The data indicate a different average for the two regions and this was used in the generation of the intensities for the lines with peak absorption only. Before estimating these intensities, the intensities of the data with measured intensities was calculated via equation 17 with the average values of  $\beta$ ,  $\beta = 0.100715E9$  for region 1 and  $\beta = 0.22147E9$  for region 2. The average absolute percent error, AAPD, the average error, E, and the maximum error,  $E_{\max}$  were computed using the measured intensities for the 1311 lines. The results are the AAPD = 13.0%,  $E = -0.00073\%$  and  $E_{\max} = 845\%$ , this is compared with the results of the Lorentz model, AAPD = 17% and  $E = -1.4\%$  ( $E_{\max}$  was not calculated in this model). It appears that the curve of growth model gives better agreement with the experimental intensities than the Lorentz model does. Thus the visible spectrum of water vapor was recalculated via the COG model in the same manner that was done for the Lorentz model. Using the COG model the intensities were calculated for lines with only the peak absorption given. These lines were merged with the data containing both S and P values. The data, which is for 300 K, was then corrected for 296 K, the reference temperature of the database. A similar procedure was used on the data without quantum identifications (unassigned lines). This yields a file with intensities for all the lines reported by Camy-Peyret et al.<sup>25-26</sup>

The water vapor data for the visible region of the spectrum is almost complete. The final step is to correct the intensities of the saturated transitions, i.e. those that had peak absorptions greater than 500. Jean-Marie Flaud has sent a list of the improved intensities for these lines, see Table 13. To make the correction, the transitions were selected from the original water vapor data in Flaud's units of  $\text{cm}^{-2} \text{atm}^{-1}$ . The intensities were then corrected to the values in Table 13 and the file was then converted to AFGL units and format and then corrected from 300 K to 296 K. The final correction file is given in Table 14. The file was merged with the other lines for the visible region.

Table 13. Flaud's Notes for Lines with P &gt; 500

			cm <sup>-2</sup> atm <sup>-1</sup> at 300 K	
13628.8617	000 - 101	221	552 - 4.74-5	P
13628.9113	542 - 643	301	488 - 3.52-5	P
13631.9693	717 - 818	301	866 - 1.12-4	
13690.0014	542 - 541	221	511 - 3.63-5	
13695.0327	440 - 441	221	802 - 8.60-5	
13708.5954	551 - 550	301	857 - 1.05-4	B
	404 - 515	202		
13766.4625	551 - 550	221	792 - 8.09-5	P
13768.9036	524 - 523	301	642 - 5.56-5	
13768.9739	642 - 643	301	551 - 3.79-5	
13782.1900	441 - 440	301	800 - 8.39-5	P
13782.2523	440 - 441	301	995 - 2.44-4	
13893.1820	432 - 331	301	627 - 5.30-5	
13897.4973	312 - 211	301	992 - 2.54-4	
13914.8369			704 - 6.13-5	
13914.9602	413 - 312	301	655 - 6.13-4	
13915.0509	524 - 423	301	999 - 3.48-4	
13929.3493	707 - 606	301	889 - 1.23-4	P
13942.5475	909 - 808	301	512 - 3.90-5	B
	845 - 744	301		
13947.2608	624 - 523	301	983 - 2.19-4	
15205.2919	515 - 616	311	531 - 3.96-5	
15402.1988	313 - 212	311	592 - 4.97-5	
15437.8123	413 - 312	311	558 - 4.46-5	P
16888.2383	220 - 221	203	563 - 6.50-5	

P = perturbed

B = blended

13628.861700	0.198E-23	23.79400.0000	0	0	0	1	0	1	2	2	1	0	0	0	161
13628.911300	0.154E-23	756.72500.0000	5	4	2	6	4	3	3	0	1	0	0	0	161
13631.949300	0.490E-23	744.16300.0000	7	1	7	8	1	8	3	0	1	0	0	0	161
13690.001400	0.157E-23	610.34100.0000	5	4	2	5	4	1	2	2	1	0	0	0	161
13695.032700	0.371E-23	188.10800.0000	4	4	0	4	4	1	2	2	1	0	0	0	161
13708.595400	0.459E-23	742.07600.0000	5	5	1	5	5	0	3	0	1	0	0	0	161
13708.595400	0.447E-23	326.62500.0000	4	0	4	5	1	5	2	0	2	0	0	0	161
13766.462500	0.354E-23	742.07600.0000	5	5	1	5	5	0	2	2	1	0	0	0	161
13768.903600	0.238E-23	446.51100.0000	5	2	4	5	2	3	3	0	1	0	0	0	161
13768.973900	0.166E-23	756.72500.0000	6	4	2	6	4	3	3	0	1	0	0	0	161
13782.190000	0.361E-23	488.13400.0000	4	4	1	4	4	0	3	0	1	0	0	0	161
13782.252300	0.105E-22	488.13400.0000	4	4	0	4	4	1	3	0	1	0	0	0	161
13893.182000	0.226E-23	283.21900.0000	4	3	2	3	3	1	3	0	1	0	0	0	161
13897.497300	0.107E-22	95.17600.0000	3	1	2	2	1	1	3	0	1	0	0	0	161
13914.836900	0.256E-24	0.00000.0000	0	0	0	0	0	0	0	0	0	0	0	0	161
13914.960200	0.259E-22	173.36500.0000	4	1	3	3	1	2	3	0	1	0	0	0	161
13915.050900	0.148E-22	300.36200.0000	5	2	4	4	2	3	3	0	1	0	0	0	161
13929.349300	0.528E-23	446.69700.0000	7	0	7	6	0	6	3	0	1	0	0	0	161
13942.547500	0.170E-23	744.06400.0000	9	0	9	8	0	8	3	0	1	0	0	0	161
13942.547500	0.172E-23	927.74400.0000	8	4	5	7	4	4	3	0	1	0	0	0	161
13947.260800	0.940E-23	446.51100.0000	6	2	4	5	2	3	3	0	1	0	0	0	161
15205.291900	0.170E-23	447.25200.0000	5	1	5	6	1	6	3	1	1	0	0	0	161
15402.198800	0.208E-23	79.49600.0000	3	1	3	2	1	2	3	1	1	0	0	0	161
15437.812300	0.188E-23	173.36500.0000	4	1	3	3	1	2	3	1	1	0	0	0	161
16888.238300	0.274E-23	134.90200.0000	2	2	0	2	2	1	2	0	3	0	0	0	161

Table 14. Corrected H<sub>2</sub>C Lines for which F > 500

Before adding the data to the database and publishing the results we are going to study the data (e.g. FASCODE plots, etc.) and compare the results with other data for this region.

## 4.0 MISCELLANEOUS TASKS

Throughout the course of the contract there were many tasks that were performed in conjunction with other groups as well as preparing data for the next version of the database. These tasks are discussed below.

### 4.1 Ozone Data for Minor Isotopic Species

A file of lines for the less abundant isotopic species of ozone was put on the VAX computer. This file is to be added to the database to upgrade the information for these isotopes of ozone. Not present in the file (1982 parameters) is the halfwidths for the transitions. The file consists of 11235 lines of data from  $934\text{ cm}^{-1}$  to  $1167\text{ cm}^{-1}$ . The file was sent to the CYBER where halfwidths of Gamache and Rothman<sup>28</sup> were added using the CYBER's mass-storage facilities. The file was transferred back to the VAX where it was reformatted to the 1986 format and the additional parameters (e.g.  $n$ ,  $R^2$ , etc.) added. The file is now on the VAX as A86:OZONE\_ISO.DAT.

### 4.2 Ozone Halfwidths for the GEISA Atlas

A magnetic tape containing the ozone data that is present on the GEISA atlas was received from Nicole Husson. The tape contained two files, one containing the temperature exponent for the halfwidth and the other file has a GEISA date code in this field. Because we have the software readily available to add our ozone halfwidths<sup>28</sup> to the GEISA atlas, we offered to do this task for Dr. Husson. This will ensure that no mis-communication can occur and

that the GEISA halfwidths for ozone are correct and match the HITRAN results line-for-line, default halfwidths included.

The files were taken from the tape using the AFGL copany routine. The tape was labelled as follows

LABEL,TAPE1,VSN=M2764,CV=EB,LK=KU,D=PE,PO=R,F=L

and copany needed a file card to describe the 77 card images per physical record on the tape, i.e.

FILE,TAPE1,FL=80,RB=77,RT=F,BT=K.

By running copany twice we were able to extract each file and save them as direct access files. The ADDHWO3 program was modified to read the GEISA data and using the mass storage file of O<sub>3</sub> halfwidths, add them to the output file. The output files were checked to ensure the program ran as expected and the two files were then transferred to a magnetic tape in the form that they were sent to us. The tape was dumped and the results appeared correct. We then sent the tape to Dr. Husson for addition to the next version of the GEISA atlas.

#### 4.3 Halfwidth and Temperature Dependence of Halfwidths for

##### Database

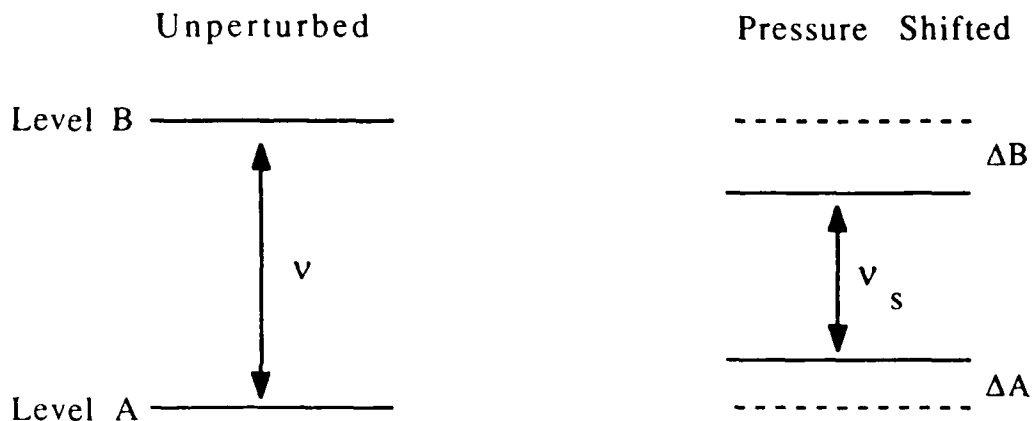
At suggestion of Linda Brown of JPL, we generated a table of the range of the halfwidths and temperature exponents of the halfwidth for each molecule on the database. To do this a program was written that read the unblocked database and stored the maximum and minimum values of  $\gamma$  and  $n$  for each molecule. After the program was run the output was taken and put into tabular form (see Table 5).

#### 4.4 Ozone Halfwidth and Shift Data Requested by Outside Groups

Dr. Mary Ann Smith of NASA Langley Research Center requested a listing of ozone shift values for lines in the region 1070  $\text{cm}^{-1}$  to 1140  $\text{cm}^{-1}$ . Using SELECT all ozone lines in this region were removed from the database. From this file only lines with  $J \leq 35$  were kept, since the shift calculations stopped at  $J = 35$ . The calculated shift values were recovered from backup tape and put on the CYBER and a program was written to add the corresponding shift to the lines of data based on the rotational quantum numbers (no vibrational dependence was considered). This only produced a small number of shift values for the ozone lines. The reason was that the calculation of the shift is specific to the initial and final state rotational quantum numbers. The listed shift values mostly had the quantum numbers reversed ( $f \rightarrow i$ ,  $i \rightarrow f$ ) from the lines Smith requested. The calculations of the shift, however, have the shift of the individual energy levels listed which allows the calculation of both  $\Delta v_{if}$  and  $\Delta v_{fi}$ . This is described below.

If one calculates the shift in the wavenumber for the transition from level A to B, the shift for the transition B to A can be calculated from the shifts in the individual levels A and B. This, of course, neglects vibrational dependence of the shift which may be important for many systems. To see this consider the following diagram,





In the unperturbed case, the wavenumber of the transition is given by

$$v(\text{cm}^{-1}) = E_B(\text{cm}^{-1}) - E_A(\text{cm}^{-1}). \quad (18)$$

When the levels are pressure shifted the wavenumber is

$$\begin{aligned} v_s(\text{cm}^{-1}) &= (E_B + \Delta B) - (E_A + \Delta A) \\ &= E_B - E_A + (\Delta B - \Delta A) \\ &= v + (\Delta B - \Delta A). \end{aligned} \quad (19)$$

The line shift is given by  $\Delta v = (\Delta B - \Delta A)$ . When the reverse transition  $B \rightarrow A$  occurs the shift is  $\Delta v = (\Delta A - \Delta B)$ . Because of the sign of the shift of the individual levels,  $\Delta v(A \rightarrow B)$  does not necessarily equal  $-\Delta v(B \rightarrow A)$ . For the cases when  $\Delta A$  and  $\Delta B$  have the same sign  $\Delta v(A \rightarrow B) = -\Delta v(B \rightarrow A)$ , when one level shifts up and the other down,  $\Delta v(A \rightarrow B) \neq -\Delta v(B \rightarrow A)$ . In these cases the shift for the reverse transitions must be calculated from the shifts of the energy levels. These shifts were calculated in the QFT-ID calculations for  $\text{O}_3$ ; thus the reverse transitions can be calculated.

The shifts for the reverse transitions were calculated and put into a file with the rotational quantum numbers, the halfwidth

and shift. The shift data was then added to the file of ozone lines. This supplied data for all the lines in the listing. The data was then sent to Dr. Smith for comparison with experimentally determined shifts for ozone lines.

The same experiment has yielded ozone halfwidths and, in a preprint, Smith stated that for  $v_1$  lines our calculations are a fairly constant 6% lower than the experimental values. For the few  $v_3$  lines that she has measured the calculations average about 3% lower than experiment. The reason for the improvement for the  $v_3$  lines is that the calculations were done for A- and B-type transitions and the vibrational constants used were from the  $v_3$  and pure rotation bands. Hence the calculated halfwidths for  $v_3$  transitions contain the vibrational dependence explicitly whereas the  $v_1$  halfwidths were calculated using ground state constants only.

Drs. Ira Nolt and Mian Abbas requested ozone halfwidths for some twenty transitions. The halfwidth data is to be used for retrieval experiments. The data were for lines in the  $40\text{ cm}^{-1}$  to  $70\text{ cm}^{-1}$  region of the spectrum. The data is listed in Table 15 and was sent to Dr. Abbas at Drexel University.

#### 4.5 Halfwidths for Water Vapor for HOT Gas Atlas

Dr. John Selby of Grumman Corp. sent a magnetic tape of transitions for water vapor which are to make up the AFGL HOT gas atlas. The data on the tape are for the reference temperature 1000 K. Selby requested that data be added to the tape, namely the air-broadened halfwidths and the temperature dependence of the halfwidths. The programs to accomplish this task reside on the CYBER computer and make use of mass storage files. The tape was loaded on to the CYBER. This was attempted by two different methods; first the CYBER COPANY routine was used and while reading

Table 15. Ozone Halfwidths sent to Dr. M. Abbas

Rotational Quantum Numbers						Halfwidths cm <sup>-1</sup> /atm
7	7	1	6	6	0	.0677
11	7	5	10	6	4	.0691
9	9	1	8	8	0	.0677
19	8	12	18	7	11	.0685
10	6	4	9	5	5	.0688
12	7	5	11	6	6	.0690
13	10	4	12	9	3	.0690
13	12	2	12	11	1	.0669
17	6	12	16	5	11	.0682
17	7	11	16	6	10	.0684
18	6	12	17	5	13	.0682
18	7	11	17	6	12	.0683
20	7	13	19	6	14	.0682
20	6	14	19	5	15	.0682
21	6	16	20	5	15	.0683
27	5	23	26	4	22	.0696

the tape a parity error was encountered. Next a BUFFER IN program was used and again a parity error was encountered while the tape was being read. I then took the tape to the AFGL VAX computer and accomplished copying the tape into a file without any problems.

The VAX file SELBY.H2O, 18072 lines of data, was transferred to the CYBER via the hyperchannel. The program to add the halfwidths along with the five halfwidth files that are input to it were put on the CYBER from backup tapes. The halfwidths were added to the file (note the file is already in the 1986 format) and the temperature exponent  $n = 0.64$  was added to all the lines. The file was hyperchanneled back to the VAX as SELBYHW.H2O. The file was visually inspected along with the output from the CYBER addition of halfwidths and it appears to be correct. The file was written to a magnetic tape and sent back to Selby.

#### 4.6 CO<sub>2</sub> Data from L. Rosenmann

Laurence Rosenmann from Ecole Centrale des Arts et Manufactures sent a Macintosh diskette containing halfwidths and temperature exponents for CO<sub>2</sub> broadened by CO<sub>2</sub>, H<sub>2</sub>O, N<sub>2</sub>, and O<sub>2</sub>. The file was written in the MacWrite application. The file was loaded into a Macintosh SE and the MacWrite file was converted to text form. The file was then transferred to the AFGL VAX computer and given the name ROSENMANN. This was accomplished by using KERMIT in the SE's communications program. Afterwards the VAX file, ROSENMANN, was edited to remove blank lines that were created in the transfer. This data will be considered for the next version of the database.

#### 4.7 Updates to the Program SELECT

There have been several changes to the program SELECT since the version 1 distribution. In particular we have tested in-house several different schemes to make the program faster. They are based on eliminating as many of the code conversions as possible. Input to the program has been made easier and the program can be run in the interactive mode to generate a data file for the batch mode. This work is aimed at making the use of the database as simple as possible.

Other changes were made that deal with problems associated with a growing database. Several times the array space had to be increased due to the addition of new vibrational bands. Because the look up procedure relies on these numbers, each time the array AVIB is increased all the positioning keys need to be changed. After doing this a few times, we added 25 extra locations for the vibrational bands to each molecule. This allows us to add new vibrational bands without having to change all the positioning keys.

## 5.0 PARTITION SUMS FOR THE DATABASE SPECIES

The total internal partition sum,  $Q(T)$ , is needed to extract the transition probability,  $R_{if}$ , from the line strength,  $S_{if}$  (see equation 1). It is also used for converting line strengths from one temperature to another. During this contract we started a program to calculate accurate partition sums for the species on the database and to consider the temperature dependence of  $Q(T)$ . Furthermore, the temperature dependence was represented by an analytical form allowing fast and accurate calculations of  $Q(T)$  without interpolation. We set a criterion of computing  $Q(T)$  to better than 1% and fitting  $Q(T)$  vs.  $T$  to better than 1%. For the molecules considered this has been accomplished.

The total internal partition sum is given by

$$Q(T) = \sum_i g_i \cdot e^{-\epsilon_i/kT} \quad , \quad (20)$$

where the sum is over all states  $i$  of the molecule,  $g_i$  is the degeneracy of the level  $i$  and includes only the nuclear spin degeneracies and degeneracies not arising from  $K$  or  $M$ ,  $k$  is the Boltzmann constant,  $\epsilon_i$  is the ro-vibrational energy of the level  $i$ , and  $T$  is the temperature in Kelvin. We have evaluated equation 20 by direct summation over the states  $i$ . We have studied the cutoff in  $i$  with respect to the accuracy of the partition sum. What is needed to evaluate  $Q(T)$  is the energy levels of the system,  $\epsilon_i$ , and the correct degeneracy factor,  $g_i$ .

The degeneracy factor is composed of several parts. There is the space degeneracy factor  $(2J+1)$  times the total nuclear degeneracy factor of each state. This nuclear factor is given by the

nuclear spin weight of each level which is different for symmetric and nonsymmetric nuclei. For the symmetric nuclei, the nuclear and rotational wavefunctions couple to give a nuclear spin degeneracy factor (these were discussed in section 1.0). These are for example the 3:1 ratio for odd:even states of  $H_2$  or  $H_2O$ . The non-symmetrical nuclei give rise to a nuclear spin factor  $g_n = \prod (2I_i + 1)$ , where  $I$  is the spin of each nucleus in question. In general one has  $(2I_1 + 1) \cdot (2I_2 + 1) \cdot (2I_3 + 1) \dots$ , one term for each unsymmetrical nuclei. This factor is usually omitted because in most applications it cancels. This arises because for most applications a ratio of partition sums is used and the unsymmetrical term is independent of the particular state. In our early test calculations we did not include the unsymmetrical nuclear spin terms. Once we were confident with our calculations, however, all terms were included explicitly. The expression for the partition sum contains the non-symmetric factor outside of the summation and the space degeneracy and nuclear-rotational wavefunction coupling degeneracy inside,

$$Q(T) = g_n \sum_i (2J_i + 1) g_i \cdot e^{-\epsilon_i / kT} \quad (21)$$

For applications where the factor  $g_n$  is needed, it is important that the term used in the calculation is the one used. Table 16 gives the non-symmetrical nuclei contributions for each species on the database that we have considered so far.

With all the statistics at hand, only the energy levels of the systems are needed to complete the calculations. The energy levels that are needed can be obtained from the database. Care was exercised to extract all levels but only for unique quantum states of the molecules. To obtain accurate sums no duplications of levels can occur. The approach was to study the band sums for the possible lower vibrational states of each molecule to be considered. For each of the vibrational states, the energy level corresponding to each

Table 16. Nuclear Spin Degeneracy Factors for  
Non-Symmetrical Nuclei.

Molecule	AFGL Isotope Code	$g_j = \prod (2I_j + 1)$
H <sub>2</sub> O	161	1
	181	1
	171	6
	162	6
CO <sub>2</sub>	626	1
	636	2
	628	1
	627	6
	638	2
	637	12
	828	1
	728	6
O <sub>3</sub>	666	1
	668	1
	686	1
N <sub>2</sub> O	446	9
	456	6
	546	6
	448	9
	447	54
CO	26	1
	36	2
	28	1
	27	6
CH <sub>4</sub>	211	1
	311	2
	212	3
NO <sub>2</sub>	646	3



unique rotational state is taken and written to a file for that molecule. Because of the structure of the database, this created two groups, one for the molecules that have the rotational quantum numbers in QLOCLO, e.g.  $\text{H}_2\text{O}$ ,  $\text{HNO}_3$ , etc., and the other for molecules that have branch information and quantum numbers in QLOCLO, e.g.  $\text{CO}_2$ ,  $\text{OH}$ , etc. The problem is further complicated by the presence of hyperfine structure for some of the molecules. Thus rotational groups 1, 3, and 4 on the database (Table 1) store quantum numbers so QLOCLO values can be compared and stored since they uniquely define the state. For group 2 molecules (branch information and integer  $J''$ )  $J''$  and  $F''$  were extracted and written to a character string and these variables were compared and saved since they are unique. For group 5 (oxygen molecule) we stored  $J''$ ,  $N''$ , and  $F''$  in the character string and for group 6  $RJ''$  and  $F''$  were stored and similar comparisons done. A single program was written to perform this task and run on the database. This generated files of rotational state information and lower state energies for each vibrational state of each isotopic species of each molecule. The files were printed and a copy delivered to L. Rothman. These files revealed some format inconsistencies that will be addressed on the next version of the database. This resulted in energy levels to use to compute the partition sums. Preliminary calculations were done for  $\text{H}_2\text{O}$  and  $\text{CO}_2$  at 300K and compared with published values. At 300K for  $^{12}\text{C}^{16}\text{O}_2$  we found  $Q = 291.1136$  compared with the value of Gray and Young<sup>29</sup> of 291.0471. For  $\text{H}_2^{16}\text{O}$ , we found  $Q(300) = 154.0377$  compared with the JPL catalogue<sup>30</sup> value of 178.115. After discussions with H. Pickett of JPL, we agreed our value was the more correct one.

We next considered what cutoff in energy was required to produce the partition sum accurate to better than 1%. This was studied by plotting the computed  $Q(T)$  vs.  $T$  for  $\text{H}_2\text{O}$  and  $\text{CO}_2$  at several temperatures and seeing if the partition sum has converged. Figures 5-16 are plots for the main isotopic species of  $\text{H}_2\text{O}$  (Figures

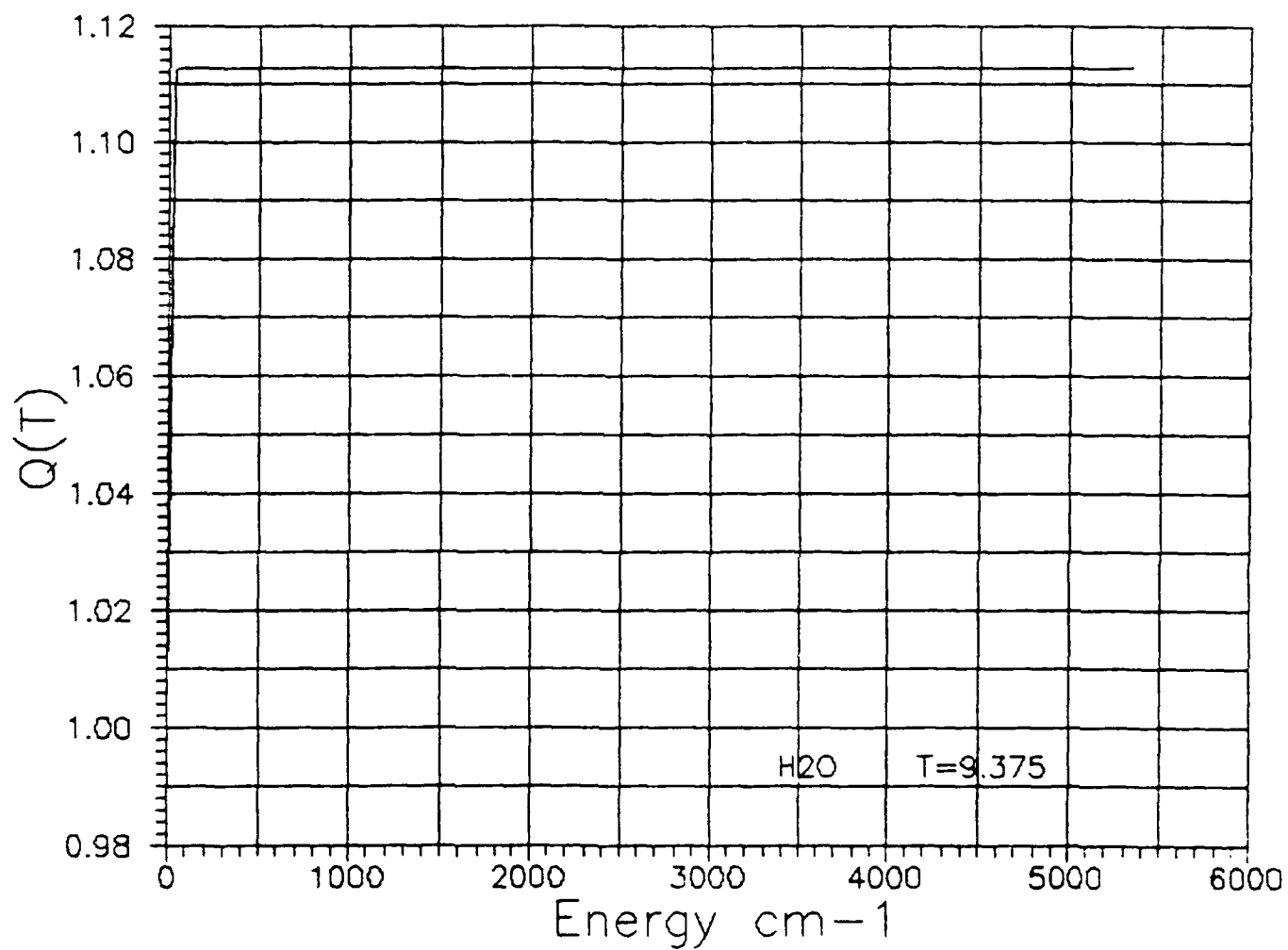


Figure 5. Total Partition Function vs. Energy for  $\text{H}_2\text{O}$  and  $\text{CO}_2$  at Various Temperatures  $\text{H}_2\text{O}$  at 9.375 K (Principal Isotope)

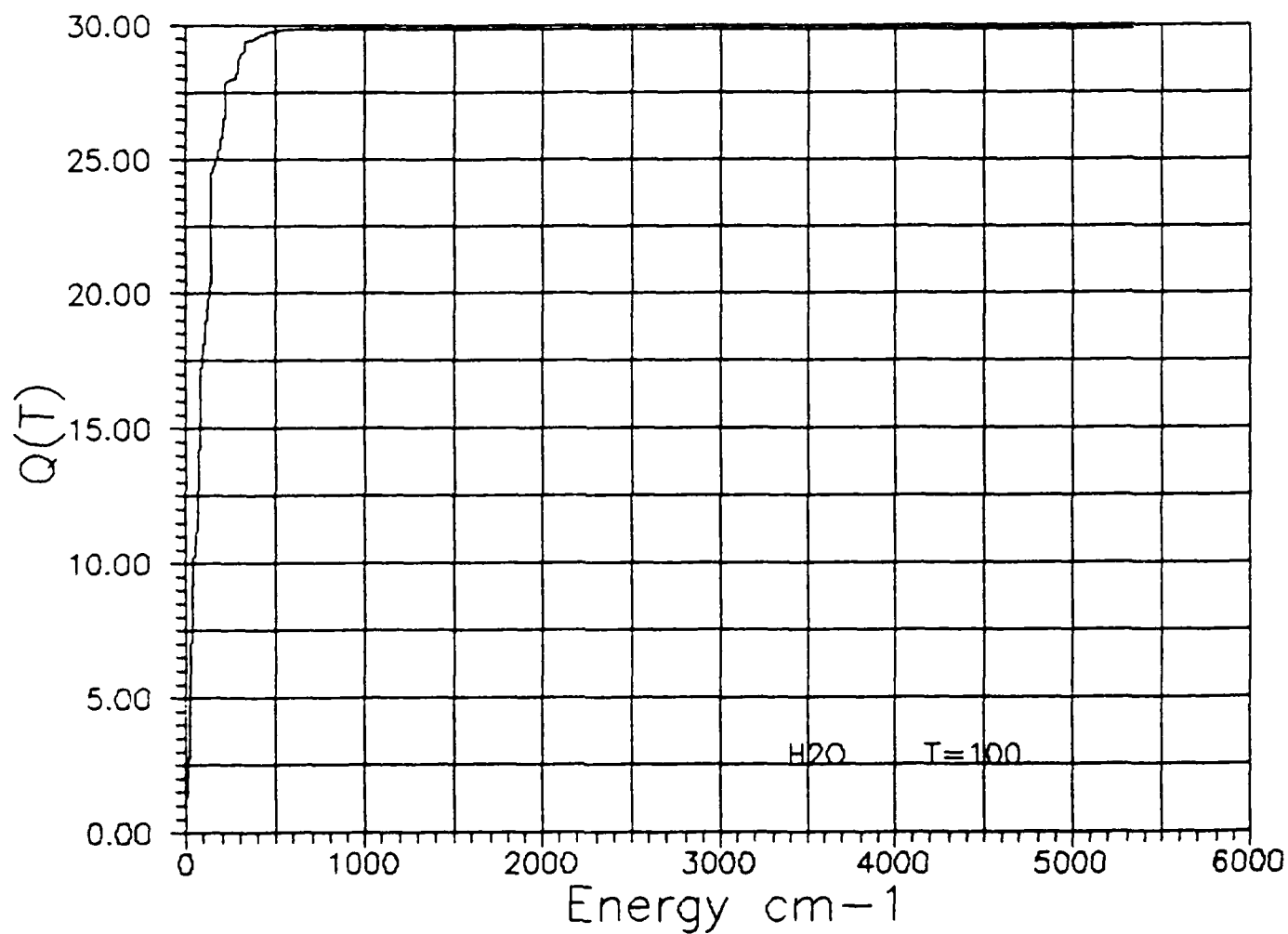


Figure 6. Total Partition Function vs. Energy for  $\text{H}_2\text{O}$  and  $\text{CO}_2$  at Various Temperatures  $\text{H}_2\text{O}$  at 100 K (Principal Isotope)

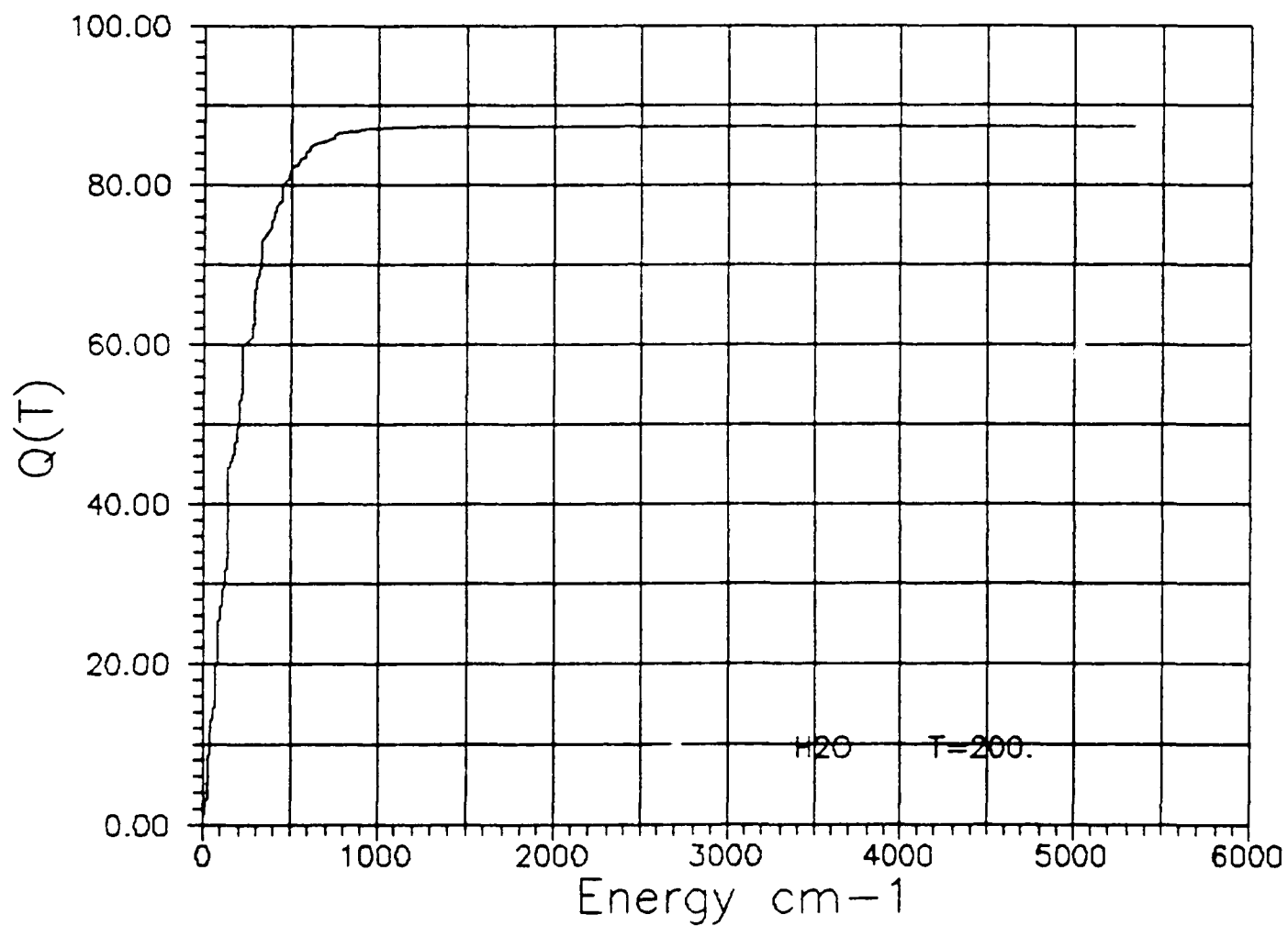


Figure 7. Total Partition Function vs. Energy for  $\text{H}_2\text{O}$  and  $\text{CO}_2$  at Various Temperatures  $\text{H}_2\text{O}$  at 200 K (Principal Isotope)

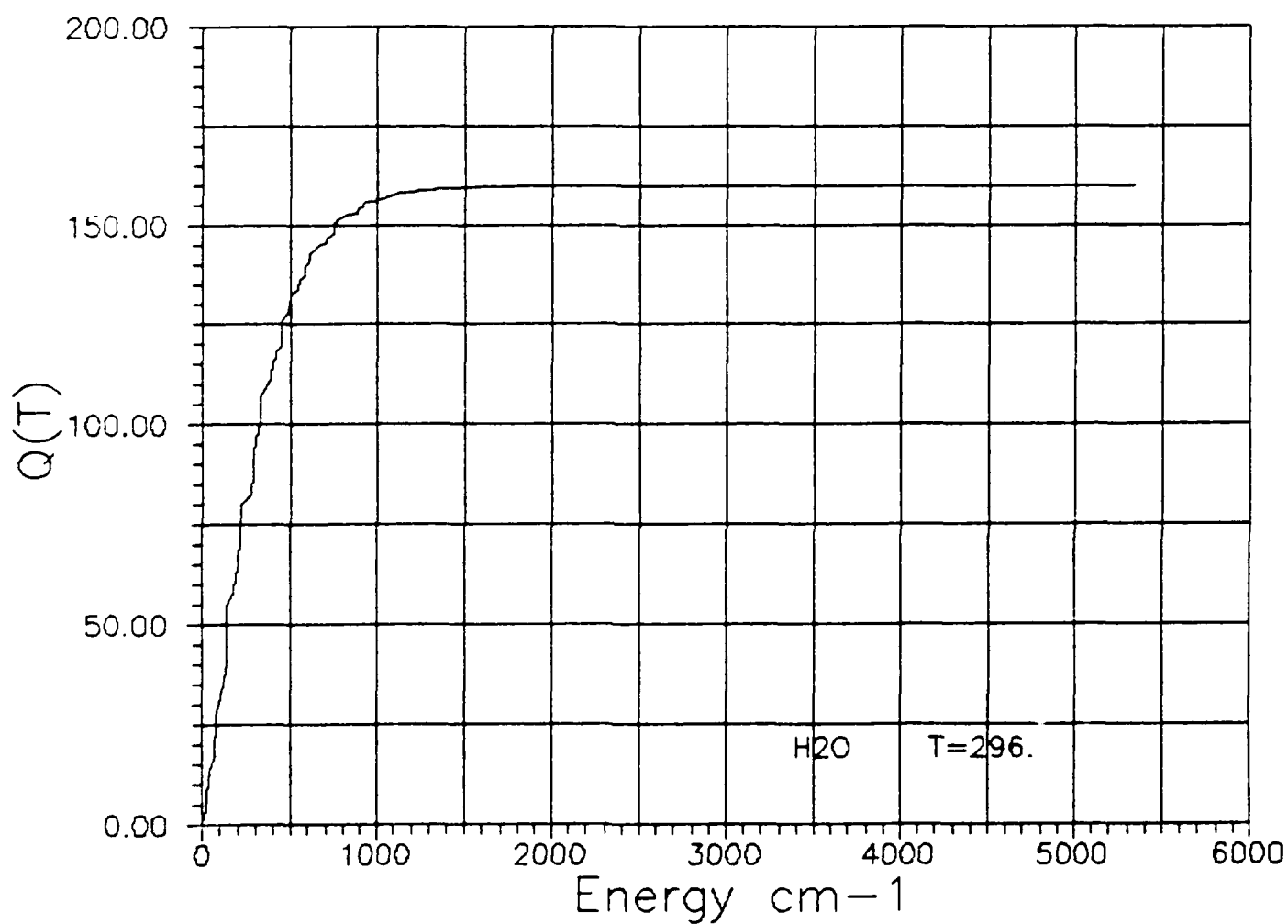


Figure 1. Total Partition Function vs. Energy for  $\text{H}_2\text{O}$  and  $\text{CCl}_2$  at Various Temperatures  $\text{H}_2\text{O}$  at 296 K (Principle Isotope)

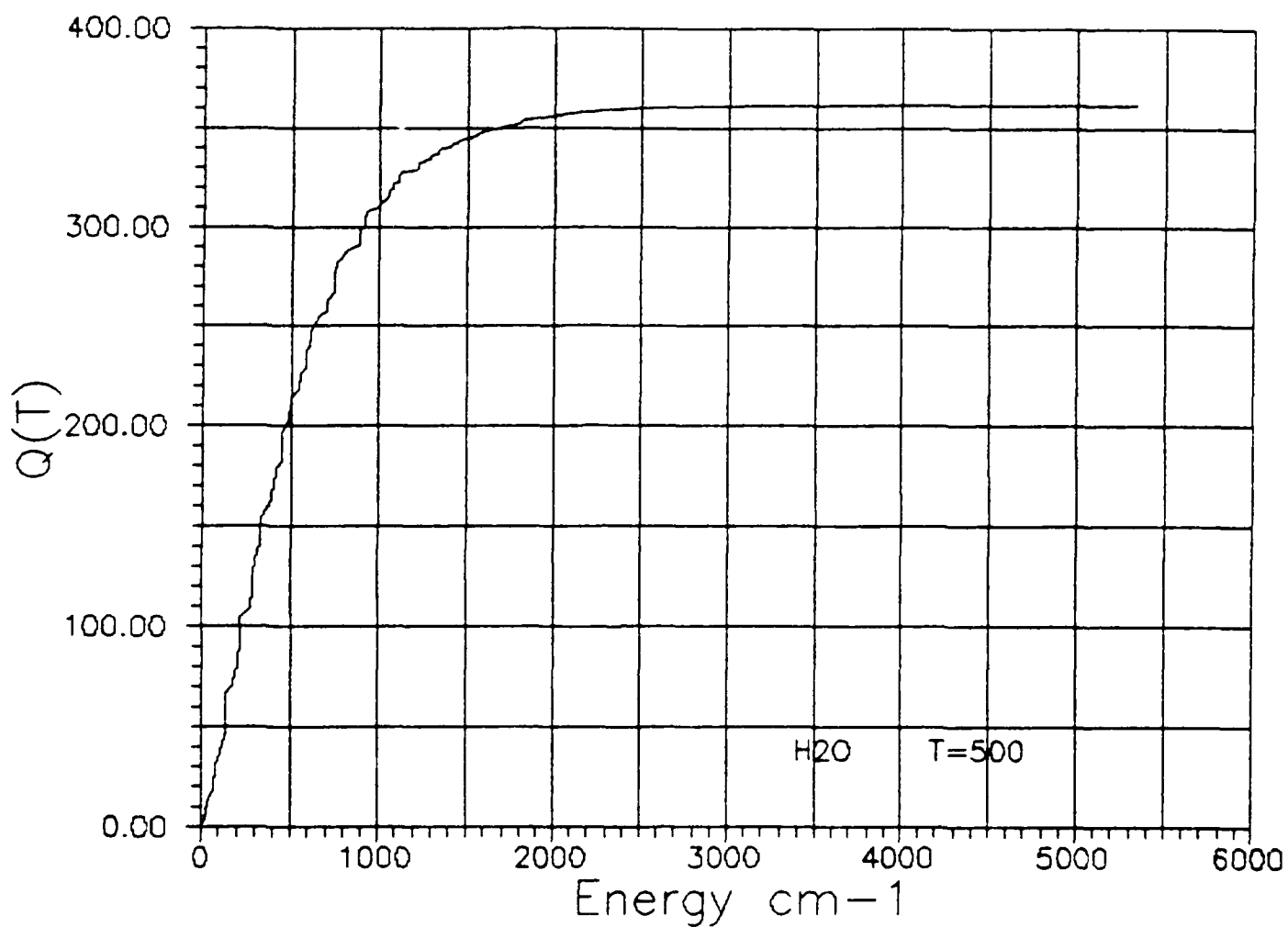


Figure 2. Total Fertilization Function vs. Energy for  $\text{H}_2\text{O}$  and  $\text{CO}_2$  at Various Temperatures  $\text{H}_2\text{O}$  at 500 K (Principal Isotope)

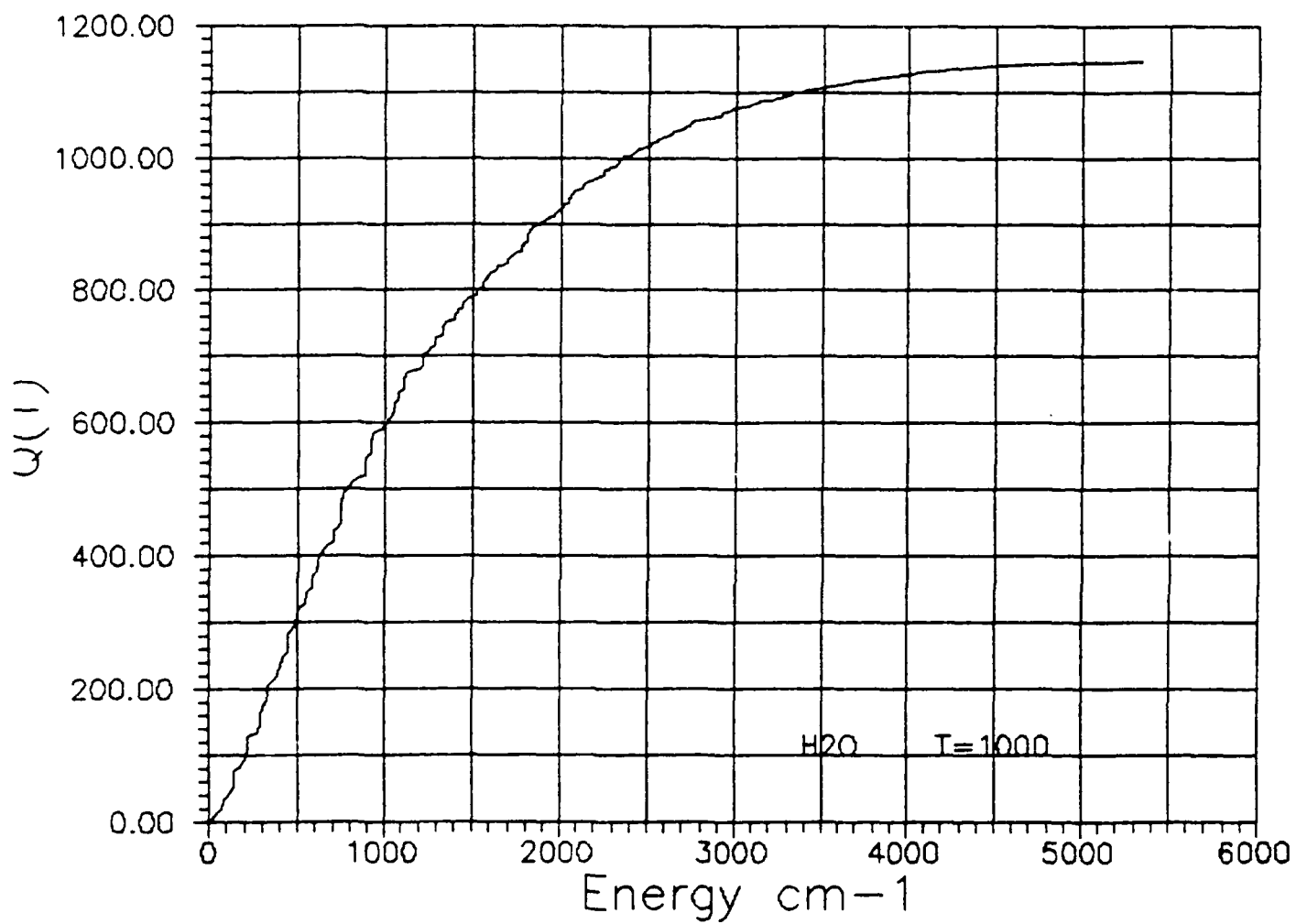


Figure 12. Total Partition Function vs. Energy for  $\text{H}_2\text{O}$  and  $\text{CO}_2$  at Various Temperatures  $\text{H}_2\text{O}$  at 1000 K (Hindible Isotope)

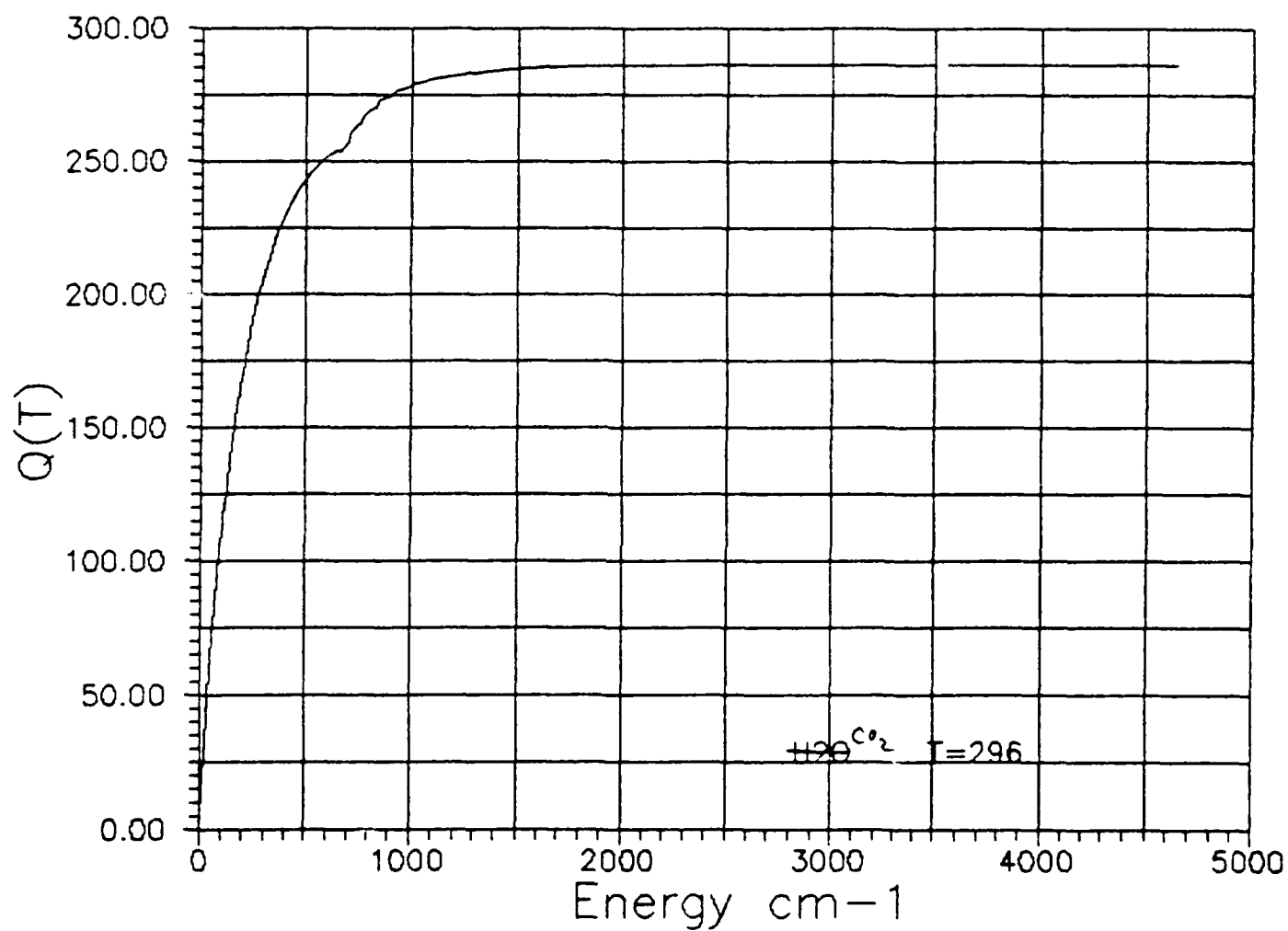


Figure 11. Total Partition Function vs. Energy for  $\text{H}_2\text{O}$  and  $\text{CO}_2$  at Various Temperatures  $\text{CO}_2$  at 296 K (Principal Isotope)



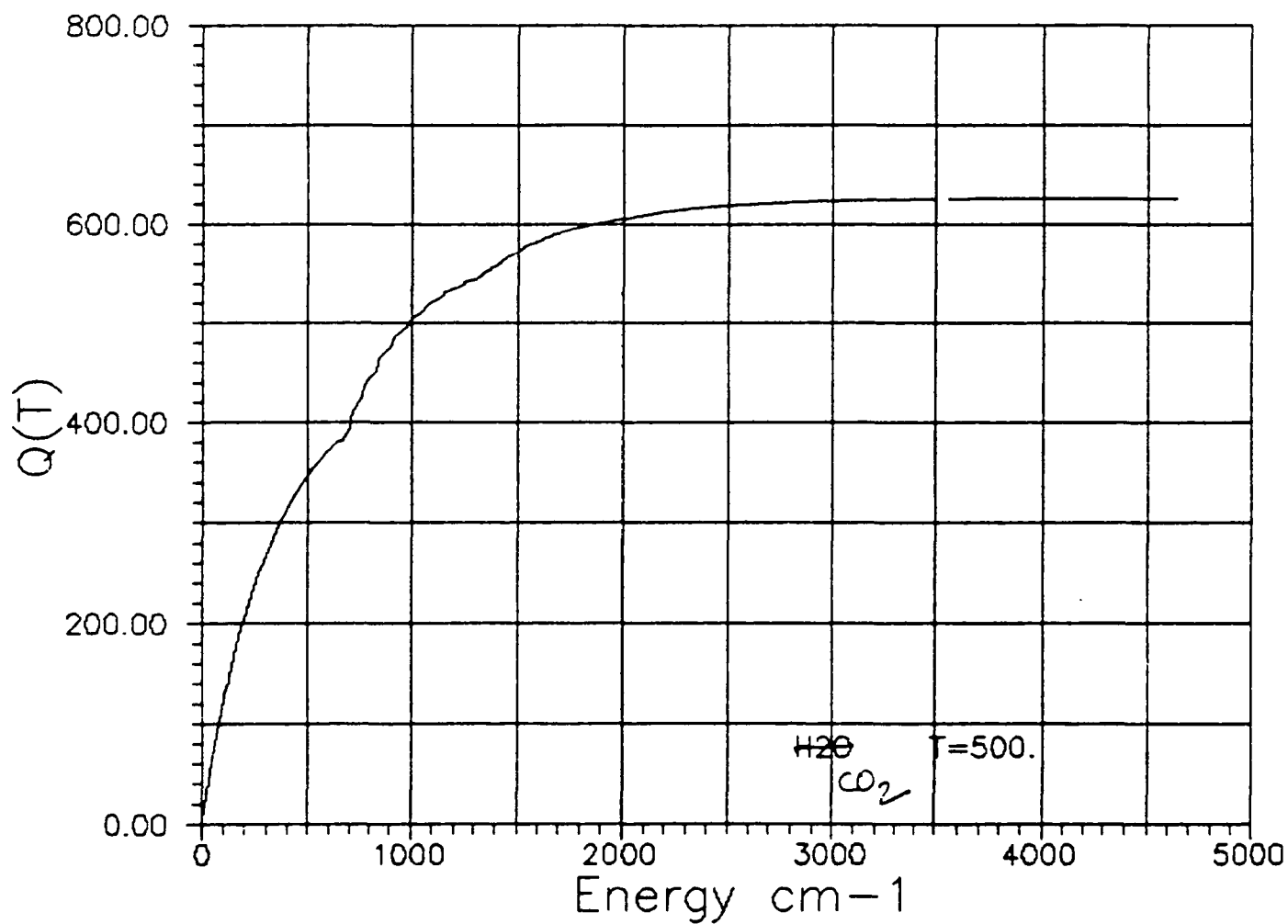


Figure 11. Total Partition Function vs. Energy for  $\text{H}_2\text{O}$  and  $\text{CO}_2$  at Various Temperatures  $\text{CO}_2$  at 500 K (Principal Isotope)

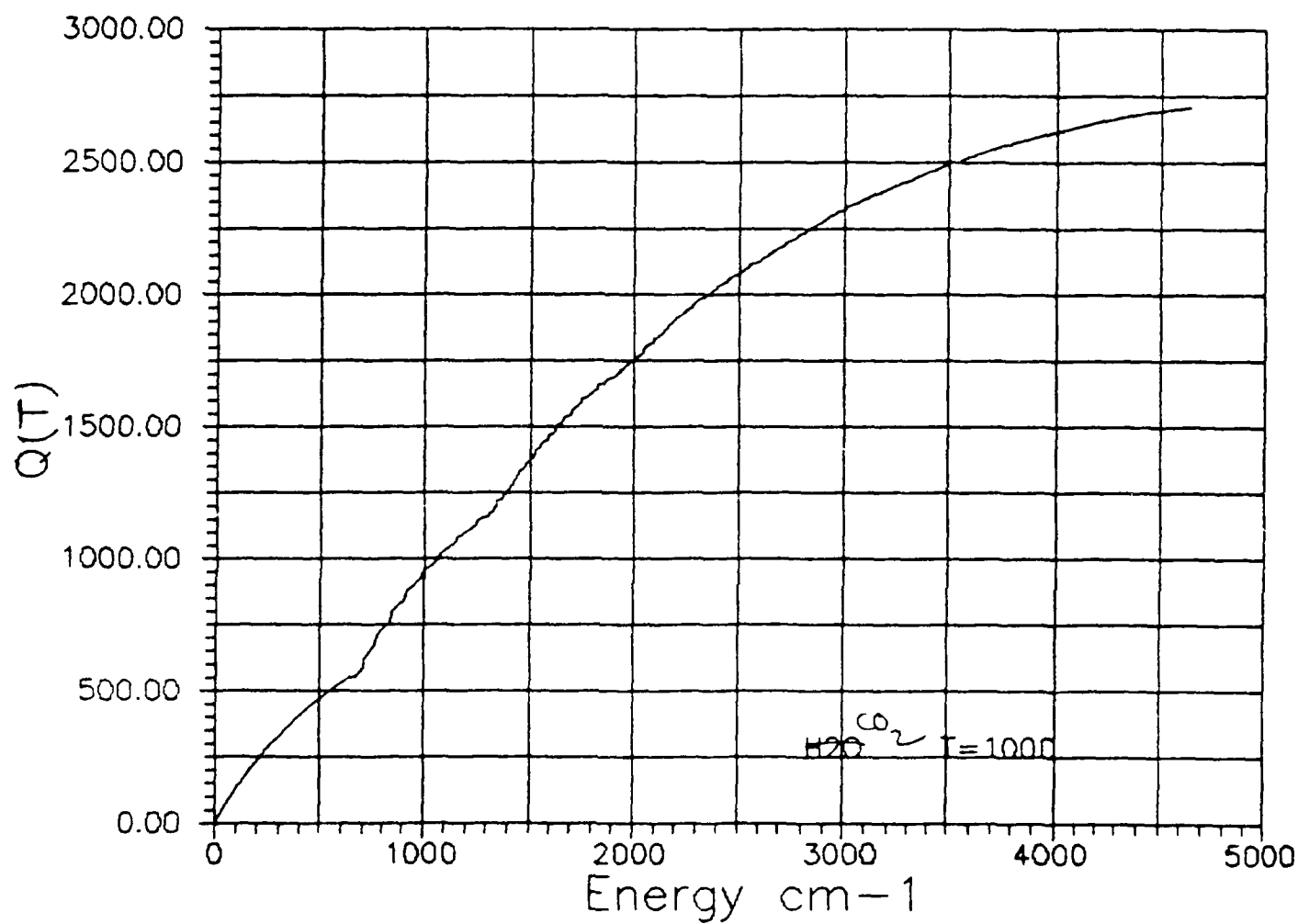


Figure 13. Total Partition Function vs. Energy for  $\text{H}_2\text{O}$  and  $\text{CO}_2$  at Various Temperatures  $\text{CO}_2$  at 1000 K (Principal Isotope)

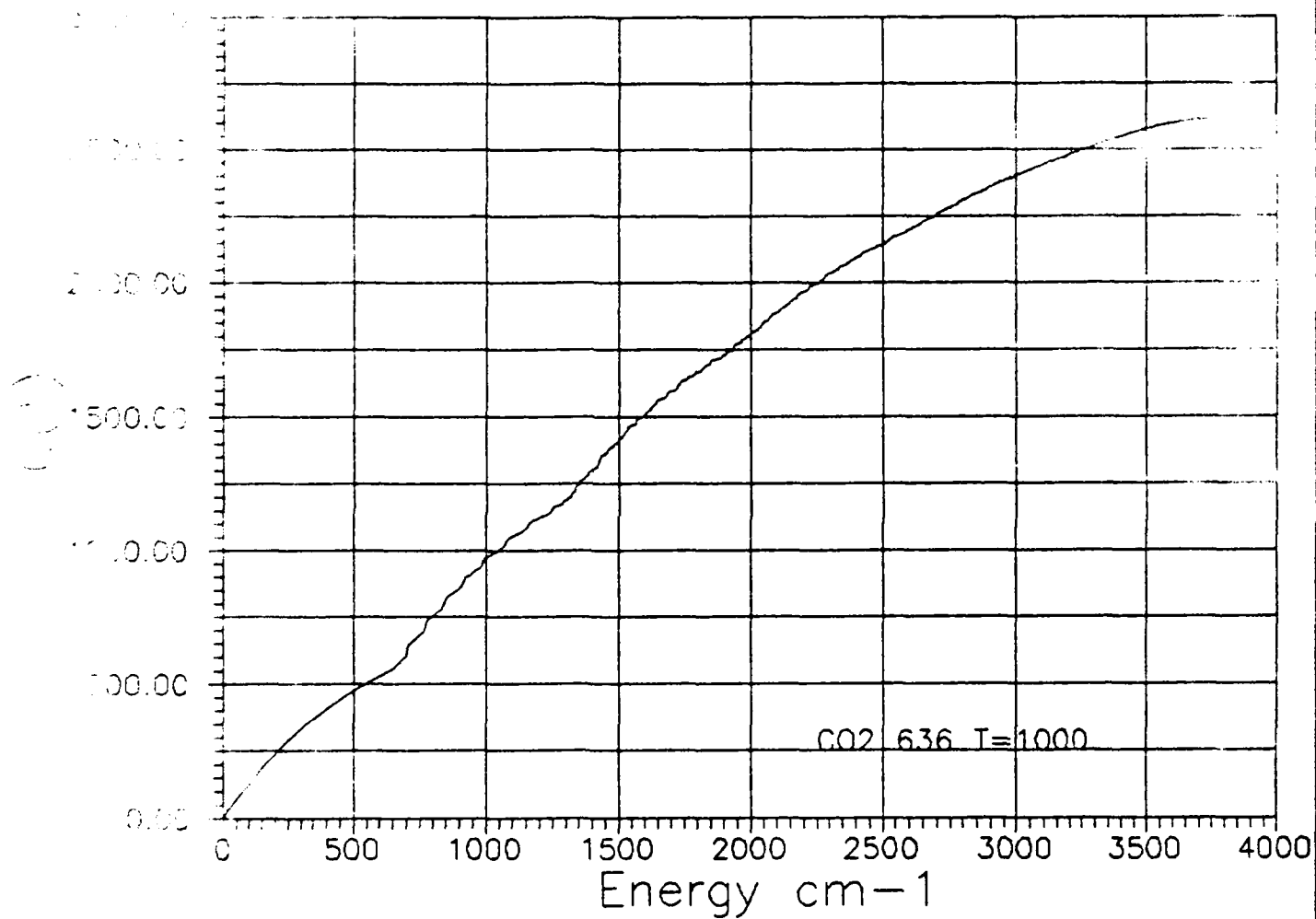


Fig. 1. Total Partition Function vs. Energy for  $\text{H}_2\text{O}$  and  $\text{CO}_2$  at Various Temperatures  $\text{CO}_2$  at 1000 K (636 Isotope)

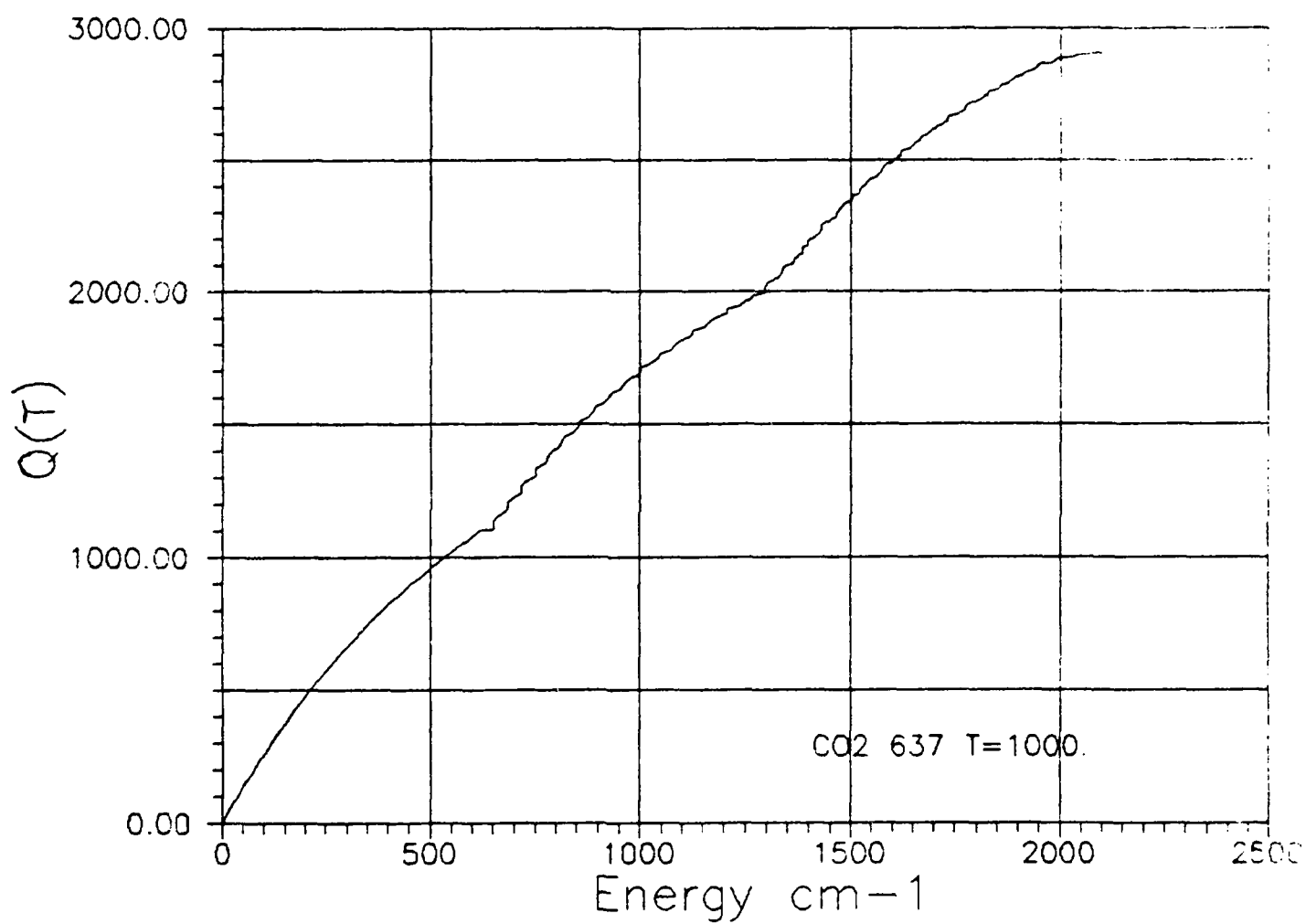


Figure 15. Total Partition Function vs. Energy for  $\text{H}_2\text{O}$  and  $\text{CO}_2$  at Various Temperatures  $\text{CO}_2$  at 1000 K (637 Isotope)

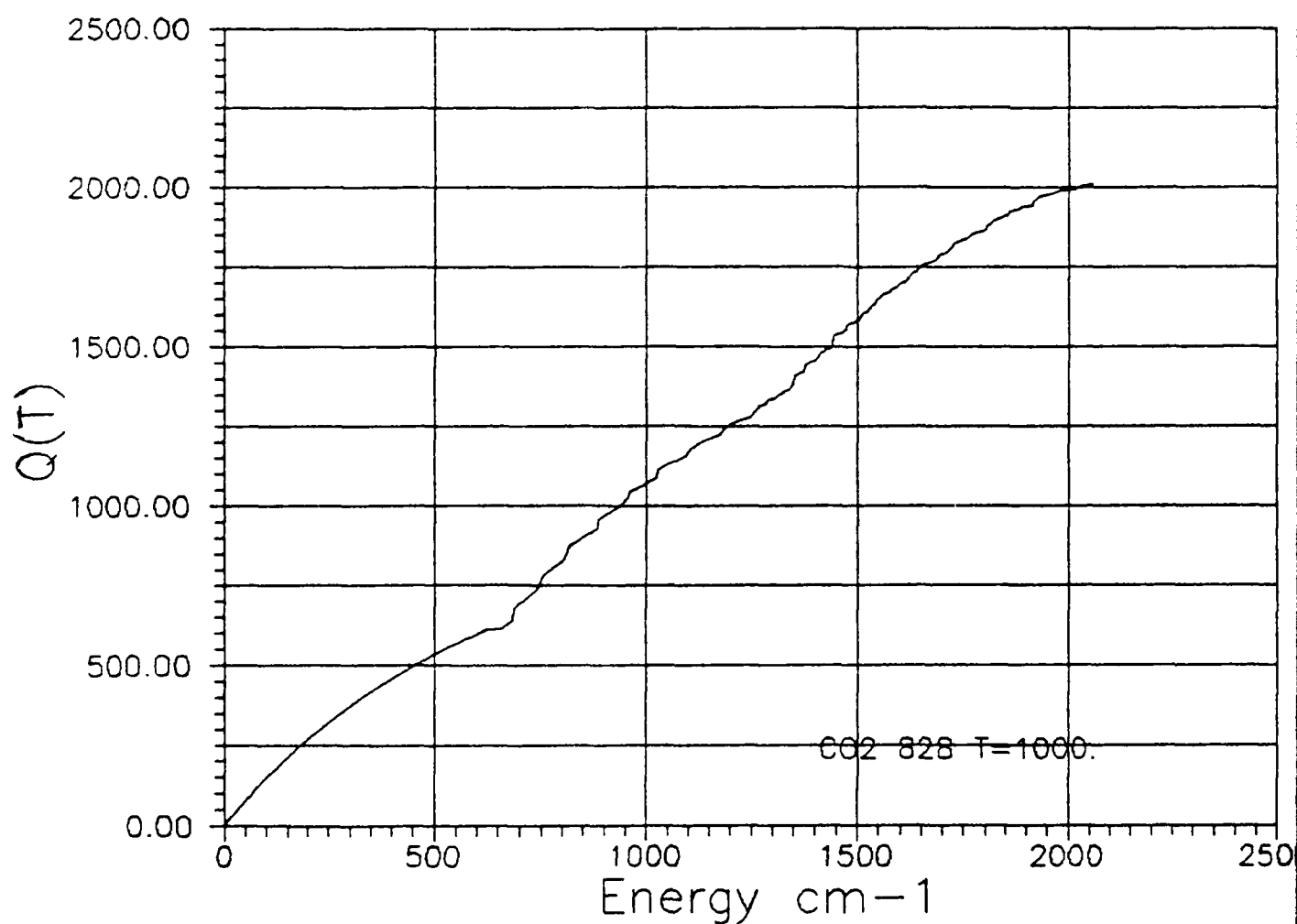


Figure 16. Total Partition Function vs. Energy for  $\text{H}_2\text{O}$  and  $\text{CO}_2$  at Various Temperatures  $\text{CO}_2$  at 1000 K (828 Isotope)

5-10) and for CO<sub>2</sub> (Figures 11-13). The figures show that the partition sums have converged. When similar plots (Figures 14-16) for the lesser isotopic species of CO<sub>2</sub> were done it became clear that the calculations did not converge.

This suggested that we did not have the "complete" set of states available to us from the energy levels extracted from the database. This was apparent for the lesser isotopic species but on closer inspection it was also true for the principal species. Our analysis indicated the partition sum could be very accurately determined by including all levels up to 5000 wavenumbers. This ensures accurate values for  $Q(T)$  up to temperatures of 500K. To show this we extracted the energy levels as a function of rotational quantum index  $(J(J+1) + Ka - Kc + 1)$  for the principal species of water vapor and ozone. These are displayed in Tables 17 and 18. The zeros in the tables are when the database has no energy value for the state. This clearly showed that we could not use the energy levels from the database only and expect partition sum to better than 1%.

We discussed different schemes to produce the needed energy levels. The approximate schemes that we tried could not produce the energy levels with the accuracy that was needed. At this point we abandoned the use of approximate schemes and decided to calculate all energy levels from molecular Hamiltonians.

The other aspect of these calculations is how to represent the partition sums as a function of temperature. The method commonly used is to calculate  $Q(T)$  for a set number of temperatures and to linearly interpolate on a  $\ln\{Q(T)\}$  vs.  $\ln\{T\}$  basis. This is not an elegant method to get  $Q(T)$  at arbitrary temperatures but is certainly applicable if all else fails. We have sought simple analytical expressions that can represent  $Q(T)$  in terms of a small number of parameters. Our first tests were on a simple two parameter power law,  $Q(T) = aT^b$ . This worked very well for the principal species of

				(161)	(181)	(171)	(162)
250	16	12	1	4796.36200	.00000	.00000	.00000
251	16	12	2	5066.36200	.00000	.00000	.00000
252	16	12	3	5336.36200	.00000	.00000	.00000
253	16	12	4	.00000	.00000	.00000	.00000
254	16	12	5	5336.36200	.00000	.00000	.00000
255	16	12	6	.00000	.00000	.00000	.00000
256	16	12	7	.00000	.00000	.00000	.00000
257	16	12	8	5560.35000	2543.60700	2554.35000	1833.75400
258	16	12	9	5560.35000	2543.60700	2554.35000	1833.75400
259	16	12	10	2952.38900	2937.39900	.00000	2037.05700
260	16	12	11	2952.38900	2937.39900	2945.18700	2037.18900
261	16	12	12	3211.05600	3197.34300	.00000	2297.11300
262	16	12	13	3211.05600	3197.34300	.00000	2297.11300
263	16	12	14	3437.29800	.00000	.00000	2339.34200
264	16	12	15	3437.29800	.00000	.00000	2339.34200
265	16	12	16	3623.76200	.00000	.00000	2360.07600
266	16	12	17	3623.76200	.00000	.00000	2360.07600
267	16	12	18	3639.53700	.00000	.00000	2502.43600
268	16	12	19	3758.42900	.00000	.00000	2523.12100
269	16	12	20	3822.24600	.00000	.00000	2557.01600
270	16	12	21	3870.21200	.00000	.00000	2659.76400
271	16	12	22	4006.97100	.00000	.00000	2836.67900
272	16	12	23	4015.17500	.00000	.00000	2836.67900
273	16	12	24	4266.33100	.00000	.00000	3043.60700
274	16	12	25	4266.33100	.00000	.00000	3043.60700
275	16	12	26	4427.11900	.00000	.00000	3275.35700
276	16	12	27	4427.11900	.00000	.00000	3275.35700
277	16	12	28	4665.36700	.00000	.00000	.00000
278	16	12	29	4665.36700	.00000	.00000	.00000
279	16	12	30	4913.24500	.00000	.00000	.00000
280	16	12	31	4913.24500	.00000	.00000	.00000
281	16	12	32	5183.53800	.00000	.00000	.00000
282	16	12	33	.00000	.00000	.00000	.00000
283	16	12	34	.00000	.00000	.00000	.00000
284	16	12	35	.00000	.00000	.00000	.00000
285	16	12	36	.00000	.00000	.00000	.00000
286	16	12	37	.00000	.00000	.00000	.00000
287	16	12	38	.00000	.00000	.00000	.00000
288	16	12	39	.00000	.00000	.00000	.00000
289	16	12	40	.00000	.00000	.00000	.00000
290	17	13	1	2981.36300	2968.66800	2974.35200	2061.39500
291	17	13	2	2981.36300	2968.66800	.00000	2061.39500
292	17	13	3	3291.14500	3277.35600	.00000	2272.09800
293	17	13	4	3291.14500	.00000	.00000	2272.16800
294	17	13	5	3567.18000	.00000	.00000	2455.38200
295	17	13	6	3567.18000	.00000	.00000	2456.77700
296	17	13	7	3810.34000	.00000	.00000	2594.14300
297	17	13	8	3810.34000	.00000	.00000	2617.72900
298	17	13	9	4017.30900	.00000	.00000	2707.58300
299	17	13	10	4027.49400	.00000	.00000	2765.74000
300	17	13	11	4174.28600	.00000	.00000	2797.31000
301	17	13	12	4221.01100	.00000	.00000	2920.75300
302	17	13	13	4291.36600	.00000	.00000	.00000
303	17	13	14	4409.31300	.00000	.00000	.00000
304	17	13	15	4409.31300	.00000	.00000	.00000
305	17	13	16	4612.79000	.00000	.00000	.00000
306	17	13	17	4612.79000	.00000	.00000	.00000
307	17	13	18	4820.37900	.00000	.00000	.00000
308	17	13	19	4820.37900	.00000	.00000	.00000
309	17	13	20	5070.90000	.00000	.00000	.00000
310	17	13	21	5070.90000	.00000	.00000	.00000
311	17	13	22	.00000	.00000	.00000	.00000
312	17	13	23	5324.66100	.00000	.00000	.00000
313	17	13	24	.00000	.00000	.00000	.00000
314	17	13	25	.00000	.00000	.00000	.00000
315	17	13	26	.00000	.00000	.00000	.00000
316	17	13	27	.00000	.00000	.00000	.00000
317	17	13	28	.00000	.00000	.00000	.00000
318	17	13	29	.00000	.00000	.00000	.00000
319	17	13	30	.00000	.00000	.00000	.00000
320	17	13	31	.00000	.00000	.00000	.00000
321	17	13	32	.00000	.00000	.00000	.00000
322	17	13	33	.00000	.00000	.00000	.00000
323	17	13	34	.00000	.00000	.00000	.00000
324	17	13	35	.00000	.00000	.00000	.00000

Table 17. Selected Energy Levels for Water Vapor in  $\text{cm}^{-1}$

1052	32	18	12	655	1052	655
1053	32	17	13	957.227	957.227	957.227
1055	32	14	16	1045.82300	.00000	.
1055	32	15	17	1138.31300	.00000	.00000
1057	32	16	15	1232.51000	.00000	.00000
1059	32	17	15	1332.39400	.00000	.00000
1061	32	18	14	1427.89700	.00000	.00000
1063	32	19	13	1546.95000	.00000	.00000
1065	32	20	12	1665.46200	.00000	.00000
1067	32	21	11	1787.41900	.00000	.00000
1069	32	22	10	1914.65800	.00000	.00000
1071	32	23	9	2047.21400	.00000	.00000
1073	32	24	8	2184.91900	.00000	.00000
1075	32	25		.00000	.00000	.00000
1077	32	26		.00000	.00000	.00000
1079	32	27		.00000	.00000	.00000
1081	32	28		.00000	.00000	.00000
1083	32	29		.00000	.00000	.00000
1085	32	30		.00000	.00000	.00000
1087	32	31		.00000	.00000	.00000
1089	32	32		.00000	.00000	.00000
1091	33	1	33	455.03520	454.99400	454.99400
1093	33	2	32	478.43900	478.38700	478.38700
1095	33	3	31	499.79020	499.73200	499.73200
1097	33	4	30	522.59390	522.52300	522.52300
1099	33	5	29	550.31340	550.24000	550.24000
1101	33	6	28	584.26840	584.18900	584.18900
1103	33	7	27	624.55070	624.45900	624.45900
1105	33	8	26	671.06350	670.99000	670.99000
1107	33	9	25	723.75060	723.67900	723.67900
1109	33	10	24	782.53330	782.47700	782.47700
1111	33	11	23	847.36200	847.32900	.00000
1113	33	12	22	918.18130	918.18130	918.18130
1115	33	13	21	994.93500	994.93500	994.93500
1117	33	14	20	1077.56500	.00000	.00000
1119	33	15	19	1166.01000	.00000	.00000
1121	33	16	18	1260.20700	.00000	.00000
1123	33	17	17	1360.09100	.00000	.00000
1125	33	18	16	1465.59400	.00000	.00000
1127	33	19	15	1576.64600	.00000	.00000
1129	33	20	14	1693.18000	.00000	.00000
1131	33	21	13	1815.11700	.00000	.00000
1133	33	22	12	1942.38500	.00000	.00000
1135	33	23	11	2074.91200	.00000	.00000
1137	33	24	10	2212.61700	.00000	.00000
1139	33	25	9	.00000	.00000	.00000
1141	33	26	8	.00000	.00000	.00000
1143	33	27	7	.00000	.00000	.00000
1145	33	28	6	.00000	.00000	.00000
1147	33	29	5	.00000	.00000	.00000
1149	33	30	4	.00000	.00000	.00000
1151	33	31	3	.00000	.00000	.00000
1153	33	32	2	.00000	.00000	.00000
1155	33	33	1	.00000	.00000	.00000

Table 18. Selected Energy Levels for  $O_3$  in  $cm^{-1}$



water vapor from 200-350K, 0.04% maximum error in reproducing  $Q(T)$ . This form failed when applied to other isotopic species and to other molecules.

A more complex analytical form based on the work of McDowell<sup>31</sup> was tried next. From McDowell, the analytical form of the rotational partition sum for a spherical top molecule is given by

$$Q_r = \sigma^* \pi^{1/2} c^{\beta/4} \beta^{-3/2} \left( 1 + \frac{15D}{4\beta B} \right) \quad (22)$$

where  $\beta = hcB/kT$  ( $B$  = rotational constant) and  $\sigma^* = (2I_Y + 1)n/\sigma$  ( $I_Y$  = nuclear spin of the  $Y$  nuclei,  $\sigma$  = classical symmetry number) and  $D$  = centrifugal distortion constant. In this expression  $\sigma$ ,  $\beta$ ,  $D$  and  $B$  were treated as adjustable constants. This proved to give good results.

We then tried a simple polynomial expression in temperature with four adjustable constants,

$$Q(T) = a + bT + cT^2 + dT^3 \quad (23)$$

This form for the partition sum proved to be the simplest for recalculation of  $Q(T)$  and it gave the most accurate results. This was the form that we chose to represent the partition sums.

We then fixed the temperature range of study to consider from 70 to 440K in 5K steps. The energy levels for each molecule were calculated via the appropriate Hamiltonian for each vibrational state and the partition sums done. The partition sums were then fitted<sup>32</sup> by the polynomial expression by first doing a least squares fit. The results of the least squares fit was used as input to a minimax (Simplex) procedure to the eight power (the power of eight was chosen by increasing the exponent until no further change in the results was observed). The standard deviation of the least squares fit was used as a step size in the Simplex minimization. This yields a

set of coefficients; a, b, c, d, for each isotopic species of each molecule studied. Below we discuss each molecule separately.

### 5.1 Water Vapor

For water vapor, there are some levels missing for the principal isotopic species (161 AFGL code) and many levels missing for the other species 181, 171 and 162. By using the index,  $J + K_a - K_c + 1$ , we have filled an array of energy levels for each isotopic species. This allows us to determine which levels are missing for each isotopic species. We then took the Watson Hamiltonian constants from C. Camy-Peyret et. al.<sup>33-34</sup> for the 161, 181 and 171 isotopic species and the Hamiltonian constants of Toth et. al.<sup>35</sup> for the HDO species (162) (the constants are given in Table 19) and used these to generate all the missing levels. In order to do this the asymmetric rotor energy program had to be made operable. After some work this was done and test calculations were made to check the integrity of the program. Calculations were made up to a cutoff in energy which relates to the maximum J level for a vibrational state. This gave us a near complete set of energy levels up to 5000  $\text{cm}^{-1}$ . Because the energy levels from the database come from the work of Camy-Peyret et al., the final energies are a consistent set.

The partition sums were then calculated using the "complete" set of energy levels. The calculations were done in part on the AFGL VAX and on an ULCAR IBM-AT-PC. In Figure 17 the convergence of the partition sum at several temperatures is shown. The partition sum has leveled off at around 2500  $\text{cm}^{-1}$ . Error analysis was also done by shifting the energy levels by the maximum error reported in the literature (0.2%), recalculating the partition sums and then forming the difference of the two values. The results

Flaud and Camy-Peyret ground state 161 Watson constants

0.00000000	E+00	Vibrational energy
27.880678	E+00	A
14.521689	E+00	B
9.277459	E+00	C
3.25199	E-02	DLK
-5.7655	E-03	DLJK
1.24894	E-03	DLJ
1.3007	E-03	dsK
5.0838	E-04	dsJ
1.2281	E-04	HLK
-1.3700	E-05	HLKJ
-1.921	E-06	HLJK
4.5061	E-07	HLJ
2.3958	E-05	hsK
-4.21	E-07	hsJK
2.2568	E-07	hsJ
-6.496	E-07	ALK
1.29150	E-07	ALKKJ
-3.681	E-08	ALJK
0.0	E-00	ALJ
8.66000	E-10	ALJJK
-1.5414	E-07	AlsK
6.17	E-10	AlsJK
0.0	E-00	AlsKJ
0.0	E-00	AlsJ
2.399	E-09	PK
6.81	E-12	PKKJ
1.704	E-10	psK
-6.49	E-12	QK
7.65	E-15	RK

Table 19. Ground State Watson Hamiltonian Constants for the Four Isotopic Species of  $H_2O$

Flaud and Camy-Peyret ground state 181 Watson constants

---

0.00000000	E+00	Vibrational energy
27.531110	E+00	A
14.522047	E+00	B
9.238056	E+00	C
3.16331	E-02	DLK
-5.6857	E-03	DLJK
1.25338	E-03	DLJ
1.2636	E-03	dsK
5.0937	E-04	dsJ
1.1805	E-04	HLK
-1.5611	E-05	HLKJ
-1.5209	E-06	HLJK
5.3638	E-07	HLJ
2.8488	E-05	hsK
-5.49	E-07	hsJK
2.7204	E-07	hsJ
-6.305	E-07	ALK
1.7035	E-07	ALPKJ
-4.454	E-08	ALJK
-2.373	E-10	ALJ
0.00000	E-10	ALJJJ
-2.2547	E-07	AlsK
0.00	E 00	AlsJK
-3.22	E-09	AlPKJ
-1.324	E-10	AlsJ
1.982	E-09	PK
0.0000	E 00	PKKJ
4.157	E-10	psK
-3.797	E-12	QK
0.00	E 00	RK

---

Tabl. 19. (Continued)

Flaud and Camy-Peyret ground state 171 Watson constants

---

0.00000000	E+00	Vibrational energy
27.695220	E+00	A
14.521875	E+00	B
9.256840	E+00	C
3.20133	E-02	DLK
-5.71998	E-03	DLJK
1.25345	E-03	DLJ
1.2885	E-03	dsK
5.0841	E-04	dsJ
1.2040	E-04	HLK
-1.6324	E-05	HLKJ
-1.378	E-06	HLJK
5.3645	E-07	HLJ
3.1329	E-05	hsK
-7.396	E-07	hsJK
2.7281	E-07	hsJ
-6.882	E-07	ALK
2.4318	E-07	ALKKJ
-6.947	E-08	ALJK
-2.759	E-10	ALJ
0.00000	E 00	ALJJK
-2.8704	E-07	AlsK
0.00	E 00	AlsJK
-7.76	E-09	AlsKJ
-1.533	E-10	AlsJ
2.031	E-09	PK
0.00	E 00	PKKJ
4.613	E-10	psK
-3.964	E-12	QK
0.00	E-15	RK

---

Table 13. (Continued)

Toth's Watson constants for HDO

0.00000000	E+00	Vibrational energy
23.413842	E+00	A
9.103323	E+00	B
6.406295	E+00	C
1.25376	E-02	DLK
1.1432	E-03	DLJK
3.60562	E-04	DLJ
2.0814	E-03	dsK
1.2143	E-04	dsJ
4.5589	E-05	HLK
-8.702	E-06	HLKJ
2.401	E-06	HLJK
3.513	E-08	HLJ
1.482	E-05	hsK
1.001	E-06	hsJK
2.112	E-08	hsJ
-1.055	E-07	ALK
0.00000	E 00	ALKKJ
0.00000	E 00	ALJK
0.000	E-08	ALK
0.00000	E 00	ALJKK
0.00000	E 00	AlsK
0.00000	E 00	AlsJK
0.00000	E 00	AlsKJ
1.09000	E-11	AlsJ
0.00000	E 00	PK
0.00000	E 00	PKKJ
0.00000	E 00	psK
0.00000	E 00	QK
0.00000	E 00	RK

Table 19. (Continued)

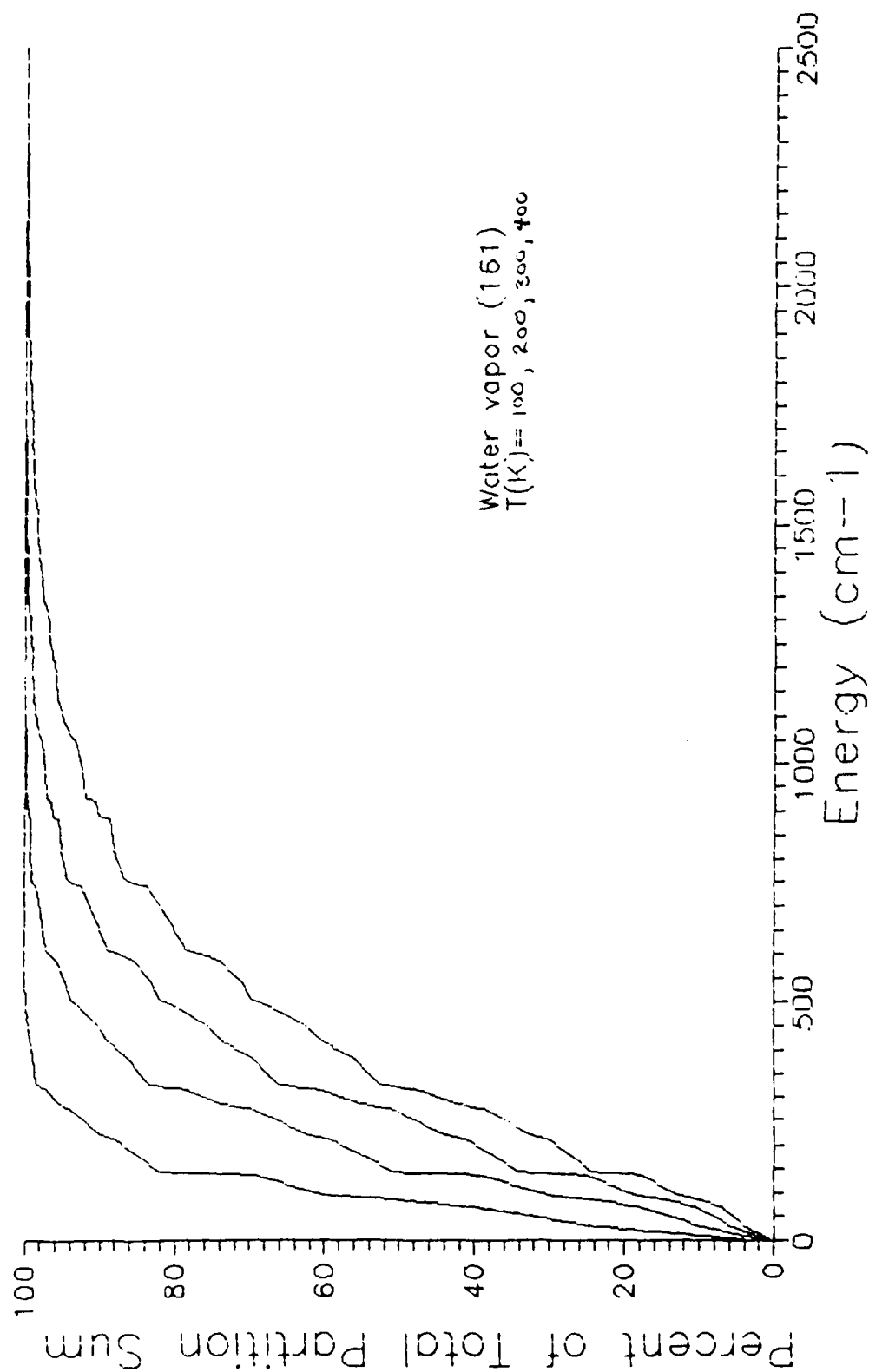


Figure 10. Convergence of Partition Sums vs. Energy (161)  
 Water Vapor at  $T = 100, 200, 300,$  and  $400$  K

of the error analysis show the partition sums accurate to  $\sim 0.3\%$ , which is certainly in the error range we desired.

The polynomial fits were done for the four isotopic variants of water vapor. Figures 18 and 19 display the % error  $[(Q(T) - \text{polynomial}) * 100 / Q(T)]$  of the fits for  $\text{H}_2^{16}\text{O}$  and for HDO. For the principal species the error remains below 0.25%, for HDO it remains below 0.02%, confirming the validity of the polynomial fit. Thus we are confident that the partition sums are accurate to better than 1%.

## 5.2 Carbon Dioxide

For carbon dioxide, all energy levels upto  $5000 \text{ cm}^{-1}$  were calculated via L. Rothman's  $\text{CO}_2$ -Generator program. This program used the most recent set of molecular constants for the isotopic species  $^{12}\text{C}^{16}\text{O}_2$ ,  $^{13}\text{C}^{16}\text{O}_2$ , and  $^{16}\text{O}^{12}\text{C}^{18}\text{O}$ . The error analysis used a shift in the energy levels of 0.2%, this is greater than the actual error for most of the lines but provides an upper limit. With this shift in energy the partition sums did not change by more than 0.3%. The partition sums were evaluated at the specified temperatures and then the results fitted by the polynomial. The resulting error of the fitting is demonstrated in Figure 20 for the principal isotopic species of  $\text{CO}_2$ . Note the fitting error remains less than -0.02% again confirming the polynomial fit and total internal partition sums accurate to better than 1%.

## 5.3 Ozone

Ozone had many energy levels missing as well as having many states coming from older less reliable sources. Because better values are available, especially for the isotopic species, we decided to



# Polynomial Fit

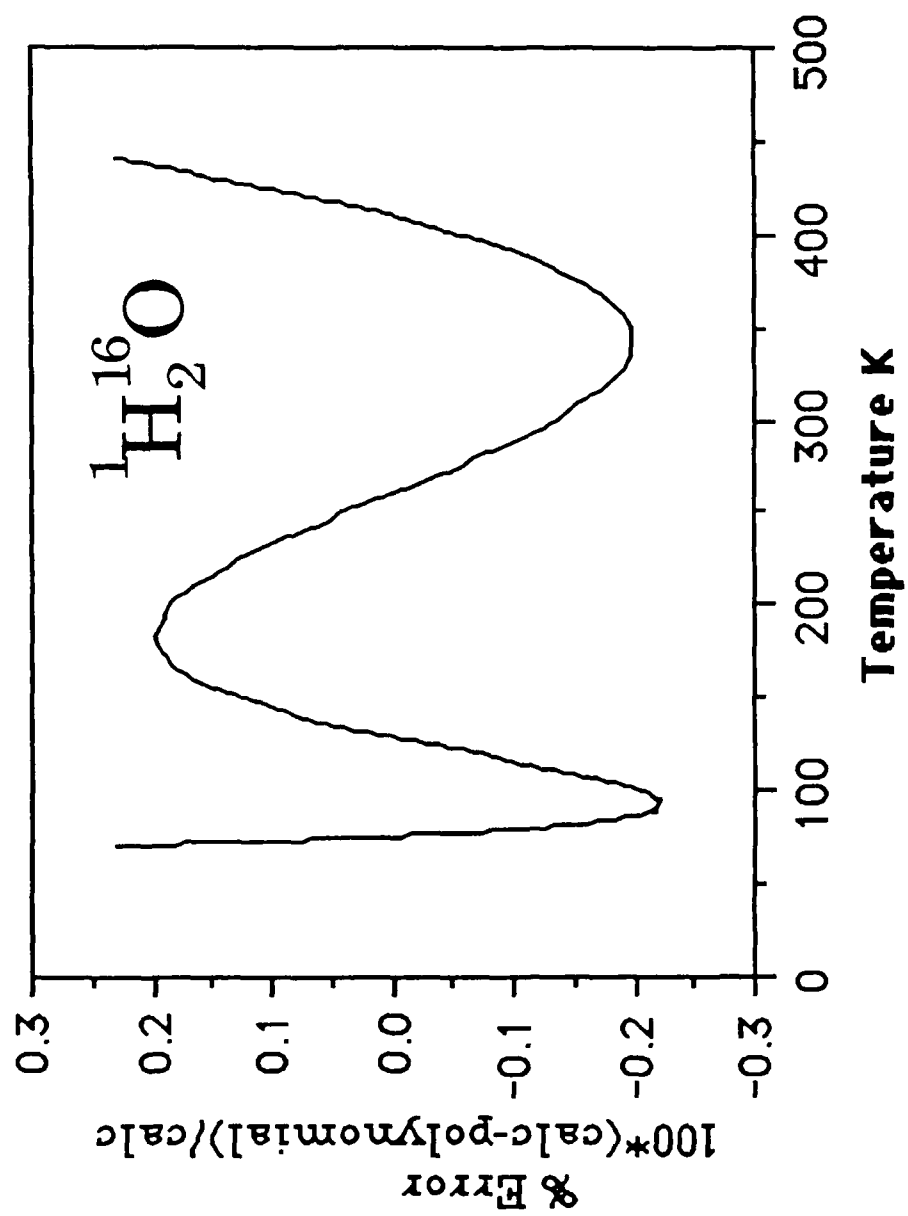


Figure 18. % Error  $|Q(T) - \text{Polynomial}| / Q(T)$  vs. T for  $\text{H}_2^{16}\text{O}$

# Polynomial Fit

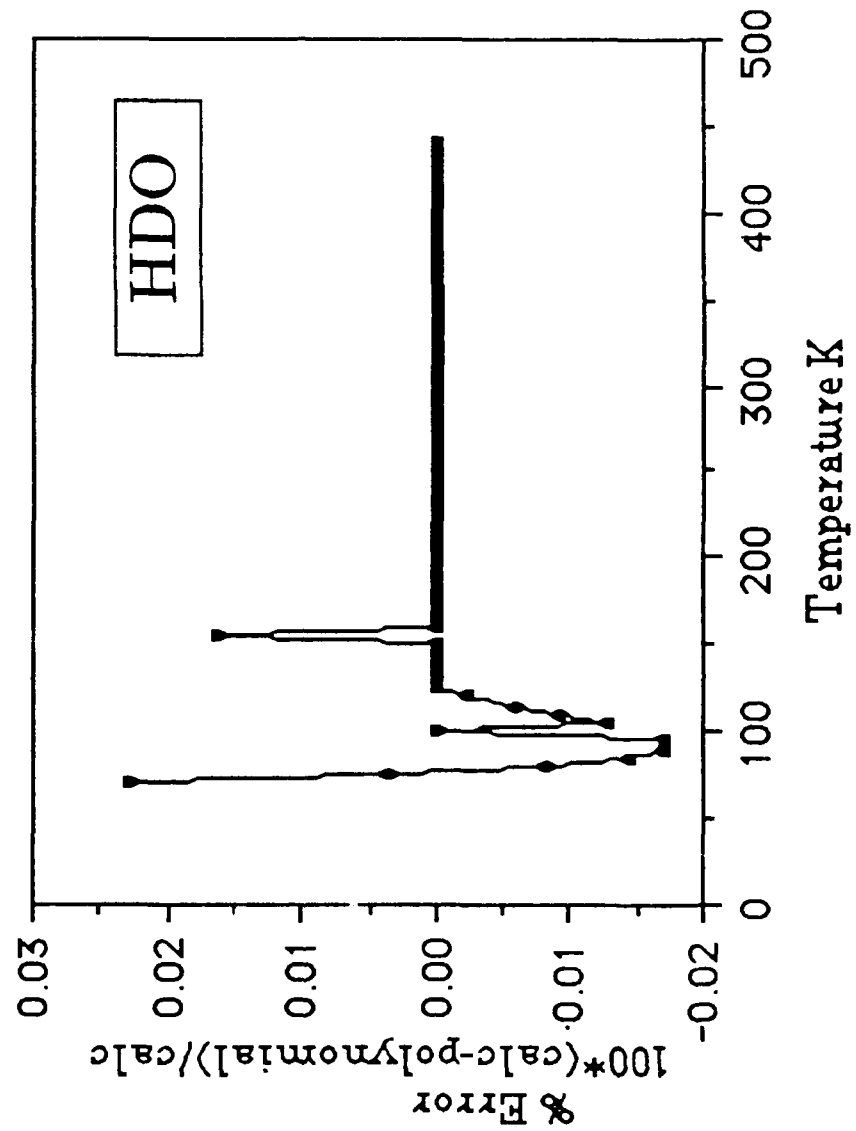


Figure 19. % Error  $|Q(T) - \text{Polynomial}| / QT$  vs. T for HDO

CO<sub>2</sub>

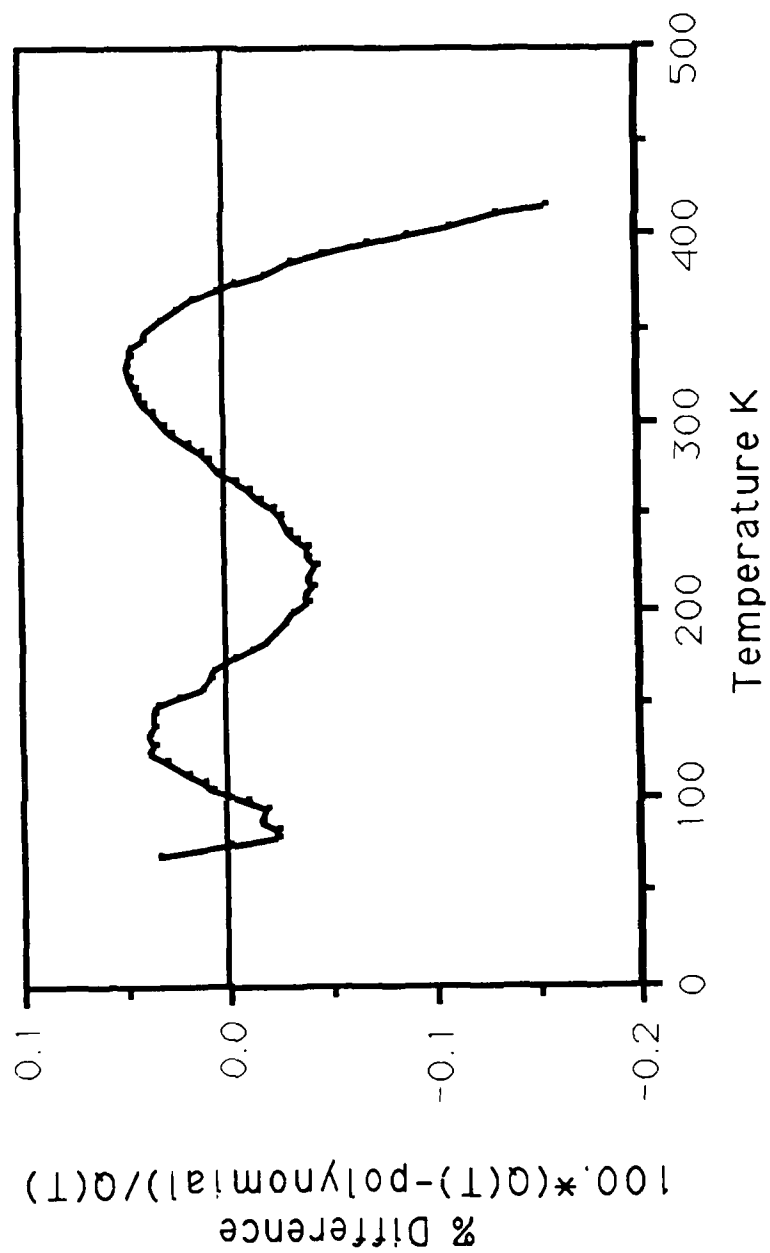


Figure 19. % Error  $|Q(T) - \text{Polynomial}|/QT$  vs.  $T$  for CO<sub>2</sub>

do the ozone partition sums from molecular constants entirely, i.e. the levels from HITRAN will not be used at all. The references for the ozone Watson Hamiltonian constants are Flaud et. al.<sup>36-41</sup> These constants are (see Table 20) for the principal species (666) for the states 000, 001, 100, 110, 011, 010, 020, 002, 101 and 200. For the 686 and 668 species the constants include the 000, 010, 001 and 100 vibrational states. Note for the principal isotopic species (666) there are ten vibrational levels and we tested the often used approximation

$$Q(T) = Q_v(T) \cdot Q_r(T) . \quad (24)$$

used for these levels. Many thousands of levels were calculated by the ASMROT program and formatted for the partition sum program. Again the 5000 cm<sup>-1</sup> cutoff was enforced to produce the final set of "complete" energy levels. The resulting partition sums and the error analysis are given in Tables 21 and 22. The error analysis shows the partition sums being good to better than 0.4% error.

The test of the approximation of  $Q_{vib}$  times  $Q_{rot}$  being equal to  $Q_{tot}$  appears very good for ozone. The difference between the actual partition sum and the approximation was never greater than 0.16% error from 100 to 400 K (see Table 23).

#### 5.4 N<sub>2</sub>O

For N<sub>2</sub>O we sorted the energy levels from the database and found many levels missing for  $J > 70$ . These energies are in the range 2500 cm<sup>-1</sup> and must be accounted for if the calculations are to be of the required accuracy. The vibrational bands of importance are:

Flaud et. al. ozone (666) ground state Watson constants

0.00000000	E+00	Vibrational energy
3.553666502	E+00	A
0.445283207	E+00	B
0.394751807	E+00	C
0.2116872	E-03	DLK
-0.184846	E-05	DLJK
0.454169	E-06	DLJ
0.323240	E-05	dsK
0.697903	E-07	dsJ
0.39896	E-07	HLK
-0.18592	E-08	HLKJ
-0.646	E-11	HLJK
0.321	E-12	HLJ
0.2293	E-08	hsK
-0.757	E-11	hsJK
0.1755	E-12	hsJ
-0.1177	E-10	ALK
0.273	E-12	ALKKJ
0.0	E-00	ALJK
0.299	E-17	ALJ
-0.325	E-15	ALJJK
0.181	E-12	AlsK
0.0	E-00	AlsJK
0.0	E 00	AlsKJ
0.0	E 00	AlsJ
0.333	E-14	PK
0.189	E-15	PKKKJ
0.0	E-00	psK
0.0	E-00	QK
0.0	E-00	RK

Table 20. Watson Hamiltonian Constants for  $O_3$  from Flaud et al.

Flaud et. al. ozone (666) 010 state Watson constants

700.931056	E+00	Vibrational energy
3.607092966	E+00	A
0.444021809	E+00	B
0.392439113	E+00	C
0.2327460	E-03	DLK
-0.1790036	E-05	DLJK
0.457106	E-06	DLJ
0.388935	E-05	dsK
0.692601	E-07	dsJ
0.48866	E-07	HLK
-0.24209	E-08	HLKJ
0.309	E-11	HLJK
0.31367	E-12	HLJ
0.31968	E-08	hsK
-0.1155	E-10	hsJK
0.1868	E-12	hsJ
-0.1582	E-10	ALK
0.4795	E-12	ALKKJ
0.0	E-00	ALJK
0.0	E-17	ALJ
0.0	E-15	ALJJK
0.636	E-12	AlsK
0.0	E-00	AlsJK
0.383	E-13	AlsKJ
0.0	E-00	AlsJ
0.498	E-14	PK
0.0	E-15	PKKKJ
0.0	E-00	psK
0.0	E-00	QK
0.0	E-00	RK

Table 20. (Continued)

Flaud et. al. ozone (666) 001 state Watson constants

1042.08398	E+00	Vibrational energy
3.50055300	E+00	A
0.44129635	E+00	B
0.390998275	E+00	C
0.208072	E-03	DLK
-0.16977	E-05	DLJK
0.456697	E-06	DLJ
0.29609	E-05	dsK
0.759513	E-07	dsJ
0.39036	E-07	HLK
-0.1802	E-08	HLKJ
0.160	E-11	HLJK
0.1704	E-12	HLJ
0.248	E-08	hsK
-0.1142	E-10	hsJK
0.2355	E-12	hsJ
-0.1141	E-10	ALK
0.317	E-12	ALKKJ
0.0	E-00	ALJK
0.2994	E-17	ALJ
-0.3251	E-15	ALJJK
0.21	E-12	AlsK
0.0	E-00	AlsJK
0.0	E-13	AlsKJ
0.0	E 00	AlsJ
0.333	E-14	PK
0.1895	E-15	PKKKJ
0.0	E-00	psK
0.0	E-00	QK
0.0	E-00	RK

Table 20. (Continued)

Flaud et. al. ozone (666) 100 state Watson constants

1103.13729	E+00	Vibrational energy
3.55669374	E+00	A
0.442736468	E+00	B
0.392568222	E+00	C
0.217495	E-03	DLK
-0.21569	E-05	DLJK
0.461481	E-06	DLJ
0.35570	E-05	dsK
0.658775	E-07	dsJ
0.41897	E-07	HLK
-0.2041	E-08	HLKJ
-0.312	E-10	HLJK
0.424	E-12	HLJ
0.98	E-09	hsK
-0.80	E-11	hsJK
0.916	E-13	hsJ
-0.12189	E-10	ALK
0.309	E-12	ALKKJ
0.0	E-00	ALJK
0.2994	E-17	ALJ
-0.3251	E-15	ALJKJ
0.15	E-12	AlSK
0.0	E-00	AlsJK
0.0	E-13	AlSKJ
0.0	E-00	AlsJ
0.333	E-14	PK
0.1895	E-15	PKKKJ
0.0	E-00	psK
0.0	E-00	QK
0.0	E-00	RK

Table 23. (Continued)



Flaud et. al. ozone (666) 020 state Watson constants

---

1399.272628	E+00	Vibrational energy
3.6624062	E+00	A
0.44274468	E+00	B
0.39007214	E+00	C
0.256077	E-03	DLK
-0.17212	E-05	DLJK
0.46006	E-06	DLJ
0.45898	E-05	dsK
0.68637	E-07	dsJ
0.610	E-07	HLK
-0.2542	E-08	HLKJ
0.186	E-10	HLJK
0.118	E-12	HLJ
0.478	E-08	hsK
-0.268	E-10	hsJK
0.238	E-12	hsJ
-0.333	E-10	ALK
0.953	E-12	ALKKJ
0.0	E-00	ALJK
0.0	E-17	ALJ
0.0	E-15	ALJJK
0.0	E-12	AlsK
0.0	E-00	AlsJK
0.0	E-13	AlsKJ
0.0	E 00	AlsJ
0.40	E-13	PK
0.0	E-00	PKKKJ
0.0	E-00	psK
0.0	E-00	QK
0.0	E-00	RK

---

Table 20. (Continued)

Flaud et. al. ozone (666) 002 state Watson constants

2063.17411	E+00	Vibrational energy
3.44883	E+00	A
0.4374296	E+00	B
0.387865	E+00	C
0.20455	E-03	DLK
-0.1426	E-05	DLJK
0.46727	E-06	DLJ
0.2075	E-05	dsK
0.7886	E-07	dsJ
0.382	E-07	HLK
-0.1474	E-08	HLKJ
0.0	E-11	HLJK
0.3215	E-12	HLJ
0.327	E-08	hsK
-0.7576	E-11	hsJK
0.1755	E-12	hsJ
-0.104	E-10	ALK
0.2739	E-12	ALKKJ
0.0	E-00	ALJK
0.2994	E-17	ALJ
-0.3251	E-15	ALJKJ
0.1812	E-12	AlsK
0.0	E-00	AlsJK
0.0	E-13	AlsKJ
0.0	E 00	AlsJ
0.333	E-14	PK
0.1895	E-15	PKKKJ
0.0	E-00	psK
0.0	E-00	QK
0.0	E-00	RK

Table 20. (Continued)

Flaud et. al. ozone (666) 101 state Watson constants

---

2110.78428	E+00	Vibrational energy
3.5019861	E+00	A
0.4385779	E+00	B
0.388266	E+00	C
0.213845	E-03	DLK
-0.1870	E-05	DLJK
0.46090	E-06	DLJ
0.4330	E-05	dsK
0.7482	E-07	dsJ
0.4085	E-07	HLK
-0.2173	E-08	HLKJ
0.22	E-10	HLJK
0.3215	E-12	HLJ
0.207	E-08	hsK
-0.7576	E-11	hsJK
0.1755	E-12	hsJ
-0.1106	E-10	ALK
0.2739	E-12	ALKKJ
0.0	E-00	ALJK
0.2994	E-17	ALJ
-0.3251	E-15	ALJJK
0.1812	E-12	AlsK
0.0	E-00	AlsJK
0.0	E-13	AlsKJ
0.0	E 00	AlsJ
0.333	E-14	PK
0.1895	E-15	PKKKJ
0.0	E-00	psK
0.0	E-00	QK
0.0	E-00	RK

---

Table 20. (Continued)

Flaud et. al. ozone (666) 200 state Watson constants

2195.87187	E+00	Vibrational energy
3.55982	E+00	A
0.4400887	E+00	B
0.390089	E+00	C
0.22394	E-03	DLK
-0.2641	E-05	DLJK
0.46579	E-06	DLJ
0.3510	E-05	dsK
0.6250	E-07	dsJ
0.468	E-07	HLK
-0.2405	E-08	HLKJ
-0.57	E-10	HLJK
0.3215	E-12	HLJ
0.143	E-08	hsK
-0.7576	E-11	hsJK
0.1755	E-12	hsJ
-0.191	E-10	ALK
0.2739	E-12	ALKKJ
0.0	E-00	ALJK
0.2994	E-17	ALJ
-0.3251	E-15	ALJJK
0.1812	E-12	AlsK
0.0	E-00	AlsJK
0.0	E-13	AlsKJ
0.0	E 00	AlsJ
0.333	E-14	PK
0.1895	E-15	PKKKJ
0.0	E-00	psK
0.0	E-00	QK
0.0	E-00	RK

Table 20. (Continued)

Flaud et. al. ozone (666) 110 state Watson constants

---

1796.26187	E+00	Vibrational energy
3.6108121	E+00	A
0.44144616	E+00	B
0.39029870	E+00	C
0.239727	E-03	DLK
-0.20753	E-05	DLJK
0.46689	E-06	DLJ
0.4321	E-05	dsK
0.6473	E-07	dsJ
0.4997	E-07	HLK
-0.2104	E-08	HLKJ
-0.84	E-10	HLJK
0.169	E-12	HLJ
-0.28	E-08	hsK
-0.33	E-10	hsJK
0.92	E-13	hsJ
-0.126	E-10	ALK
0.2739	E-12	ALKKJ
0.0	E-00	ALJK
0.2994	E-17	ALJ
-0.3251	E-15	ALJJK
0.1812	E-12	AlsK
0.0	E-00	AlsJK
0.0	E-13	AlsKJ
0.0	E 00	AlsJ
0.333	E-14	PK
0.1895	E-15	PKKKJ
0.0	E-00	psK
0.0	E-00	QK
0.0	E-00	RK

---

Table 20. (Continued)

Flaud et. al. ozone (666) 011 state Watson constants

		Vibrational energy
1726.52249	E+00	A
3.5523057	E+00	B
0.43989712	E+00	C
0.38850339	E+00	DLK
0.22865	E-03	DLJK
-0.1598	E-05	DLJ
0.45985	E-06	dsK
0.3495	E-05	dsJ
0.7610	E-07	HLK
0.464	E-07	HLKJ
-0.1876	E-08	HLJK
-0.311	E-10	HLJ
0.114	E-12	hsK
0.0	E-08	hsJK
0.0	E-11	hsJ
0.200	E-12	ALK
-0.108	E-10	ALKKJ
0.2739	E-12	ALJK
0.0	E-00	ALJ
0.2994	E-17	ALJK
-0.3251	E-15	AlsK
0.1812	E-12	AlsJK
0.0	E-00	AlsKJ
0.0	E-13	AlsJ
0.0	E 00	PK
0.333	E-14	PKKKJ
0.1895	E-15	psK
0.0	E-00	QK
0.0	E-00	RK

Table 20. (Continued)

Flaud et. al. ozone (686) ground state Watson constants

---

0.00000000	E+00	Vibrational energy
3.29049900	E+00	A
0.445399229	E+00	B
0.391329662	E+00	C
0.1808811	E-03	DLK
-0.13179	E-05	DLJK
0.44784	E-06	DLJ
0.31155	E-05	dsK
0.72905	E-07	dsJ
0.29550	E-07	HLK
-0.1475	E-08	HLKJ
-0.121	E-10	HLJK
0.439	E-12	HLJ
0.161	E-08	hsK
0.11	E-11	hsJK
0.160	E-12	hsJ
0.0	E-00	ALK
0.0	E-00	ALKKJ
0.0	E-00	ALJK
0.0	E-00	ALK
0.0	E-00	ALJJK
0.0	E-00	AlsK
0.0	E-00	AlsJK
0.0	E 00	AlsKJ
0.0	E 00	AlsJ
0.0	E-00	PK
0.0	E-00	PKKJ
0.0	E-00	psK
0.0	E-00	QK
0.0	E-00	RK

---

Table 20. (Continued)

Flaud et. al. ozone (686) 010 state Watson constants

---

693.30570	E+00	Vibrational energy
3.34155121	E+00	A
0.444188088	E+00	B
0.388900751	E+00	C
0.1990522	E-03	DLK
-0.12424	E-05	DLJK
0.450826	E-06	DLJ
0.37198	E-05	dsK
0.72243	E-07	dsJ
0.37749	E-07	HLK
-0.1709	E-08	HLKJ
-0.25	E-11	HLJK
0.332	E-12	HLJ
0.262	E-08	hsK
-0.55	E-11	hsJK
0.173	E-12	hsJ
-0.674	E-11	ALK
0.0	E-00	ALKKJ
0.0	E-00	ALJK
0.0	E-00	ALK
0.0	E-00	ALJJK
0.0	E-00	AlSK
0.0	E-00	AlsJK
0.0	E 00	AlSKJ
0.0	E 00	AlsJ
0.0	E-00	PK
0.0	E-00	PKKJ
0.0	E-00	psK
0.0	E-00	QK
0.0	E-00	RK

---

Table 20. (Continued)



Flaud et. al. ozone (686) 100 state Watson constants

1074.30756	E+00	Vibrational energy
3.290456	E+00	A
0.4428737	E+00	B
0.388777	E+00	C
0.181	E-03	DLK
-0.132	E-05	DLJK
0.448	E-06	DLJ
0.311	E-05	dsK
0.729	E-07	dsJ
0.313	E-07	HLK
-0.158	E-08	HLKJ
-0.300	E-11	HLJK
0.327	E-12	HLJ
0.217	E-08	hsK
-0.967	E-11	hsJK
0.187	E-12	hsJ
0.0	E-00	ALK
0.0	E-00	ALKKJ
0.0	E-00	ALJK
0.0	E-00	ALK
0.0	E-00	ALJJK
0.0	E-00	AlsK
0.0	E-00	AlsJK
0.0	E 00	AlsKJ
0.0	E 00	AlsJ
0.0	E-00	PK
0.0	E-00	PKKJ
0.0	E-00	psK
0.0	E-00	QK
0.0	E-00	RK

Table 20. (Continued)

Flaud et. al. ozone (686) 001 state Watson constants

---

1008.45277	E+00	Vibrational energy
3.243579	E+00	A
0.4415969	E+00	B
0.388332	E+00	C
0.17836	E-03	DLK
-0.1387	E-05	DLJK
0.45380	E-06	DLJ
0.2604	E-05	dsK
0.7713	E-07	dsJ
0.3082	E-07	HLK
-0.99	E-09	HLKJ
-0.300	E-11	HLJK
0.327	E-12	HLJ
0.217	E-08	hsK
-0.967	E-11	hsJK
0.187	E-12	hsJ
0.0	E-00	ALK
0.0	E-00	ALKKJ
0.0	E-00	ALJK
0.0	E-00	ALK
0.0	E-00	ALJJK
0.0	E-00	AlsK
0.0	E-00	AlsJK
0.0	E 00	AlsKJ
0.0	E 00	AlsJ
0.0	E-00	PK
0.0	E-00	PKKJ
0.0	E-00	psK
0.0	E-00	QK
0.0	E-00	RK

---

Table 20. (Continued)

Flaud et. al. ozone (668) ground state Watson constants

0.00000000	E+00	Vibrational energy
3.48818507	E+00	A
0.420008328	E+00	B
0.374008935	E+00	C
0.2038845	E-03	DLK
-0.190229	E-05	DLJK
0.406917	E-06	DLJ
0.29205	E-05	dsK
0.606059	E-07	dsJ
0.35200	E-07	HLK
-0.1589	E-08	HLKJ
-0.140	E-10	HLJK
0.300	E-12	HLJ
0.159	E-08	hsK
0.20	E-11	hsJK
0.112	E-12	hsJ
0.0	E-00	ALK
0.0	E-00	ALKKJ
0.0	E-00	ALJK
0.0	E-00	ALK
0.0	E-00	ALJKJ
0.0	E-00	AlsK
0.0	E-00	AlsJK
0.0	E 00	AlsKJ
0.0	E 00	AlsJ
0.0	E-00	PK
0.0	E-00	PKKJ
0.0	E-00	psK
0.0	E-00	QK
0.0	E-00	RK

Table 10. (Continued)

Flaud et. al. ozone (668) 010 state Watson constants

---

684.613410	E+00	Vibrational energy
3.53817681	E+00	A
0.418829269	E+00	B
0.371940160	E+00	C
0.223517	E-03	DLK
-0.185794	E-05	DLJK
0.409396	E-06	DLJ
0.35057	E-05	dsK
0.602338	E-07	dsJ
0.44078	E-07	HLK
-0.1832	E-08	HLKJ
-0.92	E-12	HLJK
0.315	E-12	HLJ
0.272	E-08	hsK
-0.76	E-11	hsJK
0.1500	E-12	hsJ
-0.523	E-11	ALK
-0.95	E-13	ALKKJ
0.0	E-00	ALJK
0.0	E-00	ALK
0.0	E-00	ALJKJ
0.0	E-00	Alsk
0.0	E-00	AlsJK
0.0	E 00	AlskJ
0.0	E 00	AlsJ
0.0	E-00	PK
0.0	E-00	PKKJ
0.0	E-00	psK
0.0	E-00	OK
0.0	E-00	RK

---

Table 20. (Continued)

Flaud et. al. ozone (668) 100 state Watson constants

---

1087.321	E+00	Vibrational energy
3.492163	E+00	A
0.4177232	E+00	B
0.371583	E+00	C
0.21002	E-03	DLK
-0.21110	E-05	DLJK
0.41042	E-06	DLJ
0.367	E-05	dsK
0.5909	E-07	dsJ
0.465	E-07	HLK
-0.171	E-08	HLKJ
-0.300	E-11	HLJK
0.237	E-12	HLJ
0.230	E-08	hsK
-0.113	E-10	hsJK
0.160	E-12	hsJ
0.0	E-00	ALK
0.0	E-00	ALKKJ
0.0	E-00	ALJK
0.0	E-00	ALK
0.0	E-00	ALJJK
0.0	E-00	AlsK
0.0	E-00	AlsJK
0.0	E 00	AlsKJ
0.0	E 00	AlsJ
0.0	E-00	PK
0.0	E-00	PKKJ
0.0	E-00	psK
0.0	E-00	QK
0.0	E-00	RK

---

Table 20. (Continued)

Flaud et. al. ozone (668) 001 state Watson constants

1031.144	E+00	Vibrational energy
3.437126	E+00	A
0.41623161	E+00	B
0.370827	E+00	C
0.20100	E-03	DLK
-0.18600	E-05	DLJK
0.41252	E-06	DLJ
0.2265	E-05	dsK
0.6396	E-07	dsJ
0.346	E-07	HLK
-0.171	E-08	HLKJ
-0.300	E-11	HLJK
0.237	E-12	HLJ
0.230	E-08	hsK
-0.113	E-10	hsJK
0.160	E-12	hsJ
0.0	E-00	ALK
0.0	E-00	ALKKJ
0.0	E-00	ALJK
0.0	E-00	ALK
0.0	E-00	ALJKK
0.0	E-00	AlsK
0.0	E-00	AlsJK
0.0	E 00	AlsKJ
0.0	E 00	AlsJ
0.0	E-00	PK
0.0	E-00	PKKJ
0.0	E-00	psK
0.0	E-00	QK
0.0	E-00	RK

Table 20. (Continued)

T(K)	Isotopic species AFGL notation		
	666	686	668
75.0	423.57301	442.04036	452.18747
100.0	651.93939	680.37119	696.01106
125.0	911.29072	951.06373	972.96670
150.0	1199.11158	1251.55313	1280.46761
175.0	1514.51893	1581.01883	1617.70104
200.0	1857.98773	1940.05606	1985.26019
225.0	2231.08186	2330.30476	2384.75109
250.0	2636.19739	2754.06241	2818.40078
275.0	3076.33884	3213.93102	3288.70960
300.0	3554.93599	3712.52993	3798.17253
325.0	4075.69798	4252.28448	4349.07628
350.0	4642.49715	4835.28585	4943.36631
375.0	5259.27411	5463.21039	5582.57170
400.0	5929.95802	6137.28490	6267.77471

Table 21. Partition Sums from a "Complete" Set of  $O_3$  Energy Levels

T(K)	Q(up)	% Err	Q(actual)	% Err	Q(down)
666 isotope					
100.0	653.89971	.30	651.93939	-.30	649.98887
200.0	1863.73002	.31	1857.98773	-.31	1852.27591
296.0	3487.31957	.33	3475.62583	-.34	3464.00203
300.0	3566.94909	.34	3554.93599	-.34	3542.99506
400.0	5952.39804	.38	5929.95802	-.38	5907.66662
686 isotope					
100.0	682.41710	.30	680.37119	-.30	678.33551
200.0	1946.06082	.31	1940.05606	-.31	1934.08323
296.0	3642.21345	.33	3630.04803	-.34	3617.95402
300.0	3725.01776	.33	3712.52993	-.34	3700.11563
400.0	6159.67172	.36	6137.28490	-.36	6115.03544
668 isotope					
100.0	698.10417	.30	696.01106	-.30	693.92840
200.0	1991.40759	.31	1985.26019	-.31	1979.14548
296.0	3726.35560	.33	3713.92951	-.33	3701.57603
300.0	3810.92570	.33	3798.17253	-.34	3785.49411
400.0	6290.51425	.36	6267.77471	-.36	6245.17363

Table 22. Error Analysis for the Isotopic Species of O<sub>3</sub>



Temp(K)	Error	Q <sub>actual</sub>	Q <sub>total</sub>	Q <sub>vib</sub>	Q <sub>rot</sub>
100.	.0000	651.9394	651.9395	1.0000	651.9119
200.	-.0008	1857.9880	11858.0030	1.0074	1844.3030
225.	-.0008	2231.0820	2231.0990	1.0136	2201.1150
250.	-.0002	2636.1980	2636.2020	1.0224	2578.5150
275.	.0012	3076.3390	3076.3010	1.0339	2975.4720
300.	.0035	3554.9360	3554.8120	1.0483	3391.1030
325.	.0066	4075.6980	4075.4300	1.0656	3824.6350
350.	.0101	4642.4970	4642.0260	1.0858	4275.3910
375.	.0135	5259.2740	5258.5630	1.1088	4742.7660
395.	.0155	5791.3220	5790.4260	1.1291	5128.2660

Table 20. Test of Approximation  $Q_{\text{actual}} = Q_{\text{vib}} \cdot Q_{\text{rot}}$  for the Principle Species of  $\text{O}_3$

Toth's Effective rotational constants for the 0000 state of 446 N2O

1	1	91	120	
0.0000000000	E 00			G
0.4190110012	E 00			B
1.76091933	E-07			D
-0.1652924	E-13			H
0.00000	E-18			L

Toth's Effective rotational constants for the 0110E state of 446 N2O

1	2E	80	120	
588.768	E 00			G
0.4191779259	E 00			B
1.78324547	E-07			D
-0.17146	E-13			H
0.00000	E-18			L

Toth's Effective rotational constants for the 0110F state of 446 N2O

1	2F	80	120	
588.768	E 00			G
0.4199698451	E 00			B
1.79303055	E-07			D
-0.17668	E-13			H
0.00000	E-18			L

Toth's Effective rotational constants for the 0200 state of 446 N2O

1	3	78	120	
1168.1323	E 00			G
0.419920957	E 00			B
2.49403822	E-07			D
30.82612	E-13			H
-18.9735	E-18			L

Toth's Effective rotational constants for the 0220E state of 446 N2O

1	4E	78	120	
1177.7446	E 00			G
0.420125256	E 00			B
1.196793	E-07			D
-29.5680	E-13			H
-24.48239	E-18			L

Toth's Effective rotational constants for the 0220F state of 446 N2O

1	4F	78	120	
1177.7446	E 00			G
0.420126260	E 00			B
1.8180	E-07			D
0.9510	E-13			H
0.00000	E-18			L

Table 24. Vibrational-Rotational Hamiltonian Constants for N<sub>2</sub>O from Toth

Toth's Effective rotational constants for the 1000 state of 446 N2O

1	5	76	120
1284.9		E 00	G
0.417255097		E 00	B
1.7261943		E-07	D
1.263279		E-13	H
3.492826		E-18	L

Toth's Effective rotational constants for the 0310E state of 446 N2O

1	6E	68	120
1749.0651		E 00	G
0.419583988		E 00	B
2.109928		E-07	D
11.75046		E-13	H
-12.20395		E-18	L

Toth's Effective rotational constants for the 0310F state of 446 N2O

1	6F	68	120
1749.0651		E 00	G
0.421079177		E 00	B
2.178319		E-07	D
-3.200163		E-13	H
14.50675		E-18	L

Toth's Effective rotational constants for the 0330E state of 446 N2O

1	7E	67	120
1766.912		E 00	G
0.420667057		E 00	B
1.593325		E-07	D
-29.1628		E-13	H
0.0		E-18	L

Toth's Effective rotational constants for the 0330F state of 446 N2O

1	7F	67	120
1766.912		E 00	G
0.4206713799		E 00	B
1.6806495		E-07	D
29.5664		E-13	H
0.0		E-18	L

Toth's Effective rotational constants for the 0330E state of 446 N2O

1	7E	1	2
1766.912		E 00	G
0.420667057		E 00	B
1.593325		E-07	D
-29.1628		E-13	H
0.0		E-18	L

Table 24. (Continued)

Toth's Effective rotational constants for the 0330F state of 446 N2O

1	7F	1	2	
1766.912		E 00		G
0.4206713799		E 00		B
1.6806495		E-07		D
29.5664		E-13		H
0.0		E-18		L

Toth's Effective rotational constants for the 1110E state of 446 N2O

1	8E	66	120	
1880.2657		E 00		G
0.4174647588		E 00		B
1.74899344		E-07		D
1.138277		E-13		H
0.00000		E-18		L

Toth's Effective rotational constants for the 1110F state of 446 N2O

1	8F	66	120	
1880.2657		E 00		G
0.4183730749		E 00		B
1.72005845		E-07		D
2.246281		E-13		H
0.00000		E-18		L

Table 24. (Continued)

Toth's Effective rotational constants for the 0000 state of 456 N2O

2	1	78	120
0.0000000000	E 00		G
0.4189818102	E 00		B
1.76326469	E-07		D
0.0	E-13		H
0.00000	E-18		L

Toth's Effective rotational constants for the 0110E state of 456 N2O

2	2E	68	120
588.768	E 00		G
0.4191089166	E 00		B
1.78583283	E-07		D
0.0	E-13		H
0.00000	E-18		L

Toth's Effective rotational constants for the 0110F state of 456 N2O

2	2F	68	120
588.768	E 00		G
0.4199186417	E 00		B
1.79446290	E-07		D
0.0	E-13		H
0.00000	E-18		L

Toth's Effective rotational constants for the 0200 state of 456 N2O

2	3	1	120
1168.1323	E 00		G
0.4199204111	E 00		B
2.8246994	E-07		D
58.90136	E-13		H
0.0	E-18		L

Toth's Effective rotational constants for the 0220E state of 456 N2O

2	4E	1	120
1177.7446	E 00		G
0.42003233	E 00		B
0.9542	E-07		D
0.0	E-13		H
0.0	E-18		L

Table 24. (Continued)

Toth's Effective rotational constants for the 0220F state of 456 N2O

2	4F	1	120
1177.7446		E 00	G
0.42003483		E 00	B
1.8131		E-07	D
0.0		E-13	H
0.00000		E-18	L

Toth's Effective rotational constants for the 1000 state of 456 N2O

2	5	1	120
1284.9		E 00	G
0.417127383		E 00	B
1.75528298		E-07	D
0.60935		E-13	H
0.0		E-18	L

Toth's Effective rotational constants for the 1110E state of 456 N2O

2	8E	1	120
1880.2657		E 00	G
0.4172733118		E 00	B
1.77554100		E-07	D
0.562150		E-13	H
0.00000		E-18	L

Toth's Effective rotational constants for the 1110F state of 456 N2O

2	8F	1	120
1880.2657		E 00	G
0.4181654622		E 00	B
1.76635130		E-07	D
2.288250		E-13	H
0.00000		E-18	L

Table 24. (Continued)

Toth's Effective rotational constants for the 0000 state of 546 N2O

3	1	79	120	
0.0000000000	E 00			G
0.404857965155	E 00			B
1.64294216	E-07			D
1.867536	E-13			H
0.00000	E-18			L

Toth's Effective rotational constants for the 0110E state of 546 N2O

3	2E	69	120	
588.768	E 00			G
0.4050372717	E 00			B
1.65680840	E-07			D
0.0	E-13			H
0.00000	E-18			L

Toth's Effective rotational constants for the 0110F state of 546 N2O

3	2F	69	120	
588.768	E 00			G
0.40578110957	E 00			B
1.66742291	E-07			D
0.0	E-13			H
0.00000	E-18			L

Toth's Effective rotational constants for the 0200 state of 546 N2O

3	3	1	120	
1168.1323	E 00			G
0.40571242618	E 00			B
2.224294126	E-07			D
21.26045	E-13			H
0.0	E-18			L

Toth's Effective rotational constants for the 0220E state of 546 N2O

3	4E	1	120	
1177.7446	E 00			G
0.405951230	E 00			B
1.21815	E-07			D
0.0	E-13			H
0.0	E-18			L

Toth's Effective rotational constants for the 0220F state of 546 N2O

3	4F	1	120	
1177.7446	E 00			G
0.405950430	E 00			B
1.69110	E-07			D
0.0	E-13			H
0.00000	E-18			L

Table 24. (Continued)

Toth's Effective rotational constants for the 1000 state of 546 N2O

3	5	1	120
1284.9		E 00	G
0.403263631305		E 00	B
1.5980072		E-07	D
3.702650		E-13	H
0.0		E-18	L

Toth's Effective rotational constants for the 0310E state of 546 N2O

3	6E	1	120
1749.0651		E 00	G
0.405410701		E 00	B
1.9139457		E-07	D
0.0		E-13	H
0.0		E-18	L

Toth's Effective rotational constants for the 0310F state of 546 N2O

3	6F	1	120
1749.0651		E 00	G
0.4067990584		E 00	B
1.99573470		E-07	D
0.0		E-13	H
0.0		E-18	L

Toth's Effective rotational constants for the 1110E state of 546 N2O

3	8E	1	120
1880.2657		E 00	G
0.40348977155		E 00	B
1.61182100		E-07	D
0.657200		E-13	H
0.00000		E-18	L

Toth's Effective rotational constants for the 1110F state of 546 N2O

3	8F	1	120
1880.2657		E 00	G
0.40435854185		E 00	B
1.57574110		E-07	D
0.244250		E-13	H
0.00000		E-18	L

Table 24. (Continued)



Toth's Effective rotational constants for the 0000 state of 448 N2O

4	1	78	120
0.0000000000	E 00		G
0.39557789529	E 00		B
1.58345694	E-07		D
0.0	E-13		H
0.00000	E-18		L

Toth's Effective rotational constants for the 0110E state of 448 N2O

4	2E	68	120
588.768	E 00		G
0.39575970106	E 00		B
1.60023584	E-07		D
0.0	E-13		H
0.00000	E-18		L

Toth's Effective rotational constants for the 0110F state of 448 N2O

4	2F	68	120
588.768	E 00		G
0.396471172725	E 00		B
1.61077378	E-07		D
0.0	E-13		H
0.00000	E-18		L

Toth's Effective rotational constants for the 0200 state of 448 N2O

4	3	1	120
1168.1323	E 00		G
0.396278094345	E 00		B
2.05540250	E-07		D
11.96215	E-13		H
0.0	E-18		L

Toth's Effective rotational constants for the 1000 state of 448 N2O

4	5	1	120
1284.9	E 00		G
0.394111321136	E 00		B
1.49508691	E-07		D
3.498220	E-13		H
0.0	E-18		L

Table 14. (Continued)

Toth's Effective rotational constants for the 0310E state of 448 N2O

4	6E	1	120	
1749.0651		E 00		G
0.3959890999		E 00		B
1.836545		E-07		D
0.0		E-13		H
0.0		E-18		L

Toth's Effective rotational constants for the 0310F state of 448 N2O

4	6F	1	120	
1749.0651		E 00		G
0.3972774667		E 00		B
1.93453325		E-07		D
0.0		E-13		H
0.0		E-18		L

Toth's Effective rotational constants for the 1110E state of 448 N2O

4	8E	1	120	
1880.2657		E 00		G
0.3943490062		E 00		B
1.52755220		E-07		D
0.0		E-13		H
0.0		E-18		L

Toth's Effective rotational constants for the 1110F state of 448 N2O

4	8F	1	120	
1880.2657		E 00		G
0.3952190532		E 00		B
1.47157125		E-07		D
0.0		E-13		H
0.0		E-18		L

Table 24. (Continued)

Toth's Effective rotational constants for the 0000 state of 447 N2O

5	1	78	120	
0.0000000000		E 00		G
0.406672154476		E 00		B
1.66397195		E-07		D
0.0		E-13		H
0.0		E-18		L

Table 24. (Continued)

Toth's Effective rotational constants for the 0110E state of 447 N2O

5	2E	68	120	
588.768		E 00		G
0.4068471		E 00		B
1.6836		E-07		D
0.0		E-13		H
0.0		E-18		L

Toth's Effective rotational constants for the 0110F state of 447 N2O

5	2F	68	120	
588.768		E 00		G
0.4075991		E 00		B
1.7139		E-07		D
0.0		E-13		H
0.0		E-18		L

Toth's Effective rotational constants for the 0200 state of 447 N2O

5	3	1	120	
1168.1323		E 00		G
0.40748554120		E 00		B
2.222921200		E-07		D
13.82892		E-13		H
0.0		E-18		L

Toth's Effective rotational constants for the 1000 state of 447 N2O

5	5	1	120	
1284.9		E 00		G
0.4050539924		E 00		B
1.6100012		E-07		D
3.37195		E-13		H
0.0		E-18		L

Table 24. (Continued)

Toth's Effective rotational constants for the 1110E state of 447 N2O

5	8E	1	120	
1880.2657		E 00		G
0.40528198274		E 00		B
1.62997350		E-07		D
0.0		E-13		H
0.0		E-18		L

Toth's Effective rotational constants for the 1110F state of 447 N2O

5	8F	1	120	
1880.2657		E 00		G
0.40616960105		E 00		B
1.60573455		E-07		D
0.0		E-13		H
0.0		E-18		L

Table 24. (Continued)

ivlow	vibrational state	ivlow	vibrational state
1	0000	5	1000
2	0110E, 00110F	6	0310E, 0310F
3	0200	7	0300E, 0300F
4	0200E, 0200F	8	1110E, 1110F

For N<sub>2</sub>O the energy levels can be expressed by the formula:

$$E_{v_r} = G + B - DX^2 + HX^3 + LX^4, \quad (25)$$

where  $X = J(J + 1)$  and G, B, D, H and L are effective constants given in reference 41 (see also Table 24). The missing J levels for each isotopic species and each vibrational state are given below in Table 25 while the band origins for the vibrational states from Toth<sup>42</sup> are given in Table 26.

Table 25. Last J-Level for N<sub>2</sub>O Data From the AFGL Database  
Vibrational State

isotopic species	0000	0110	0200	0220	1000	0310	0300	1110
446	91	80	78	78	76	68	67	66
456	78	68						
546	79	69						
448	78	68						
447	77	60						

Table 26. Band Origins for the Various Vibrational Levels

Vib. Level	Band Origin in $\text{cm}^{-1}$ for Isotopic Species				
	446	456	546	448	447
0100	588.768	575.5	585.320	584.1	586.3
0200	1168.1323	1144.3334	1159.9717	1155.1399	
0220	1177.7446				
1000	1284.9		1269.8920	1246.8846	1264.7047
0310	1749.0651				
0300	1766.912				
1110	1880.2657	1860.1913	1862.7670	1839.9361	

Some 4000 energy levels were calculated to fill the  $\text{N}_2\text{O}$  energy array. Because of the time necessary for file transfer to and from the VAX an energy cutoff of  $5000 \text{ cm}^{-1}$  was enforced bringing the number of calculated levels to 2888. The complete set of energy levels (to  $5000 \text{ cm}^{-1}$ ) was then used to calculate the partition sums for  $\text{N}_2\text{O}$ . In the error analysis part of the calculations, the recalculated (high J) levels are flagged by a negative sign and a shift of 0.5% is used. For all other levels the 0.2% shift was used. Table 27 lists the partition sums for  $\text{N}_2\text{O}$ . The error analysis gave approximately a 0.5% error at 500 K for the 546 species as the largest error.

#### 5.4.1 CO

The total internal partition sums for CO were calculated; however, the polynomial fit has not yet been done. For this molecule

T(K)	Isotopic species AFGL notation				
	446	456	546	448	477
75.0	124.77949	124.78836	129.13001	132.15226	128.54835
100.0	166.33257	166.35749	172.13874	176.17161	171.36247
200.0	342.09902	343.05349	354.26476	362.50801	352.45213
225.0	391.78094	393.28109	405.81071	415.03689	403.44352
250.0	445.02930	447.16813	461.06764	471.07548	457.80734
270.0	490.54599	493.22996	508.29755	518.68522	503.95600
296.0	554.01800	557.39564	574.13339	584.53580	567.70333
300.0	564.24195	567.71963	584.73393	595.07935	577.89900
325.0	631.08477	635.10712	654.00040	663.55749	644.02468
350.0	703.26770	707.61797	728.70833	736.61184	714.35619
400.0	864.98315	868.84845	895.63565	897.03323	867.81020
500.0	1265.20127	1259.64420	1305.56265	1278.03489	1225.49795

Table 27. Partition Sums for  $N_2O$  from a "Complete" Set of Energy Levels



the energy levels were calculated using the Dunham expansion. The original program and Dunham coefficients were supplied to us by R. Tipping, University of Alabama. Because the number of levels is relatively small we have calculated all levels from  $J = 0$  to 74 for the ten lowest vibrational levels ( $v = 0, 9$ ). This generates energies to  $\approx 28,000 \text{ cm}^{-1}$ . The calculations were done for the four isotopic species of CO on the database.

### 5.5 Methane

For the methane molecule, complete energy level listings for the ground states of the  $^{12}\text{CH}_4$  and  $^{13}\text{CH}_4$  species were obtained from Dr. Linda Brown, Jet Propulsion Laboratory. The energies are given for  $J$  up to 31 ( $\sim 5000. \text{ cm}^{-1}$ ). These were merged with the upper vibrational state energies from the database to get a "complete" set of energies. The partition sums were calculated for these species and are given in Table 28. In Figure 21 a plot of the partition sum for each species of carbon vs. energy at 400 K is presented. We note the sums have converged. The polynomial coefficients for the temperature expression were then calculated for this molecule.

### 5.6 Nitrogen Dioxide

For nitrogen dioxide only the principal isotopic species is present on the database,  $^{14}\text{N}^{16}\text{O}_2$ . The coupling of the rotational wave functions and the nuclear statistics for the symmetric oxygen atoms for this molecule is the same as for symmetric  $\text{O}_3$ , i.e. the only allowed levels are for  $K_a + K_c + v_3$  even. All energy levels were determined via theory. The molecular constants were obtained for

TABLE 23		
Partition Functions for CH <sub>4</sub> vs. T		
T	Q	ln Q
0.0	1.000000	0.000000
10.0	1.000000	0.000000
20.0	1.000000	0.000000
30.0	1.000000	0.000000
40.0	1.000000	0.000000
50.0	1.000000	0.000000
60.0	1.000000	0.000000
70.0	1.000000	0.000000
80.0	1.000000	0.000000
90.0	1.000000	0.000000
100.0	1.000000	0.000000
150.0	1.000000	0.000000
200.0	1.000000	0.000000
250.0	1.000000	0.000000
300.0	1.000000	0.000000
350.0	1.000000	0.000000
400.0	1.000000	0.000000
450.0	1.000000	0.000000
500.0	1.000000	0.000000
550.0	1.000000	0.000000
600.0	1.000000	0.000000
650.0	1.000000	0.000000
700.0	1.000000	0.000000
750.0	1.000000	0.000000
800.0	1.000000	0.000000
850.0	1.000000	0.000000
900.0	1.000000	0.000000
950.0	1.000000	0.000000
1000.0	1.000000	0.000000

Table 23. Partition Functions for CH<sub>4</sub> vs. T

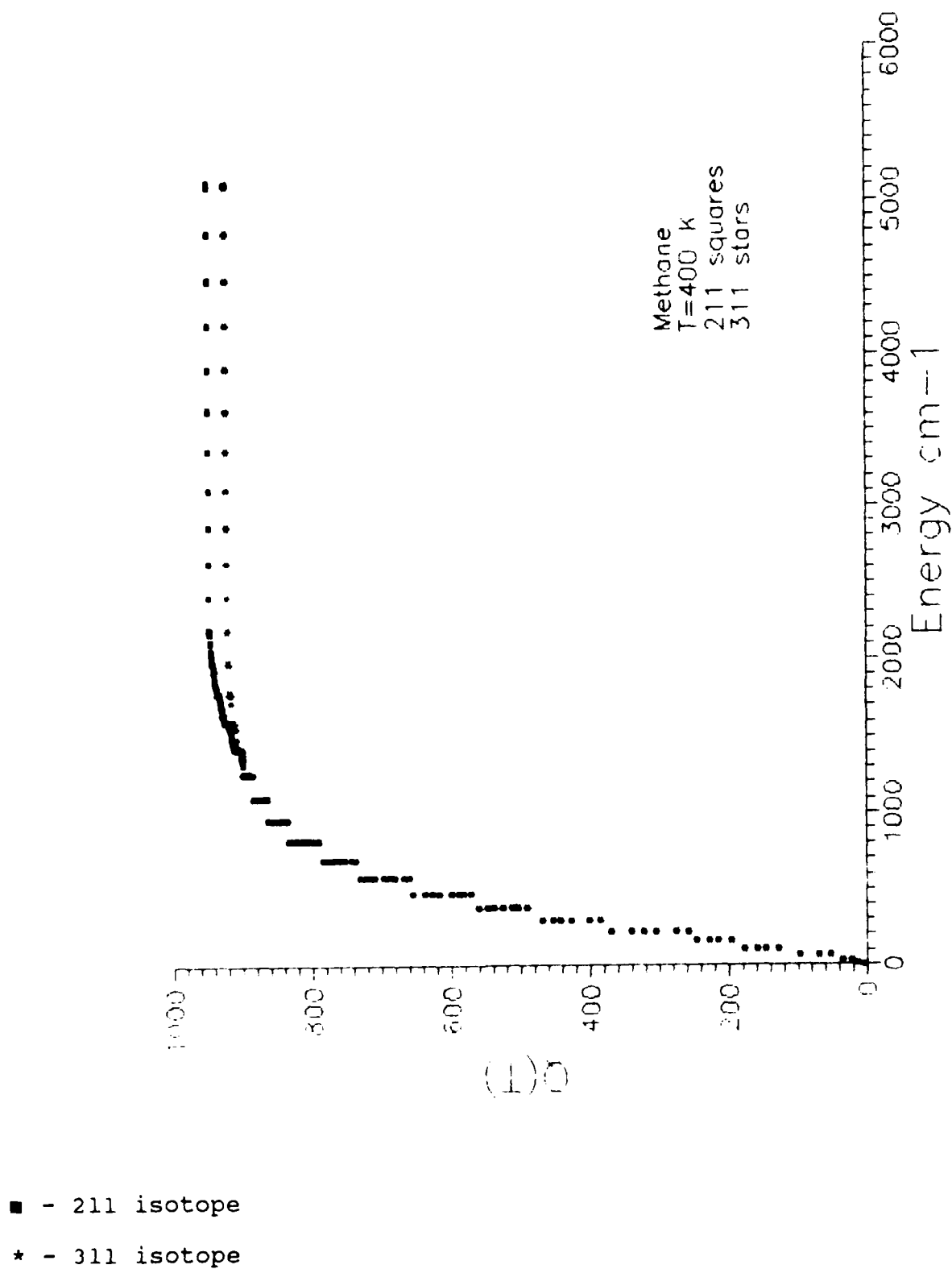


Figure 11. Partition Sum vs. Energy for  $^{12}\text{CH}_4$  and  $^{13}\text{CH}_4$  at 400 K

the first eleven vibrational states of NO<sub>2</sub>. The constants were taken from reference 43 for the 000, 010, 020, 100, 001, 030 and 011 bands and from reference 44 for the 120, 101, 130 and the 111 bands. All energies from  $J = 0$  to 75 were calculated and those less than 5000 cm<sup>-1</sup> were retained.

Nitrogen dioxide has an unpaired electron which complicates its structure. The rotational quantum numbers are labeled by  $N$ ,  $K_a$  and  $K_c$  (note  $K_a$  and  $K_c$  can be combined into one quantum number  $\tau = K_a - K_c$ ) where  $N$  is the angular momentum, rotational and electron orbital, and  $K_a$  and  $K_c$  are the prolate and oblate limit of  $K$ . The electron spin ( $S = 1/2$ ) and rotational angular momentum ( $N$ ) couple to give the total electron and rotational angular momentum  $J = N \pm S = N \pm 1/2$ , thus the spin-rotation interaction splits the energy levels into two components. The energy can be expressed as a rotational energy,  $E_r$  given by diagonalizing the Watson Hamiltonian, and a contribution due to the spin-rotation interaction. The spin-rotation interaction terms determined up to second order are:

$$F_1 = \frac{E_r}{hc} + \frac{1}{2(N+1)} \left[ \begin{aligned} &(\epsilon_{aa} - \bar{\epsilon}) K_a^2 + \bar{\epsilon} N(N+1) + \gamma \frac{(\epsilon_{bb} - \epsilon_{cc})}{4} \delta_{1,K_a} N(N+1) \\ &+ \eta_{aaaa} K_a^4 - \frac{(\epsilon_{aa} - \bar{\epsilon})}{4B} K_a^2 \left( 1 - \frac{K_a^2}{(N+1)^2} \right) \end{aligned} \right] \quad (26)$$

for  $J = N + 1/2$ , and

$$F_2 = \frac{E_r}{hc} + \frac{1}{2N} \left[ (\epsilon_{aa} - \epsilon) K_a^2 + \epsilon N(N+1) + \gamma \frac{(\epsilon_{bb} - \epsilon_{cc})}{4} \delta_{1,K} N(N+1) \right. \\ \left. + \eta_{aaaa} K_a^4 - \frac{(\epsilon_{aa} - \epsilon)}{4B} K_a^2 \left( 1 - \frac{K_a^2}{N^2} \right) \right] \quad (27)$$

for  $J = N - 1/2$  ( $N > 0$ )

In these equations  $\epsilon = (1/2)(\epsilon_{bb} - \epsilon_{cc})$ ;  $B = (1/2)(B+C)$ ;  $\gamma = -1$  for  $N$  odd and  $\gamma = +1$  for  $N$  even. The spin-rotation constants are given in terms of the  $\epsilon_{aa}$ ,  $\epsilon_{bb}$ ,  $\epsilon_{cc}$  and  $\eta_{aaaa}$ . From the papers listed above, spin-rotation constants are available for the following bands: 000, 010, 120, 101, 130, and 111. For the other bands, 020, 100, 001, 030 and 011, only the rotation energy was calculated and a splitting factor of 2 was multiplied times these levels in the partition sums, i.e. the degeneracy factor.

We started by calculating the rotational contribution to the energy levels. All states for  $N = 0$  to 75 were considered with the cutoff at  $5000 \text{ cm}^{-1}$ . The calculations had some difficulties: for lower values of  $N$  the calculations matched the published values, however, extrapolation to higher values was clearly incorrect. For example, the state **44 6 38** is present on the database and has an energy of  $1105.6 \text{ cm}^{-1}$ , the calculated value from diagonalizing the Watson Hamiltonian was  $402.9 \text{ cm}^{-1}$ . From the calculations there were many other examples of levels that were incorrect, some wild extrapolations, negative energies, etc. In order to calculate the partition sums accurate to one percent, these levels must be evaluated. We looked at several ways to estimate the missing levels, e.g. filling in with levels that were present on the database and

trying fits for the other missing levels. For NO<sub>2</sub>, the rotational constants B and C are approximately equal to give a near prolate symmetric top but the limiting energy formula does not give accurate enough results for the calculations. We also investigated the change in energy with respect to K<sub>a</sub> and again this was of little help for prediction of the energies that were needed.

We then considered the fitting procedure that is normally used to give the Watson Hamiltonian constants. As one goes up in the terms of the Hamiltonian the constants get smaller and smaller. However, these multiply angular momentum to larger and larger powers. Thus, if one of the upper constants is off by a small amount, the calculations diverge as J increases. We then took the ground state Watson constants from Camy-Peyret et. al.<sup>43</sup> (this publication references the work of W. Lafferty, N.B.S. for the ground state Hamiltonian constants) and set the three highest constants,  $h_K$ ,  $h_{KN}$ , and  $L_K$ , to zero (these are angular momentum to the sixth, sixth, and eighth powers, respectively). The calculations were repeated with these constants and compared with the published values (those on the HITRAN database). Table 29 gives examples for some levels that were in error before.

Table 29. Comparison of Calculated Energies in cm<sup>-1</sup> with Published Values

State	E(calc)	E(pub)	% diff
29 10 20	1099.8	1102.	0.2
12 12 0	1102.1	1109.	0.62
44 6 38	1105.6	1105.6	0.0
51 1 51	1106.8	1106.7	-0.005

The agreement is very good and it appears that this was the problem. We tested eliminating only the highest constant  $L_K$  (this is

0.00000000	E+00	Vibrational energy
8.00236557	E+00	A
0.43370699	E+00	B
0.41044632	E+00	C
0.268804	E-02	DLK
-0.19492	E-04	DLJK
0.300692	E-06	DLJ
0.3566	E-05	dsK
0.31772	E-07	dsJ
0.29445	E-05	HLK
-0.1953	E-07	HLKJ
-0.379	E-09	HLJK
0.513	E-12	HLJ
- 0.1591	E-06	hsk
0.205	E-12	hsJK
0.0	E-07	hsJ
0.0000	E-08	ALK
0.0	E-07	ALKKJ
0.0	E-08	ALJK
0.000	E-08	ALK
0.0	E-10	ALJJK
0.0	E-07	ALsK
0.0	E-10	ALsJK
0.00	E-00	ALsKJ
0.00	E-00	ALsJ
0.0	E-09	PK
0.0	E-12	PKKJ
0.0	E-10	psK
0.0	E-12	PK
0.0	E-15	PK

	0	75	0	1.0	1.0							
	0	1	1	1	1	1	1	1	1	1	1	1
	0	75	0									
	0	75										
0.5000			E-04	.1				E-09				

125

Flaud and Camy-Peyret (010) state 400 Watson constants  
2 010

749.65370	E+00	Vibrational energy
0.373872	E+00	G
0.4336339	E+00	B
0.4095654	E+00	C
0.34257	E-02	DLE
0.21855	E-04	DLJK
0.3077	E-06	DLJ
0.795	E-05	dSK
0.3103	E-07	dSJ
0.4108	E-05	HLK
0.356	E-07	HLKJ
0.0	E-09	HLJK
0.513	E-12	HLJ
0.0	E-06	hSK
0.0	E-12	hSJJK
0.0	E-07	hSJ
0.0	E-08	HLK
0.0	E-07	HLKKJ
0.0	E-08	HLJK
0.000	E-08	HLK
0.0	E-10	HLJJK
0.0	E-07	HLsK
0.0	E-10	HLsJK
0.00	E-06	HLsKJ
0.00	E-06	HLsJ
0.0	E-09	PK
0.0	E-12	PRKJ
0.0	E-10	PSK
0.0	E-12	PK
0.0	E-15	PK
0 75	0 1.0 1.0	
0 1	1 1 1 1 1 1 1 1 1 1	
0 75	0	
0 75		
0.5000	E-04 .1	E-09

Table 30. (Continued)



1 Flaud and Camy-Peyret (020) state 466 Watson constants

2 020											
1498.355		E+00	Vibrational energy								
8.7838		E+00	A								
0.433538		E+00	B								
0.408687		E+00	C								
0.4579		E-02	DLK								
-0.24699		E-04	DLJK								
0.300692		E-06	DLJ								
0.620		E-05	dsk								
0.31772		E-07	dsJ								
0.495		E-05	HLK								
-0.397		E-07	HLKJ								
0.0		E-09	HLJK								
0.513		E-12	HLJ								
0.0		E-06	hsk								
0.0		E-12	hsJK								
0.0		E-07	hsJ								
0.0		E-08	ALK								
0.0		E-07	ALKKJ								
0.0		E-08	ALKJ								
0.000		E-08	ALK								
0.0		E-10	ALJJK								
0.0		E-07	Alsk								
0.0		E-10	AlsJK								
0.00		E-00	AlsKJ								
0.00		E-00	AlsJ								
0.0		E-09	PK								
0.0		E-12	PKKJ								
0.0		E-10	psK								
0.0		E-12	QK								
0.0		E-15	KK								
0	75	0	1.0	1.0							
0	1	1	1	1	1	1	1	1	1	1	1
0	75	0									
0	75										
0.5000		E-04	.1						E-09		

Table 30. (Continued)

2 100

0.5000

Table 30. (Continued)

1 Flaud and Camy-Peyret (001) state 466 Watson constants

2 001			
1616.853	E+00	Vibrational energy	
7.773806	E+00	A	
0.4309453	E+00	B	
0.407373	E+00	C	
0.25063	E-02	DLK	
-0.21196	E-04	DLJK	
0.3050	E-06	DLJ	
0.355	E-05	dsk	
0.3072	E-07	dsJ	
0.2372	E-05	HLK	
-0.828	E-08	HLKJ	
-0.1182	E-09	HLJK	
0.56	E-12	HLJ	
0.0	E-06	hsk	
0.0	E-12	hsJK	
0.0	E-07	hsJ	
0.0000	E-08	ALK	
0.0	E-07	ALKKJ	
0.0	E-08	ALJK	
0.0	E-08	ALK	
0.0	E-10	ALJJK	
0.0	E-07	Alsk	
0.0	E-10	AlsJK	
0.0	E 00	AlsKJ	
0.0	E 00	AlsJ	
0.0	E-09	PK	
0.0	E-12	PKKJ	
0.0	E-10	psK	
0.0	E-12	RK	
0.0	E-15	RK	
0 75	0 1.0	1.0	
0 1	1 1	1	1 1 1 1 1 1 1
0 75	0		
0 75			
0.5000	E-04 .1		E-09

Table 30. (Continued)

Flaud and Camy-Peyret (030) state 466 Watson constants

2 030											
2245.991	E+00	Vibrational energy									
0.2233	E+00	A									
0.433460	E+00	B									
0.407800	E+00	C									
0.54	E-02	DLK									
0.273	E-04	DLJK									
0.300692	E-06	DLJ									
0.720	E-05	dsk									
0.31772	E-07	dsJ									
0.000	E-05	HLK									
0.0	E-07	HLKJ									
0.0	E-09	HLJK									
0.0	E-12	HLJ									
0.0	E-06	hsk									
0.0	E-12	hsJK									
0.0	E-07	hsJ									
0.0	E-08	ALK									
0.0	E-07	ALKKJ									
0.0	E-08	ALJK									
0.000	E-08	ALK									
0.0	E-10	ALJJK									
0.0	E-07	Alsk									
0.0	E-10	AlsJK									
0.00	E-06	AlsKJ									
0.00	E-06	AlsJ									
0.0	E-09	PK									
0.0	E-12	PKKJ									
0.0	E-10	psK									
0.0	E-12	QR									
0.0	E-15	RK									
0 75	0 1.0 1.0										
0 1	1 1 1 1 1 1 1 1 1 1										
0 75	0										
0 75											
0.5000	E-04 .1	E-09									

Table 30. (Continued)

2 011

[illegible]

Table 30. (Continued)

Flaud and Camy-Peyret (120) state 466 Watson constants

2 120											
2805.512	E+00	Vibrational energy									
0.9059	E+00	A									
0.431563	E+00	B									
0.406092	E+00	C									
0.468384	E-02	DLK									
0.243	E-04	DLJK									
0.306	E-06	DLJ									
0.3566	E-05	dSK									
0.318	E-07	dSJ									
0.449	E-05	HLK									
0.0	E-07	HLKJ									
0.0	E-09	HLJK									
0.513	E-12	HLJ									
0.0	E-06	hSK									
0.0	E-12	hsJK									
0.0	E-07	hsJ									
0.0	E-08	ALK									
0.0	E-07	ALKKJ									
0.0	E-08	ALJK									
0.000	E-08	ALK									
0.0	E-10	ALJJK									
0.0	E-07	AlSK									
0.0	E-10	AlSJK									
0.00	E-00	AlSKJ									
0.00	E-00	AlSJ									
0.0	E-09	PK									
0.0	E-12	PKKJ									
0.0	E-10	pSK									
0.0	E-12	GK									
0.0	E-15	KK									
0 75	0 1.0	1.0									
0 1	1 1	1 1	1 1	1 1	1 1	1 1	1 1	1 1	1 1	1 1	1 1
0 75	0										
0 75											
0.5000	E-04	.1						E-09			

Table 30. (Continued)

1 Flaud and Camy-Peyret (101) state 466 Watson constants

2 101											
2906.069	E+00	Vibrational energy									
7.853192	E+00	A									
0.4286512	E+00	B									
0.4049507	E+00	C									
0.26952	E-02	DLK									
-0.21203	E-04	DLJK									
0.3070	E-06	DLJ									
0.65	E-05	dsK									
0.327	E-07	dsJ									
0.3428	E-05	HLK									
0.0	E-07	HLKJ									
0.0	E-09	HLJK									
0.513	E-12	HLJ									
0.0	E-06	hsK									
0.0	E-12	hsJK									
0.0	E-07	hsJ									
0.0000	E-08	ALK									
0.0	E-07	ALKKJ									
0.0	E-08	ALJK									
0.000	E-08	ALK									
0.0	E-10	ALJJK									
0.0	E-07	ALsK									
0.0	E-10	ALsJK									
0.00	E 00	ALsKJ									
0.00	E 00	ALsJ									
0.0	E-09	PK									
0.0	E-12	PKKJ									
0.0	E-10	psK									
0.0	E-12	RK									
0.0	E-15	RK									
0	75	0	1.0	1.0							
0	J	J	1	J	1	1	1	1	1	1	1
0	75	0									
0	75										
0.5000	E-04	.1						E-09			

Table 30. (Continued)

2 130

Table 30. (Continued)



2 111

[illegible]

Table 30. (Continued)

the  $P_z^8$  term) and calculating the energy. The results agree very well with the published values so we feel it was only the LK constant that was responsible for the error in the diagonalizations. This constant was removed from all the sets of Hamiltonian constants and the energies were calculated for all levels of  $\text{NO}_2$ ; this generated 15,984 rotational energy levels. In Table 30, the Watson Hamiltonian constants used in the calculations are given. These are from the papers cited above with the modifications discussed in the text. We wrote a program to calculate the spin-rotation splitting to the energy levels for the six bands that constants are available for. These constants are given in Table 31.

Table 31. Spin-Rotation Interaction Constants for  $\text{NO}_2$

Band	$\epsilon = 1/2(\epsilon_{bb}-\epsilon_{cc})$	$\epsilon_{aa}-\epsilon$	$\epsilon_{bb}-\epsilon_{cc}$	$\eta_{aaaa}$
000	$-0.14601935 \times 10^{-2}$	0.18180028	$0.34220076 \times 10^{-2}$	$-0.1710183 \times 10^{-3}$
010	$-0.15193 \times 10^{-2}$	0.199308	$0.384 \times 10^{-2}$	$-0.20074 \times 10^{-3}$
120	$-0.16733 \times 10^{-2}$	0.21940	$0.446 \times 10^{-2}$	$-0.24054 \times 10^{-3}$
101	$-0.15513 \times 10^{-2}$	0.17648	$0.3708 \times 10^{-2}$	$-0.1733 \times 10^{-3}$
130	$-0.17321 \times 10^{-2}$	0.236906	$0.48675 \times 10^{-2}$	$-0.26952 \times 10^{-3}$
111	$-0.16189 \times 10^{-2}$	0.193993	$0.41165 \times 10^{-2}$	$-0.20228 \times 10^{-3}$

Applying this, a total of 24,384 energy levels were generated for  $\text{NO}_2$ , 16804 states which have the spin-rotation interaction included and 7580 states which do not and have an additional factor of 2 in the partition sum degeneracy factor. The non-symmetrical nitrogen nucleus  $\text{I}^{14}\text{N}$  gives a nuclear statistical factor of  $g_j = 2(I + 1) = 3$ . The partition sums were calculated over the temperature grid to allow fitting the polynomial to  $Q(T)$ . The polynomial fit reproduced the sums to better than 0.4%. Comparison of our calculated value at

225K with the value given on the JPL Catalogue gives  $Q(\text{ULCAR}) = 8835$  and  $Q(\text{JPL}) = 8750$ .

### 5.7 Approximate Partition Sums

As part of the work on calculating the total internal partition sums for the molecules on the database, we tested an approximation that is often used for evaluating the partition sum. The approximation is to replace the total internal partition sum by a product of the vibrational partition sum and the rotational partition sum, i.e.  $Q(T) = Q_v(T) \cdot Q_r(T)$ . Rather than doing a direct sum on twenty to thirty thousand energy levels, two smaller direct sums are done. The vibrational sum is usually over 5 to 10 terms and the rotational sum can be over several hundred to a thousand or so levels or can be approximated by analytical formula or by classical values.

The approximation made would be strictly true if the shape of each upper vibrational potential curve was the same as the ground state potential curve. This is not the case, however, so we must ask the question "How much does the change in the shape of the potential curve affect the rotational energies and does this have a noticeable effect on the partition sums?" What we must do to answer this is to consider the ro-vibrational energies since the assumption comes from writing  $E_{vr} = E_v + E_r$ . For most of the levels at the bottom of the potential, the difference in energy causes little change in the calculated partition sum ( $<0.1\%$ ) over temperatures below 250-300 K. Above these temperatures, upper levels become important and we expect to see some deviation between the two partition sums. We desire to know how great this deviation can be. This will be important for the larger systems where molecular constants are not available for many of the low lying vibrational bands. It is for these systems where the approximation must be

made. This study will help determine the accuracy of the partitions sums calculated using  $Q_v \cdot Q_r$ .

We have tested the approximation for  $H_2O$ ,  $CO_2$  and  $O_3$ . For water vapor the calculations were done for the principal isotopic species and for monodeuterated water. The direct summation for the vibrational partition sums was over 8 and 10 vibrational levels respectively. The values of the vibrational energy levels are given in Table 32 for all the species we have tested except  $CO_2$  for which all of the values published were used (see L.S. Rothman, Appl. Opt. 25, 1795 (1986)). For  $H_2O$ ,  $CO_2$  and  $O_3$  the error was of order 0.1% in the temperature range of interest. For HDO the error was low until around 275-300 K where the error went to ~1%. This is shown in Figure 22. Also given in the figure is the approximation using the classical value for the rotational partition sum. Note this is clearly greater than the 1% level we have set for the calculations.

We decided to also test the approximation that is used in the FASCODE program<sup>21</sup> for the partition sums as a function of temperatures. In the program the partition sum at temperature T is approximated by the product  $Q_v(T) \cdot Q_r(T)$ , where  $Q_v(T)$  is calculated by direct summation and  $Q_r(T)$  is approximated by  $Q_r(296K) \cdot (T/296K)^{1.5}$ . In Figure 23 the calculated  $Q(T)$  is plotted vs. the FASCODE approximation for HDO. The % error plot reveals that the approximation starts around 3% low at 70K and increases to roughly 0.5% high at 420 K. The approximation is not too severe in the temperatures of atmospheric interest, this is, however, only for one species and larger deviations may be observed for other molecules.

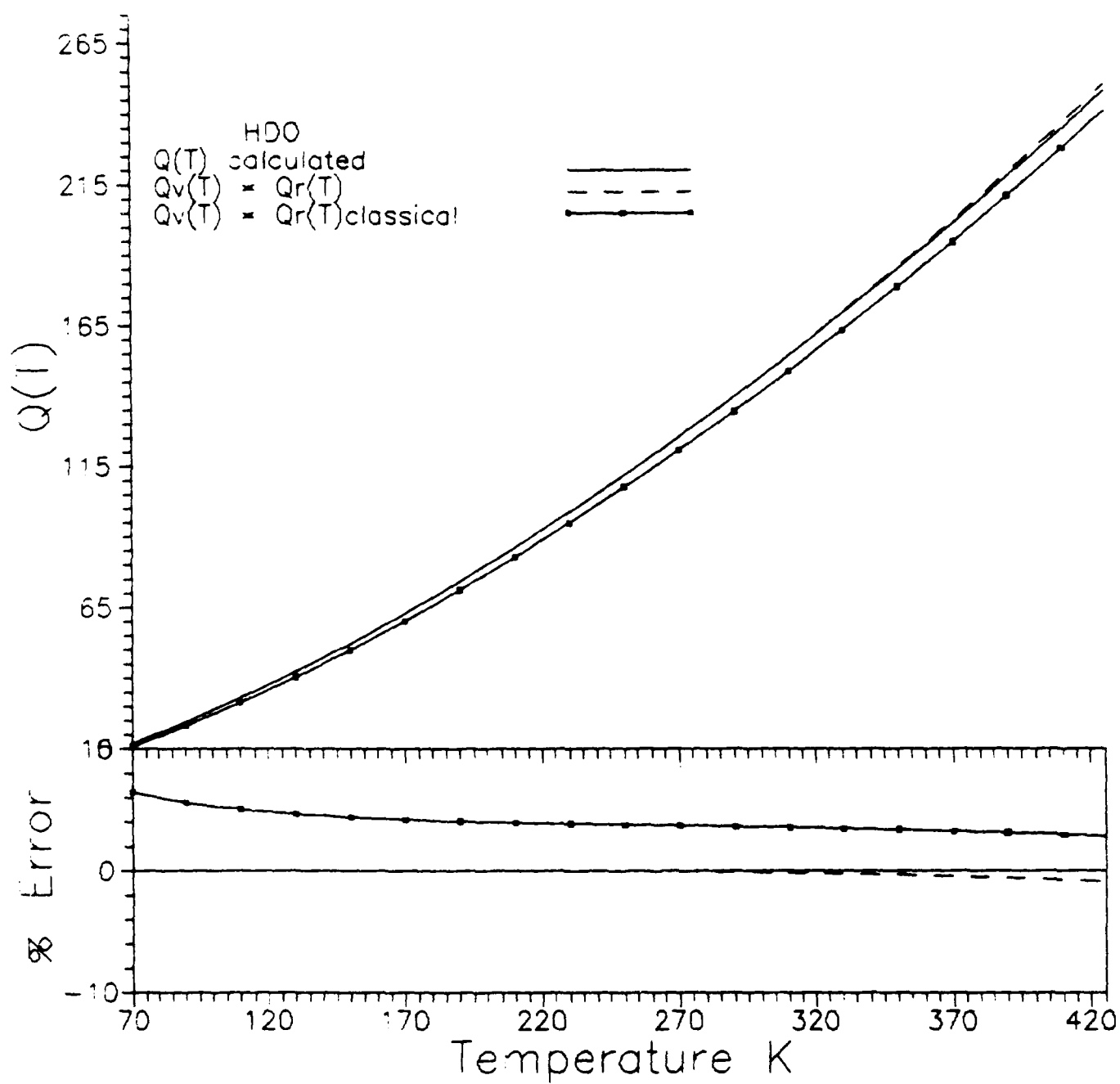


Figure 12.  $Q(T)$  Calc,  $Q_v(T) \times Q_r(T)$ ,  $Q_v(T) \times Q_r(T)$  Classical, vs. Temperature and % Error vs. Temperature

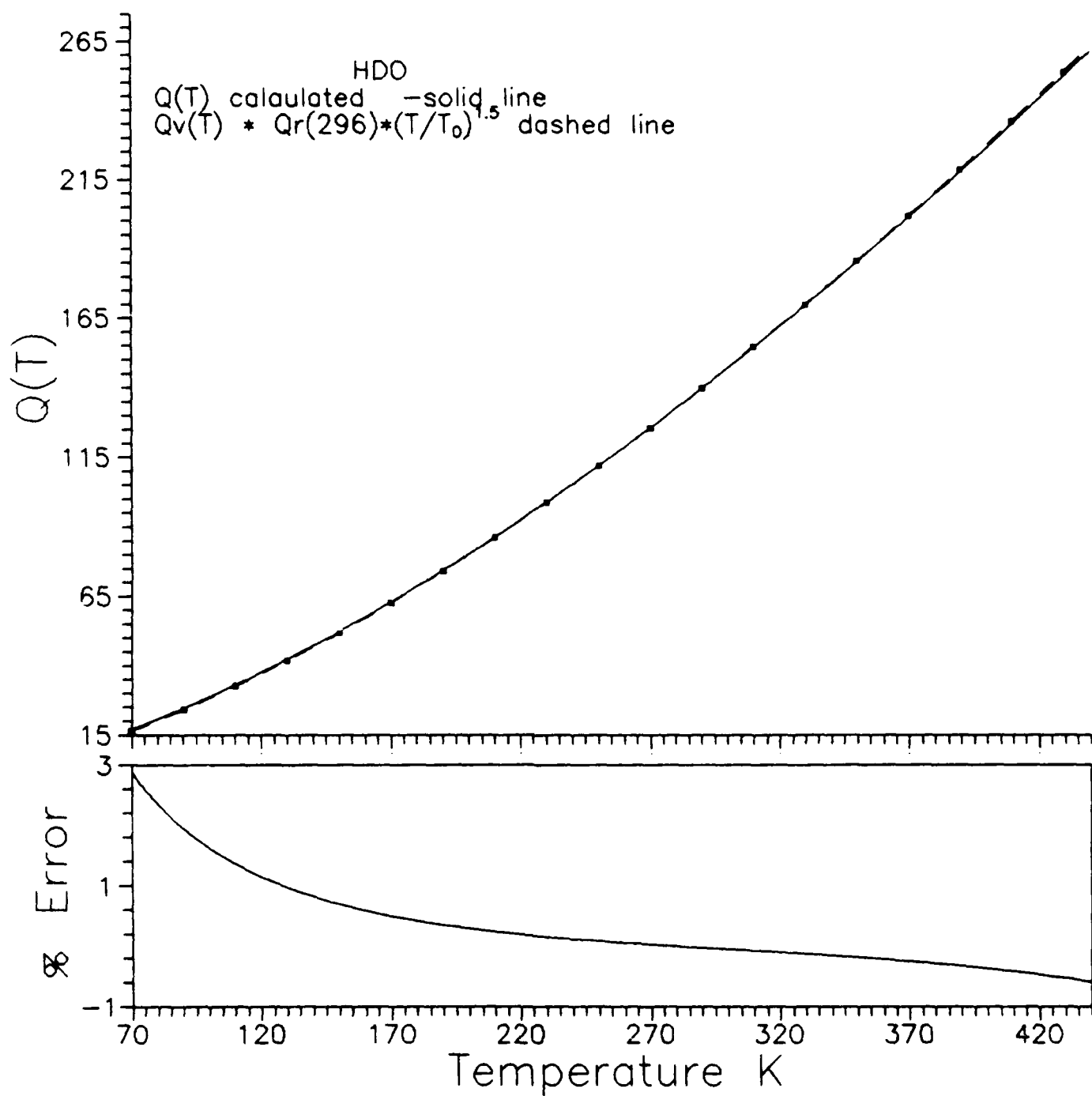


Figure 23.  $Q(T)$  Calc,  $Q_v(T) * Q_r(296K) * (T/T_0)^{1.5}$  vs. Temperature and % Error vs. Temperature, i.e. the FASCCM Approx.

Table 32. Vibrational Energies in  $\text{cm}^{-1}$ 

level	$\text{H}_2\text{O}$	$\text{HDO}$	$^{16}\text{O}_3$
1	0.0	0.0	0.0
2	1594.7	1403.4	700.9
3	3151.6	2723.7	1042.1
4	3657.1	2782.0	1103.1
5	3755.9	3707.4	1399.3
6	4666.8	4100.1	2063.2
7	5235.0	4145.6	2110.8
8	5331.3	5363.6	2195.9
9		6415.6	1796.3
10		6452.1	1726.5

### 5.8 Nuclear Statistical Factors for Non-Symmetric Nuclei

We decided to calculate the internal partition sum explicitly. This generates nuclear statistical factors that cancel in usual applications of the partition sums and hence these terms are normally omitted. It is more for the sake of clarity that they are included here, i.e. rather than trying to explain what factors we are leaving out from the sum for each isotopic variant we are simply calculating the partition sum correctly. In order to use these sums, e.g. calculating  $R$  from  $S$ , these factors must be used. We review them here for the species we have considered to date. The fact of having non-symmetric nuclei means that the spin of the nucleus has not been accounted for in the coupling between rotational wavefunctions and the spins of symmetric nuclei (the usual  $g_i$  terms,

e.g. 0 or 1 for asymmetric/symmetric ozone). The nuclear statistical factor generates additional multiplying terms of  $g_j = (2I+1)$  for each non-symmetric nuclei, where  $I$  is the spin of the nucleus in question. We write the internal partition sum as

$$Q(T) = g_j \sum_i g_i e^{-E_i/kT} \quad (28)$$

where  $g_j$  can be taken out of the sum because it is the same for all states. In the discussion below use is made of the AFGL isotopic labeling scheme, e.g. 161 represents the  $H_2^{16}O$  species of water vapor.

## $H_2O$

- 161 The hydrogen nuclei are symmetric and couple with the rotational wave functions to give the 3:1 (odd:even states) ratio. The  $^{16}O$  nucleus has spin zero so the additional factor is  $g_j = [2*(0)+1] = 1$ .
- 181 This is similar to 161, because  $^{18}O$  has spin zero the factor is the same as for 161,  $g_j = [2*(0)+1] = 1$ .
- 171 Again the symmetric hydrogen nuclei couple with the rotational wavefunctions to give the 3:1 ratio (odd:even). The  $^{17}O$  nuclei has a spin of  $5/2$  to give a factor of  $g_j = [2*(5/2)+1] = 6$ .
- 162 The hydrogen nuclei are not symmetric so there is no coupling with the rotational wavefunctions ( $g_i = 1$ ). The nuclear spins are  $I(H) = 1/2$ ,  $I(D) = 1$  and  $I(^{16}O)=0$  to give a factor of  $g_j = [2*(1/2)+1] [2*(1)+1] [2*(0)+1] = 2*3*1 = 6$ .



## CO<sub>2</sub>

- 626 There is coupling of the spin zero oxygens with the rotational wavefunctions, <sup>12</sup>C has zero spin therefore one has  $g_j = 1$ .
- 636 Same argument for the oxygens as above, <sup>13</sup>C has spin 1/2 to give  $g_j = [2*(1/2)+1] = 2$ .
- 628 No symmetric nuclei so we get  $\Pi[2I_j+1]$  but all the spins are zero so  $g_j = 1$ .
- 627  $g_j = [2*(0)+1] [2*(0)+1] [2*(5/2)+1] = 1*1*6 = 6$
- 638  $g_j = [2*(0)+1] [2*(1/2)+1] [2*(0)+1] = 1*2*1 = 2$ .
- 637  $g_j = [2*(0)+1] [2*(1/2)+1] [2*(5/2)+1] = 1*2*6 = 12$ .
- 628  $g_j = [2*(0)+1] [2*(0)+1] [2*(0)+1] = 1*1*1 = 1$ .
- 728  $g_j = 2*(5/2)+1 [2*(0)+1] [2*(0)+1] = 6*1*1 = 6$ .

## O<sub>3</sub>

- 666 Symmetric end oxygens couple with rotational wavefunctions to give the 1:0 (even:odd) ratio. The central oxygen (non-symmetric) has spin zero to give  $g_j = [2*(0)+1] = 1$ .
- 668 No coupling between rotational wavefunctions and spin so all three oxygens contribute to give  $g_j = [2*(0)+1] [2*(0)+1] [2*(0)+1] = 1*1*1 = 1$ .

686 Coupling for the 1:0 ratio as for 666, the central  $^{18}\text{O}$  has zero spin to give  $g_j = [2*(0)+1] = 1$ .

## $\text{N}_2\text{O}$

446 There are no symmetric nuclei for this molecule thus one has  $g_j = \prod [2I_j+1]$ . One has for 446,  $g_j = [2*(1)+1] [2*(1)+1] [2*(0)+1] = 3*3*1 = 9$ .

$$456 \quad g_j = [2*(1)+1] [2*(1/2)+1] [2*(0)+1] = 3*2*1 = 6.$$

$$546 \quad g_j = [2*(1/2)+1] [2*(1)+1] [2*(0)+1] = 2*3*1 = 6.$$

$$448 \quad g_j = [2*(1)+1] [2*(1)+1] [2*(0)+1] = 3*3*1 = 9.$$

$$447 \quad g_j = [2*(1)+1] [2*(1)+1] [2*(5/2)+1] = 3*3*6 = 54.$$

## $\text{CO}$

$$26 \quad g_j = [2*(0)+1] [2*(0)+1] = 1*1 = 1.$$

$$36 \quad g_j = [2*(1/2)+1] [2*(0)+1] = 2*1 = 2.$$

$$28 \quad g_j = [2*(0)+1] [2*(0)+1] = 1*1 = 1.$$

$$27 \quad g_j = [2*(0)+1] [2*(5/2)+1] = 1*6 = 6.$$

## CH<sub>4</sub>

211 Here the symmetric hydrogens give rise to coupling with rotational wavefunctions for the ratio of 5:3:2 for A:F:E states. The central carbon is what contributes to  $g_j$  to give  $g_j = [2*(0)+1] = 1$ .

311 Same as above for coupling and  $g_j = [2*(1/2)+1] = 2$ .

## NO<sub>2</sub>

446 The symmetric oxygens couple with the rotational wavefunctions to give 1:0 (even:odd) ratio. The central nitrogen gives  $g_j = [2*(1)+1] = 3$ .

## 6.0 REFERENCES

1. L. S. Rothman, R. R. Gamache, A. Barbe, A. Goldman, J. R. Gillis, L. R. Brown, R. A. Toth, J.-M. Flaud and C. Camy-Peyret, "AFGL atmospheric absorption line parameters compilation: 1982 edition," *Appl. Opt.* **22**, 2247 (1983).
2. L. S. Rothman, A. Goldman, J. R. Gillis, R. R. Gamache, H. M. Pickett, R. L. Poynter, N. Husson and A. Chedin, "AFGL trace gas compilation: 1982 edition," *Appl. Opt.* **22**, 1616 (1983).
3. L. S. Rothman, R. R. Gamache, A. Goldman, L. R. Brown, R. A. Toth, H. M. Pickett, R. L. Poynter, J.-M. Flaud, C. Camy-Peyret, A. Barbe, N. Husson, C. P. Rinsland and M. A. H. Smith, "The HITRAN database: 1986 edition," *Appl. Opt.* **26**, 4058 (1987).
4. C. H. Townes and A. L. Schawlow, "Microwave Spectroscopy," McGraw-Hill Publishing Company, New York, 1955.
5. N. Husson et al., "The GEISA Spectroscopic Line Parameters Data Bank in 1984," *Ann. Geophys.* **4**, 185 (1986).
6. A. Bauer, M. Godon and B. Duterage, *JQSRT* **33**, 167 (1985).
7. R. W. Davies and B. A. Oli, *JQSRT* **20**, 95-120 (1978).
8. P. Varanasi, *JQSRT* **15**, 191-196 (1975); P. Varanasi and S. Sarangi, *JQSRT* **15**, 473-482 (1975); W. G. Planet, G. L. Tettemer and J. S. Knoll, *JQSRT* **20**, 547-556 (1978); R. S. Eng and A. W. Mantz, *J. Mol. Spectrosc.* **74**, 331-344 (1979); W. G. Planet and G. L. Tettemer, *JQSRT* **22**, 345-354 (1979); G. L. Tettemer and W. G. Planet, *JQART* **24**, 343-345 (1980).
9. V. Malathy Devi, B. Fridovich, G. D. Jones and D. G. S. Snyder, *J. Mol. Spectrosc.* **105**, 61-69 (1984).
10. J. M. Colmont and N. Monnanteuil, *J. Mol. Spectrosc.* **104**, 122-128 (1984).

11. A. Barbe, P. Marché, C. Meunier and P. Jouve, *J. Phys.* 44, 1015-1017 (1983).
12. P. Varanasi, private communication.
13. P. Varanasi, *JQSRT* 25, 187-188 (1981); T. Nakazawa and M. Tanaka, *JQSRT* 28, 471-480 (1982).
14. P. Varanasi, L. P. Giver and F. P. J. Valero, *JQSRT* 30, 481-490 (1983).
15. R. R. Gamache, *J. Mol. Spectrosc.* 114, 31-41 (1985).
16. J. P. Bouanich, R. Farreng and C. Brodbeck, *Can. J. Phys.* 61, 192 (1983).
17. J. M. Hartmann, M. Y. Perrin, J. Taine and L. Rosenmann, private communication.
18. B. J. Connor and H. E. Radford, private communications.
19. V. M. Devi, B. Fridovich, G. D. Jones, D. G. S. Snyder, P. P. Das, J.-M. Flaud, C. Camy-Peyret and K. N. Rao, *J. Mol. Spectrosc.* 93, 179 (1982).
20. J. M. Devi, B. Fridovich, G. D. Jones, D. G. S. Snyder and A. Neuendorffer, *Appl. Opt.* 21, 1537 (1982).
21. S. A. Clough, F. X. Kneizys, L. S. Rothman and W. O. Gallery, *Proc. Soc. Photo-Opt. Instrum. Eng.* 277, 152 (1981).
22. S. T. Massie, A. Goldman, D. G. Murcray and J. C. Gille, *Appl. Opt.* 24, 3426 (1985).
23. R. R. Gamache and R. W. Davies, *J. Mol. Spectrosc.* 104, 283-299 (1985).
24. R. R. Gamache and L. S. Rothman, *J. Mol. Spectrosc.* 128, 360-369 (1988).

25. C. Camy-Peyret, J.-M. Flaud, J.-Y. Mandin, J.-P. Chevillard, J. Brault, D. A. Ramsay, M. Vervloet and J. Chauville, *J. Mol. Spectrosc.* 113, 208-228 (1985).
26. J.-Y. Mandin, M.-P. Chevillard, C. Camy-Peyret, J.-M. Flaud and J. Brault, *J. Mol. Spectrosc.* 116, 167-190 (1986).
27. R. R. Gamache and R. W. Davies, *Appl. Opt.* 22, 4013-4019 (1983).
28. R. R. Gamache and L. S. Rothman, *Appl. Opt.* 24, 1651-1656 (1985).
29. L. D. Gray and A. T. Young, *J. Quant. Spectrosc. Radiat. Transfer* 9, 569-589 (1969).
30. R. L. Poynter and H. M. Pickett, "Submillimeter, Millimeter, and Microwave Spectral Line Catalogue," JPL publication 80-23 Revision 2, June 1, 1984.
31. R. S. McDowell, *J. Quant. Spectrosc. Radiat. Transfer* 38, 337-346 (1987).
32. R. Hawkins, private communication, 1988.
33. C. Camy-Peyret and J.-M. Flaud, *Mol. Phys.* 32, 523-537 (1976).
34. C. Camy-Peyret, J.-M. Flaud and N. Papineau, *C. R. Acad. Sc. Paris*, t 290, Serie B, 537-540 (30 Juin 1980).
35. R. A. Toth, V. D. Gupta and J. W. Brault, *Appl. Opt.* 21, 3337-3347 (1982).
36. J.-M. Flaud, C. Camy-Peyret, V. M. Devi, C. P. Rinsland and Mary Ann Smith, *J. Mol. Spectrosc.* 118, 334-344 (1986).
37. C. Camy-Peyret, J.-M. Flaud, A. Perrin, V. M. Devi, C. P. Rinsland and Mary Ann Smith, *J. Mol. Spectrosc.* 118, 345-354 (1986).

38. J.-M. Flaud, C. Camy-Peyret, V. M. Devi, C. P. Rinsland and Mary Ann Smith, J. Mol. Spectrosc. 124, 209-217 (1987).
39. V. M. Devi, J.-M. Flaud, C. Camy-Peyret, C. P. Rinsland and Mary Ann Smith, J. Mol. Spectrosc. 125, 174-183 (1987).
40. J.-M. Flaud, Principal isotopic species, private communications, 1988.
41. J.-M. Flaud, 668,686 isotopic species, private communications, 1988.
42. R. A. Toth, JOSA B3, 1263-1281 (1982).
43. C. Camy-Peyret, J.-M. Flaud, A. Perrin and K. N. Rao, J. Mol. Spectrosc. **95**, 72-79 (1982).
44. A. Perrin, J.-M. Flaud and C. Camy-Peyret, Infrared Phys. **22**, 343-348 (1982)

## 7.0 ACKNOWLEDGEMENT

We would like to thank Dr. Robert Hawkins of the Air Force Geophysics Laboratory for his assistance in fitting the partition sums to the polynomial expressions. We would also like to thank Drs. Jean-Marie Flaud and Claude Camy-Peyret of the University of Paris for their suggestions and for discussions on the visible spectral region of water vapor.



## APPENDIX A

### Presentations Made Under Contract

Abstract of Paper Given at the 41st Symposium on Molecular  
Spectroscopy at The Ohio State University, June 1986

## TEMPERATURE DEPENDENCE OF N<sub>2</sub>-BROADENED HALFWIDTHS OF H<sub>2</sub>O

ROBERT R. GAMACHE and LAURENCE S. ROTHMAN

The temperature dependence of N<sub>2</sub>-broadened halfwidths of water was studied for rotational vibrational transitions of atmospheric importance. The halfwidths were calculated using cutoff free theory<sup>1</sup> with Anderson-Tsao-Curnutte<sup>2</sup> interruption functions and trajectories correct to first-order-in-time<sup>3</sup>. The calculations were carried out for pure rotational transitions and for  $\nu_2$  transitions. The temperature dependence was calculated assuming the exponential form

$$\gamma(T_0) = \gamma(T) \left\{ \frac{T}{T_0} \right\}^n$$

The exponent  $n$  has been calculated for different rovibrational transitions and the calculations have been performed over the temperature range 200 K to 1000 K to be applicable to both atmospheric studies as well as hot sources. The trends in  $n$ , such as vibrational dependence,  $J$  dependence, etc., are examined and recommended values are given.

1. D. Korff and R. P. Leavitt, Phys. Lett. A 53, 351(1975); D. Robert and J. Bonamy, J. Phys. (Paris) 40, 923(1979); R. P. Leavitt and D. Korpf, J. Chem. Phys. 74, 2180(1981).
2. P. W. Anderson, Phys. Rev. 76, 647-661(1949); 80, 511-513(1950); C. J. Tsao and B. Curnutte, J. Quant Spectrosc. Radiat. Transfer 2, 41-91(1962).
3. R. R. Gamache and R. W. Davies, J. Mol. Spectrosc. 109, 283-299(1985).

This work has been supported by the Air Force Office of Scientific Research through AFGL task 2310G1.

Address of Gamache: University of Lowell Center for Atmospheric Research, 450 Aiken Street, Lowell, MA 01854.

Address of Rothman: Optics Division, Air Force Geophysics Laboratory, Hanscom AFB, MA 01731.

Time Required: 10 min.

Session in which paper is recommended for presentation. 5  
High resolution IR & THEORY

Paper for Meeting at the Atmospheric Spectroscopy Applications  
(ASA) Workshop at Rutherford Appleton Laboratory, Oxfordshire, UK,  
1-3 September 1987

## Temperature Dependence Line Widths and Shifts

Robert R. Gamache  
University of Lowell, Center for Atmospheric Research  
450 Aiken Street, Lowell, MA 01854  
and  
Laurence S. Rothman  
Air Force Geophysics Laboratory  
Hanscom AFB, MA 01731

The temperature dependence of the pressure-broadened line widths and the pressure induced line shift are investigated. Line width and shift calculations were done for two major constituents of the terrestrial atmosphere, ozone and water vapor. For ozone some 126 ro-vibrational transitions belonging to either the pure rotation or the  $\nu_3$  band were studied via QFT-ID<sup>1</sup> calculations over a temperature range of 200-500 K. H<sub>2</sub>O has been studied<sup>2</sup> over a temperature range of 200-1000 K to yield results applicable to atmospheric studies as well as hot sources. Forty-seven rotational transitions important to atmospheric studies were considered and the calculations were done for both the pure rotation and  $\nu_2$  bands of water. The halfwidths were calculated using a cutoff free theory with Anderson-Tsao-Curnutte (ATC) interruption functions and trajectories correct to first order in time.<sup>2</sup> In both studies the transitions span a wide range of J" (1 to 14 for H<sub>2</sub>O and 1-35 for O<sub>3</sub>) with the full manifold of K<sub>a</sub>" being sampled.

The calculations were done with nitrogen as the perturbing gas and the calculations included the dipole(H<sub>2</sub>O or O<sub>3</sub>)-quadrupole(N<sub>2</sub>) and the quadrupole(H<sub>2</sub>O or O<sub>3</sub>)-quadrupole(N<sub>2</sub>) interactions. The vibrational dependence was explicitly considered in all the calculations and a Lennard-Jones potential was used to give the first-order-in-time trajectories. The molecular constants used in the calculations<sup>1,2</sup> were the best available in the literature. In these calculations all terms were included (real and imaginary) and no adjustment of the molecular parameters was done.

By evaluating the halfwidth at a series of temperatures, the variation with temperature can be determined in terms of a particular model. The halfwidth in cm<sup>-1</sup>/atm is expressed as the product of density, velocity, and the optical cross-section,

$$\gamma(T) = \rho(T) \cdot v(T) \cdot \sigma(T) \quad (1)$$

The temperature dependence of the density( $n_0 \cdot 273.15/T$ ) and the velocity( $(8kT/\pi\mu)^{1/2}$ ) are known. Here we assume the temperature dependence of the optical cross-section follows a power law, i.e.  $\sigma(T) = \sigma_0 \cdot T^m$ , where  $\sigma_0$  is independent of temperature. The halfwidth from Eq. (1) is considered at two temperatures, T<sub>1</sub> and T<sub>2</sub>, and the ratio is taken to give

$$\frac{\gamma(T_1)}{\gamma(T_2)} = \left[ \frac{T_1}{T_2} \right]^{-1/2} \cdot \left[ \frac{T_1}{T_2} \right]^m \quad (2)$$

Setting  $n = -1/2 + m$  produces the usual formula

$$\gamma(T_1) = \gamma(T_2) \cdot \left( \frac{T_1}{T_2} \right)^{-n} \quad (3)$$

The temperature dependence of the halfwidth is contained in the value of the exponent  $n$ . This model also gives the temperature dependence,  $m$ , of the optical cross-section which can be useful for other studies.

A similar power law form was tried for the line shift,

$$\Delta(T) = a T^b \quad (4)$$

However, we have found that for some transitions an exponential law,  $\Delta(T) = ae^{bT}$ , fits the calculated line shifts better.

To determine the temperature exponent, the halfwidth or shift is evaluated at a number of temperatures and the results least-squares fitted to the particular model. For example, for the halfwidth a plot (linear regression) of the set of points  $\ln(T_2/T_1)$  vs.  $\ln(\gamma(T_1)/\gamma(T_2))$  yields a straight line of slope  $-n$ . Furthermore, the correlation coefficient of the fit of the points to a straight line relates to the validity of the assumed temperature dependence of the optical cross-section, i.e., the closer the correlation coefficient is to  $|1|$  the more valid the assumption.

A full description of the results, with tables, is presented in references 1 and 2, here we only summarize the results.

In figure 1 we show a typical input set of points and the resulting straight line from regression for the pure rotation transition  $2_2 0 \leftarrow 3_1 3$  of water vapor. All the points fall on the straight line as seen in the figure. This is confirmed by the correlation coefficient of the fit which was 0.99998 for this transition. For all of the transitions studied here, the correlation coefficient for the halfwidth was equal to one to three significant figures confirming the assumed temperature dependence of the optical cross-section, i.e.,  $\sigma_0 \cdot T^m$ .

In figures 2 and 3 the temperature exponents for the halfwidth are plotted vs. rotational quantum numbers for  $H_2O$  and  $O_3$  respectively. Note there appears to be no structure that would help one predict  $n$  for a particular transition.

Figures 4 and 5 show the temperature dependence of the shift results from assuming the power law and exponential law fits. Note in figure 4 the power law gives the best results whereas it is the reverse in figure 5. Although the shift calculations are still in a preliminary stage, they are useful to show trends. The results indicate large variations in the multiplying and exponential coefficients in both models with transition. It does not appear that these coefficients can be predicted with any certainty nor does the use of an average value seem warranted. There remains much to be done on this subject.

#### Summary

#### Temperature dependence of the halfwidth

For both water vapor and ozone it appears that the temperature dependence of the halfwidth cannot be expressed by a simple relation dependent on  $J''$  or any other quantum number. There is some vibrational dependence, but the variation with rotational transition overshadows this. The fluctuation in the results is much greater for  $H_2O$  when compared with the results for  $O_3$ .

The calculations give an average temperature exponent of  $n=0.68$  and  $n=0.76$  for air-broadening of water vapor lines and ozone lines respectively.

It is suggested that whenever possible temperature exponents calculated for specific ro-vibrational transitions be used.

#### Temperature dependence of the line shifts

Although still in a preliminary stage, the results of the shift calculations indicate the temperature dependence is best described by a power law for some lines and by an exponential law for other lines. There seems to be much greater variability of the line shift with temperature as compared to the halfwidth. The dependence varies greatly from line to line. The results suggest that this may be important in certain planetary atmospheres or hot plumes.

#### References

1. R. R. Gamache, J. Mol. Spectrosc. 114, 31-41(1985).
2. R. R. Gamache and L. S. Rothman, "Temperature Dependence of  $N_2$ -Broadened Halfwidths of Water Vapor: the Pure Rotation and  $\nu_2$  Bands," submitted to J. Mol. Spectrosc. July 1987.

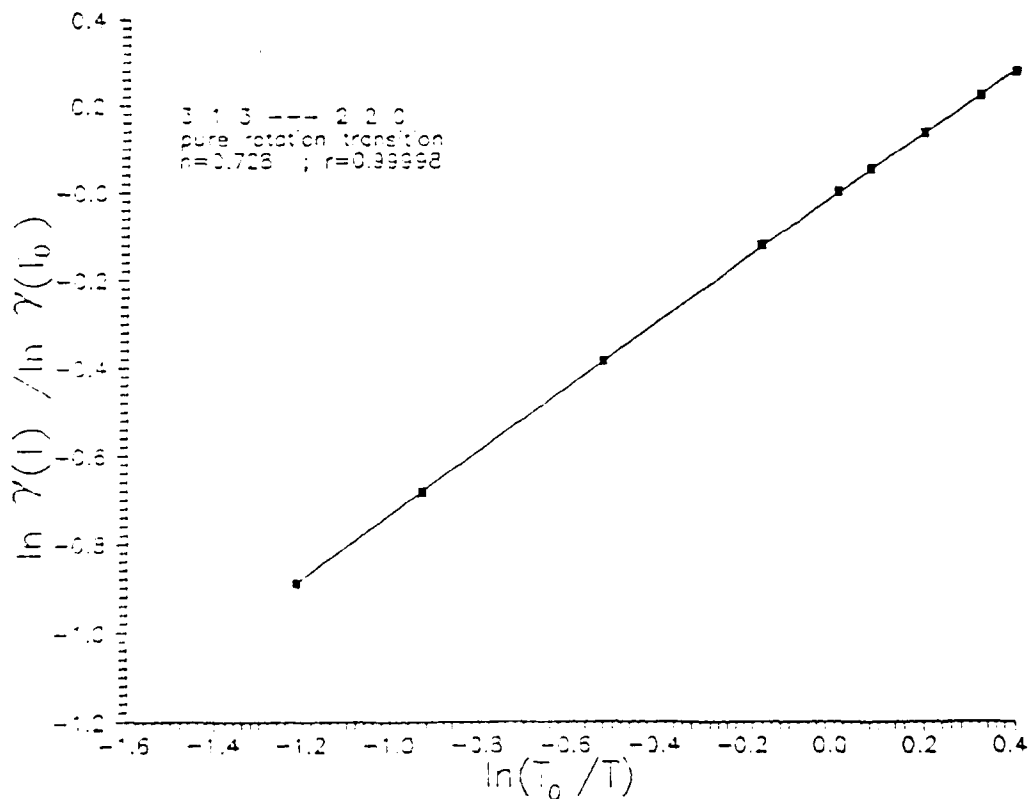


Figure 1

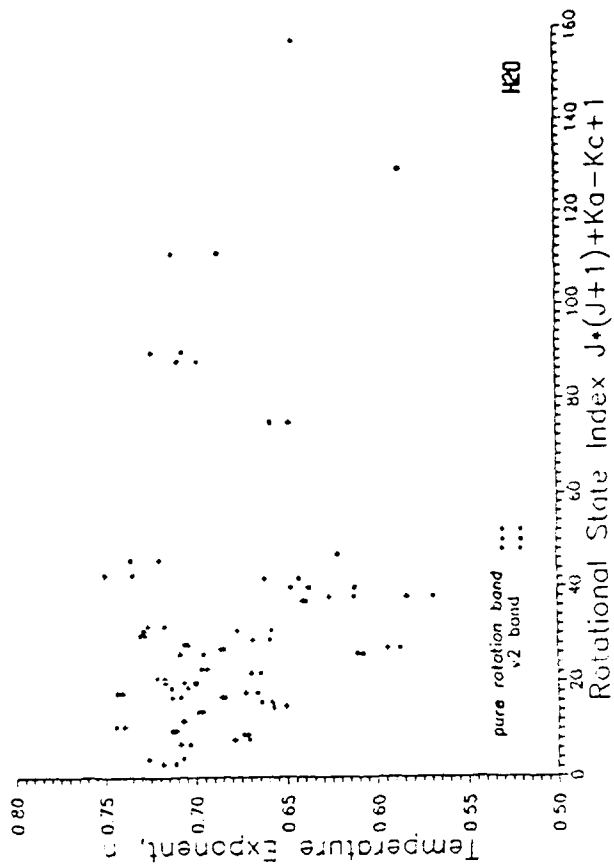


Figure 3

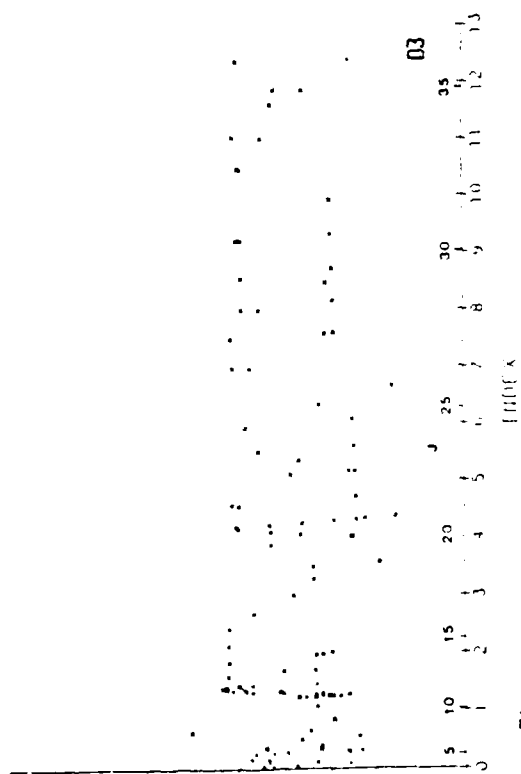


Figure 2

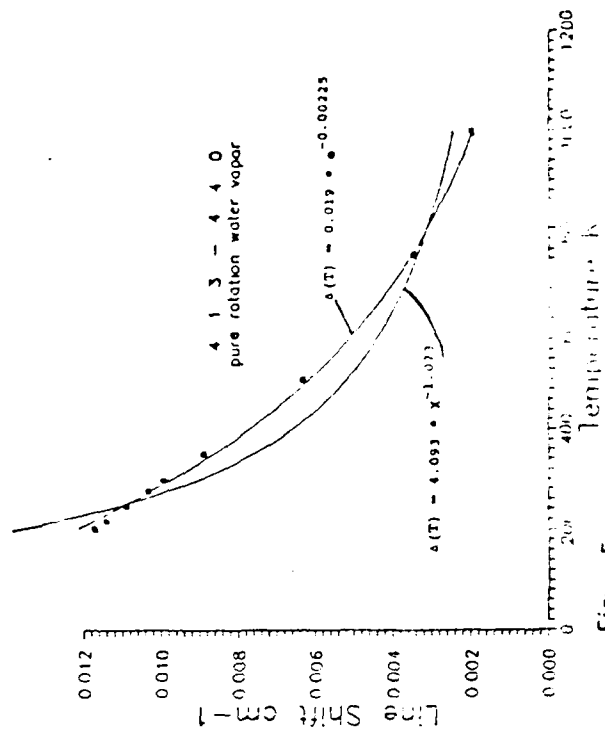


Figure 5

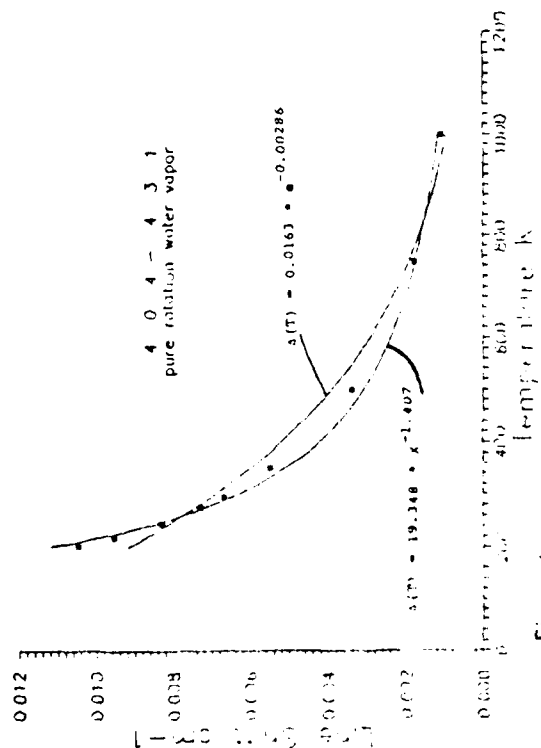


Figure 4



Abstract for Paper Given at the 10th Colloquium on High Resolution  
Molecular Spectroscopy at the University of Burgundy, Dijon, France,  
14-18 September 1987

## TEMPERATURE DEPENDENCE OF LINE WIDTHS AND SHIFTS

Robert R. Gamache  
University of Lowell Center for Atmospheric Research  
Lowell, MA 01854, USA

Laurence S. Rothman  
Air Force Geophysics Laboratory  
Hanscom AFB, MA 01731, USA

The temperature dependence of the pressure broadened line width and the temperature dependence of the pressure induced line shift are investigated. The model considers the optical cross-section to vary with temperature as  $\sigma(T) = \sigma_0 \cdot T^m$  where  $\sigma_0$  is independent of temperature. From this model the temperature dependence of the half-width is given by

$$\gamma(T) = \gamma(T_0) \left\{ \frac{T}{T_0} \right\}^{-n} \quad (1)$$

and the temperature dependence of the line shift is

$$\Delta\nu(T) = \Delta\nu(T_0) \frac{S(T)}{S(T_0)} \left( \frac{T}{T_0} \right)^{-n'} \quad (2)$$

In expression (2),  $S(T)$  is the sign of the line shift at temperature  $T$  and is necessary in order to avoid mathematical discontinuities. The temperature dependence of the line

width and shift is contained in the exponents  $n$  and  $n'$  respectively.

The temperature dependence of  $N_2$ -broadened halfwidths has been studied over a temperature range of 200-500°K for ozone and from 200-1000°K for water vapor. For  $O_3$ , 126 ro-vibrational transitions were studied and both the pure rotation and  $\nu_3$  transitions were included. For water vapor, some hundred transitions were studied for pure rotation and for  $\nu_2$  transitions. The transitions were selected for their importance in atmospheric applications, to consider a wide range of the rotational quantum number  $J''$ , and the full manifold of  $Ka''$  for particular  $J''$  values. The results yield average temperature exponents of ozone and water vapor of  $n = 0.77$  and  $n = 0.68$ , respectively. The results for both molecules are compared here.

The temperature dependence of the line shift for  $N_2$ -broadening of  $O_3$  are also presented. The calculated line shifts are somewhat in question, however, only the trend with temperature was studied. The values of  $n'$  presented show large fluctuations. The many problems observed are discussed in this work.

Abstract for the 43rd Symposium on Molecular Spectroscopy at The  
Ohio State University, June 1988

# SIMPLIFIED EXPRESSION FOR THE TOTAL INTERNAL PARTITION SUM AS A FUNCTION OF TEMPERATURE

ROBERT R. GAMACHE, ROBERT HAWKINS, and LAURENCE S. ROTHMAN

The total internal partition sums have been calculated for the molecules and their isotopic variants on the HITRAN database. The calculations employed near complete sets of energy levels for all relevant rotation-vibration states generated from the molecular constants. All degeneracies were accounted for in the calculations. The calculations were performed over a temperature range of 75K to 400K. The accuracies of the resulting partition sums will be shown. For generalized applications, the internal partition sums have been fitted to the expression

$$Q(T) = a + b \cdot T + c \cdot T^2 + d \cdot T^3,$$

where a, b, c and d are constants adjusted by means of a least-squares minimax procedure. The maximum deviation of the fit is on the order of a few tenths of a percent.

---

Address of Gamache: The Center for Atmospheric Research,  
The University of Lowell, Lowell, MA 01854

Address of Hawkins and Rothman: Optics Division, Air Force Geophysics  
Laboratory, Hanscom AFB, MA 01731

Time required: 10 min.

Session in which paper is recommended for presentation: 5

Abstract of Paper Given at 1988 AFGL Annual Review Conference on  
Transmission Models

## New Method for Temperature Corrections to the HITRAN Line Intensities

Robert R. Gamache<sup>1</sup>, Robert Hawkins<sup>2</sup>, and Laurence S. Rothman<sup>2</sup>

1. Center for Atmospheric Research, University of Lowell,  
450 Aiken St., Lowell, MA 01854
2. AFGL/OPI, Hanscom AFB, MA 01731

The total internal partition sums have been calculated for the molecules and their isotopic variants on the HITRAN database. The calculations employed near complete sets of energy levels for all relevant rotation-vibration states generated from the molecular constants. All degeneracies were accounted for in the calculations. The calculations were performed over a temperature range of 75K to 400K. The accuracies of the resulting partition sums will be shown. For generalized applications, the internal partition sums have been fit to the a simple four parameter Taylor series expansion. The maximum deviation of the fit is on the order of a few tenths of a percent. This scheme will be used on future editions of the HITRAN database to enable users to simply make temperature corrections to the line intensities and retain information about isotopes as well.

## APPENDIX B

### Publications Made Under Contract



Temperature Dependence of N<sub>2</sub>-Broadened Halfwidths of Ozone

ROBERT R. GAMACHI

*Center for Atmospheric Research, The University of Lowell, 450 Aiken Street  
Lowell, Massachusetts 01854*

The temperature dependence of N<sub>2</sub>-broadened halfwidths of ozone has been studied over a temperature range of 200–500 K. Assuming the form  $\gamma(T) = \gamma(T_0)(T_0/T)^n$ , the exponent  $n$  has been determined from QFT-ID calculations for 126 ro-vibrational transitions of ozone selected to consider a wide range of the rotational quantum number  $J'$  (1 to 35), the full manifold of  $K'_a$  for particular  $J'$ , values and transitions important to stratospheric studies. The results give an average temperature exponent of  $n = 0.77$  for nitrogen-broadening. The temperature exponents are transition dependent but the fluctuation about the average value is small ( $\pm 6\%$ ). The value of  $n$  as a function of  $J'$  and  $K'_a$  is investigated. Comparison of the present results with experiment and other theoretical calculations shows good agreement. Based on the results an average temperature exponent for air-broadening of  $n = 0.76$  is suggested. © 1985 Academic Press, Inc.

## 1. INTRODUCTION

The use of balloon-borne and ground-based spectrometers to study and monitor the atmosphere has greatly increased our knowledge of many regions of the atmosphere. It is well recognized (1, 2) that in order to reduce the data from these methods an accurate knowledge of the broadening coefficients for ro-vibrational transitions is necessary. For atmospheric applications the temperature dependence of the halfwidth must be understood as well as the halfwidth at a given temperature for all species under consideration. Here we are concerned with the molecule ozone which has a very rich spectrum and is known to play an important role in the temperature regulation of the lower atmosphere, air chemical cycles, and climate and which must be well determined in order to extract information on trace atmospheric constituents in the far IR (3).

A fair amount of effort has been invested in the determination of accurate halfwidths for ro-vibrational transitions of ozone perturbed by atmospheric gases, i.e., N<sub>2</sub>, O<sub>2</sub>, air, O<sub>3</sub>. Several experimental measurement efforts have been performed (4–10) yielding halfwidths for some one to two hundred transitions, mostly for N<sub>2</sub>-broadening with some O<sub>2</sub>-, air-, and self-broadening results as well. Theoretical calculations using the conventional ATC method (11) have been performed (12–15). The last two of these studies (14, 15), using the most up to date molecular constants, produced results that were too low compared with experiment. Recently the QFT-ID method (16) was used to study 127 transitions of ozone broadened by N<sub>2</sub>, O<sub>2</sub>, and air; comparison with experiment gave agreement to 7%. Using this method, halfwidths have been calculated (17) for N<sub>2</sub>-broadening of ozone for all the unique rotational transitions of ozone with

## The HITRAN database: 1986 edition

L. S. Rothman, R. R. Gamache, A. Goldman, L. R. Brown, R. A. Toth, H. M. Pickett, R. L. Poynter, J.-M. Flaud, C. Camy-Peyret, A. Barbe, N. Husson, C. P. Rinsland, and M. A. H. Smith

A description and summary of the latest edition of the AFGL HITRAN molecular absorption parameters database are presented. This new database combines the information for the seven principal atmospheric absorbers and twenty-one additional molecular species previously contained on the AFGL atmospheric absorption line parameter compilation and on the trace gas compilation. In addition to updating the parameters on earlier editions of the compilation, new parameters have been added to this edition such as the self-broadened halfwidth, the temperature dependence of the air-broadened halfwidth, and the transition probability. The database contains 348947 entries between 0 and 17,900  $\text{cm}^{-1}$ . A FORTRAN program is now furnished to allow rapid access to the molecular transitions and for the creation of customized output. A separate file of molecular cross sections of eleven heavy molecular species, applicable for qualitative simulation of transmission and emission in the atmosphere, has also been provided.

### I. Introduction

The high-resolution transmission molecular absorption database (known under the acronym HITRAN) is a compilation of spectroscopic parameters from which a wide variety of computer simulation codes are able to calculate and predict the transmission and emission of radiation in the atmosphere. This database is a prominent and long running effort established by the Air Force at the Air Force Geophysics Laboratory (AFGL) in the late 1960s in response to the requirement of a detailed knowledge of infrared transmission properties of the atmosphere. With the advent of sensitive detectors, rapid computers, and higher resolution spectrometers, a large database representing the dis-

crete molecular transitions that affect radiative propagation throughout the electromagnetic spectrum became a necessity. A wide range of applications for HITRAN has evolved including detection of trace and weakly absorbing features in the atmosphere, atmospheric modeling efforts, laser transmission studies, remote sensing, lidar, and a reference base for fundamental laboratory spectroscopic research. The HITRAN database has been periodically updated and enhanced since it first became generally available.<sup>1-4</sup> The most recent edition of the HITRAN database was made available in late 1986. This latest version now unites the data on twenty-eight molecular species with bands covering regions from the millimeter through visible portion of the spectrum. Originally the database contained for each molecular transition the following basic parameters: (1) resonant frequency; (2) line intensity; (3) air-broadened halfwidth; and (4) lower state energy (as well as unique quantum identifications). Additional parameters have recently been provided which permit new capabilities for remote sensing in the atmosphere and capabilities to deal with nonlocal thermodynamic equilibrium effects in the upper atmosphere. The overall structure of the database has been expanded to include files of cross-sectional data on heavy molecular species such as the chlorofluorocarbons (CFCs) and oxides of nitrogen which are not yet amenable to line-by-line representation. This has added to HITRAN the capability of qualitative detection of anthropogenic gases in the window regions of the infrared. Ongoing research efforts will gradually move some of these data to the main body of the database. The new file structure of HITRAN is shown in Fig. 1. New parameters have been added to the

L. S. Rothman is with U.S. Air Force Geophysics Laboratory, Optical Physics Division, Hanscom Air Force Base, Massachusetts 01731; R. R. Gamache is with University of Lowell, Center for Atmospheric Research, Lowell, Massachusetts 01854; A. Goldman is with University of Denver, Physics Department, Denver, Colorado 80208; J.-M. Flaud and C. Camy-Peyret are with P. & M. Curie University, Laboratory of Molecular & Atmospheric Physics, 75252 Paris, France; A. Barbe is with Rheims University, Faculty of Sciences, 51062 Rheims, France; N. Husson is with Ecole Polytechnique, Dynamic Meteorology Laboratory, 91128 Palaiseau, France; C. P. Rinsland and M. A. H. Smith are with NASA Langley Research Center, Hampton, Virginia 23665; the other authors are with Jet Propulsion Laboratory, Pasadena, California 91109.

Received 17 April 1987.

## Temperature Dependence of N<sub>2</sub>-Broadened Halfwidths of Water Vapor: The Pure Rotation and $\nu_2$ Bands

ROBERT R. GAMACHE

*University of Lowell, Center for Atmospheric Research, 450 Aiken Street, Lowell, Massachusetts 01854*

AND

LAURENCE S. ROTHMAN

*Air Force Geophysics Laboratory, Hanscom AFB, Massachusetts 01731*

The temperature dependence of N<sub>2</sub>-broadened halfwidths of H<sub>2</sub>O has been studied over a temperature range of 200-1000 K to yield results applicable to atmospheric studies as well as hot sources. Forty-seven rotational transitions important to atmospheric studies were considered and the calculations were done for both the pure rotation and the  $\nu_2$  bands of water. The transitions span a range of  $J''$  from 1 to 14 with the manifold of  $K''_a$  being sampled. The halfwidths were calculated using a cutoff-free theory with Anderson-Tsao-Cornut interruption functions and trajectories correct to first order in time. Assuming the form  $\gamma(T) = \gamma(T_0)(T_0/T)^n$ , the exponent  $n$  has been determined for each transition. The results show strong fluctuations in  $n$  with the rotational quantum numbers and a lesser dependence on the particular vibrational band. The results give average temperature exponents for N<sub>2</sub> broadening of  $\bar{n}(\text{pure rotation}) = 0.684$  and  $\bar{n}(\nu_2) = 0.676$ . Based on the results, an average value of  $n = 0.68$  is recommended, and it is suggested that values calculated for specific rotational transitions be used when available. © 1988 Academic Press, Inc.

### 1. INTRODUCTION

The use of spectroscopy, via balloon-borne or ground-based spectrometers, has greatly increased our knowledge of the constituents and chemistry of the atmosphere. The successful retrieval of stratospheric information from remotely sensed data requires that accurate spectral parameters (e.g., line intensities, line widths, and line frequencies) be known (1). In addition to these parameters, the temperature variation of the parameters must be known, from 200 to 300 K for atmospheric studies and in the range of 1000 K for hot sources. This paper focuses on water vapor. Although a minor constituent of the terrestrial atmosphere, water vapor has a very rich spectrum and is of major importance for considering the absorption of infrared radiation in the atmosphere (2). It plays a prominent role in determining atmospheric transmission to solar or laser radiation and has a profound effect on the heat balance of the lower atmosphere (3). This species is of primary concern in the characterization of hot sources. Furthermore, in order to extract information about trace gas constituents of the atmosphere, the principle absorbers must be well characterized (4).

For water vapor, a fair amount of effort has gone into determining halfwidths for a number of rovibrational transitions both experimentally (5-19) and theoretically

0022-2852/88 \$3.00

Copyright © 1988 by Academic Press, Inc.

All rights reserved. No part may be reproduced.

0001